

EXPERIMENTAL AND COMPUTER STUDIES

OF THE

THERMOLYSIS OF SOME METHYLSILANES

A Thesis presented by

ALAN CHARLES BALDWIN

for the degree of

DOCTOR OF PHILOSOPHY

of the

UNIVERSITY OF LEICESTER

Department of Chemistry
University of Leicester

September 1976

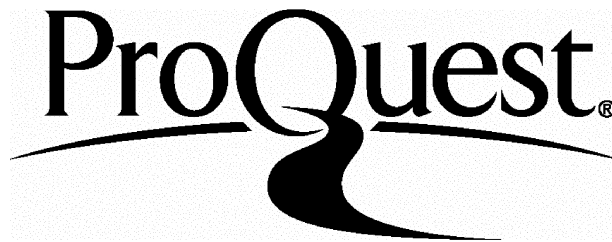
ProQuest Number: U622442

All rights reserved

INFORMATION TO ALL USERS

The quality of this reproduction is dependent upon the quality of the copy submitted.

In the unlikely event that the author did not send a complete manuscript and there are missing pages, these will be noted. Also, if material had to be removed, a note will indicate the deletion.



ProQuest U622442

Published by ProQuest LLC(2015). Copyright of the Dissertation is held by the Author.

All rights reserved.

This work is protected against unauthorized copying under Title 17, United States Code.
Microform Edition © ProQuest LLC.

ProQuest LLC
789 East Eisenhower Parkway
P.O. Box 1346
Ann Arbor, MI 48106-1346



THESIS
S16361
14.12.76

x75301766x

To my Mother and Father
with thanks for all their
help and encouragement.

ACKNOWLEDGEMENTS

I wish to thank my supervisor, Dr. Iain Davidson, for his continued help, encouragement, and valued guidance throughout the course of this work.

I would also like to thank all the many members of the department who have assisted or advised me in the past three years. In particular, I must thank Mrs Ann Crane for tracing the diagrams and Sue Jackson for typing this thesis.

Finally, the award of a maintenance grant from S.R.C. is gratefully acknowledged.

CONTENTS

		<u>Page</u>
Chapter 1	Introduction	1
1.1	Thermolysis of Methylsilanes	1
1.2	Computer Modelling	7
1.3	The Experimental Method	8
Chapter 2	Apparatus and Experimental Procedure	9
2.1	The Flow System	10
2.2	The Sampling System	25
2.3	Experimental Procedure	28
2.4	An Experiment to Test the Assumptions of 'Perfect Mixing' and 'Perfect Pulse Behaviour' Directly.	35
Chapter 3	The Theory of the Pulsed Stirred Flow Technique	38
3.1	Time Dependent Response of a Pulsed Stirred-Flow Reactor	40
3.2	Derivation of Rate Constants in Terms of Experimentally Accessible Parameters	45
3.3	Application of Derived Equations in Practise	48
3.4	Advantages of the Pulsed Stirred-Flow System	50
Chapter 4	Computer Modelling	51
4.1	Approximate Solutions - The Steady State Approach	52
4.2	Numerical Solutions	54

4.3	Gear's Method for the Solution of Systems of Ordinary Differential Equations	58
Chapter 5	Experimental Results	62
5.1	Inert Tracer Experiments	63
5.2	Measurement of a Known Reaction	66
5.3	Thermolysis of Tetramethylsilane	68
Chapter 6	Discussion	77
6.1	The Numerical Accuracy of the Experimental Results	79
6.2	The Mechanism of Thermolysis of Tetramethylsilane	80
6.3	The Mechanism of Thermolysis of Other Methylsilanes	93
Appendix 1	Calibration of the Gas Density Detector	105
Appendix 2	Calibration of the Pressure Transducer	106
Appendix 3	Computer Program to Calculate the Area of a Peak Using Simpson's Rule	108
Appendix 4	Computer Program for the Numerical Solution of Systems of Differential Equations	110
Appendix 5	Numerical Results for the Thermal Isomerisation of Cyclopropane	119
Appendix 6	Numerical Results for the Thermolysis of Tetramethylsilane	122
References		140

LIST OF FIGURES

Figure		Page
2.1	The Flow System	11
2.2	Photograph of Reaction Vessels	12
2.3	Diagram of a Reaction Vessel	12
2.4	Furnace Wiring Diagram	14
2.5	Furnace Temperature Profile	14
2.6	The Sampling Valve	18
2.7	The G.L.C. System	20
2.8	The Traps	20
2.9	The Gas Density Detector	23
2.10	The Sampling System	26
2.11	The Trapping Valve	23
2.12	A Typical Chromatogram	30
2.13	Apparatus Used for Data Logging of G.L.C. Peaks	33
2.14	Modification to the System for Time Dependent Measurements	36
2.15	System Used for Time Delay Measurements	36
3.1	Graph of Reactant Concentration within the Reactor against Time	44
3.2	Graph of Product Concentration within the Reactor against Time	44
4.1	Macroscopic Flowchart of Gear's Algorithm	60
5.1	Comparison of Experimental Response Curve and Calculated Points for Injection of an Inert Pulse	64

5.2	Plot of log(cyclopropane) against log(propene)	67
5.3	Arrhenius Plot for the Thermal Isomerisation of Cyclopropane	67
5.4	Order Plots of Data Obtained from Unpacked Reaction Vessels	70
5.5	Order Plots of Data Obtained from Packed Reaction Vessel	71
5.6	Arrhenius Plot for the Formation of Methane in the Thermolysis of Tetramethylsilane	72
5.7	Arrhenius Plot for the Formation of Methane in the Thermolysis of Tetramethylsilane in a Packed Vessel	73
5.8	Arrhenius Plot Showing Reproducibility of High Temperature Results	75

LIST OF TABLES

Table		Page
2.1	Some Typical Chromatographic Data	31
5.1	Typical Product Distributions	69
5.2	Summary of Arrhenius Parameters	75
6.1	Mechanism of Thermolysis of Tetramethylsilane	85
6.2	Arrhenius Parameters for the Mechanism of Thermolysis of Tetramethylsilane	86
6.3	Sources of Arrhenius Parameters	87
6.4	Experimental Details for the Thermolysis of Trimethylsilane	95

6.5	Mechanism of Thermolysis of Trimethylsilane	97
6.6	Arrhenius Parameters for the Mechanism of Thermolysis of Trimethylsilane	99
6.7	Sources of Arrhenius Parameters	101

CHAPTER ONE

INTRODUCTION

INTRODUCTION

1.1 Thermolysis of Methylsilanes

The thermolysis of several methylsilanes have been studied to determine bond dissociation energies and to investigate the reactions of silicon centred radicals. Until recently, the complex mechanistic behaviour revealed by these studies has prevented the establishment of mutually consistent reaction and bond energy schemes. The thermolysis of hexamethyldisilane (HMDS) has been extensively studied¹⁻⁶ under widely differing conditions. In a static system with mass spectrometric analysis of reaction products, kinetic data were obtained and interpreted as relating to a radical non chain mechanism, so that the observed Arrhenius parameters could be identified with those for the initial rupture of the silicon-silicon bond¹, reaction (1).



$$\log_{10}(k_1/\text{s}^{-1}) = 13.5 - 282 \text{ kJ mol}^{-1}/2.303 \text{ RT}$$

This value of 282 kJ mol⁻¹ for the silicon-silicon bond dissociation energy, in conjunction with electron impact data⁶, led to values for the silicon-methyl and silicon-hydrogen bond dissociation energies of 318 and 339 kJ mol⁻¹ respectively, all of which seemed sensible at the time.

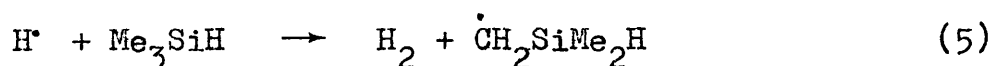
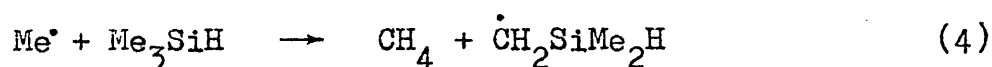
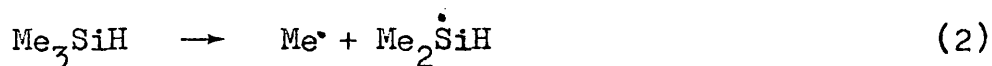
Davidson and Lambert⁸ then investigated the thermolysis of trimethylsilane (TMS) in order to obtain experimental values for the silicon-methyl and silicon-hydrogen bond dissociation energies. In a stirred-flow system between 943K and 1031K they found that the products were mainly methane and hydrogen, with

smaller quantities of 1,1,3,3-tetramethyl-1,3-disilacyclobutane, 1,1,3-trimethyl-1,3-disilacyclobutane, 1,3-dimethyl-1,3-disilacyclobutane, the disilanes $\text{Si}_2\text{H}_m\text{Me}_{(6-m)}$ where $m=0,1,2$, and the disilamethylenes $\text{CH}_2\text{Si}_2\text{H}_n\text{Me}_{(6-n)}$ where $n=1,2$. The rate constants for the formation of methane and hydrogen were given by

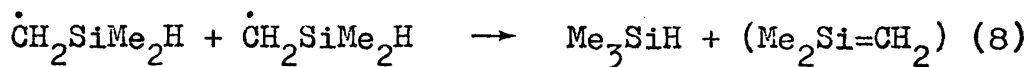
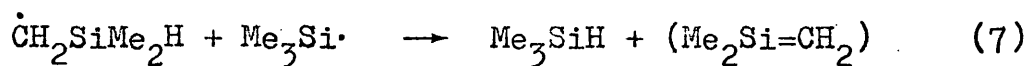
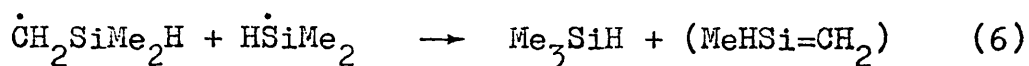
$$\log_{10}(k/s^{-1}) = 15.9 - 320 \text{ kJ mol}^{-1}/2.303 \text{ RT}$$

$$\log_{10}(k/s^{-1}) = 15.6 - 336 \text{ kJ mol}^{-1}/2.303 \text{ RT}$$

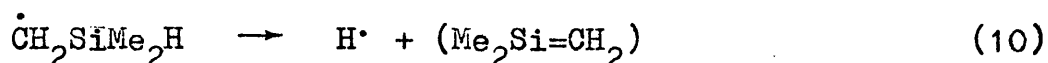
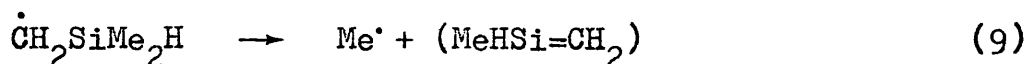
respectively. In view of the close agreement between these activation energies and the values of the silicon-methyl and silicon-hydrogen bond dissociation energies obtained as described above, it was concluded that the thermolysis proceeded by a non-chain sequence, reactions (2)-(5), in which the formation of methane and hydrogen were rate determined by reactions (2) and (3).



The higher silanes in the products resulted from combination of the radicals produced in reactions (2)-(5). The formation of the three disilacyclobutanes implies the prior formation of the double bonded intermediates⁹, $(\text{Me}_2\text{Si}=\text{CH}_2)$ and $(\text{MeHSi}=\text{CH}_2)$. As the reaction was assumed to be non-chain it was proposed that these were formed in radical disproportionation reactions, (6)-(8),



and not in the radical dissociation reactions, (9)-(10).

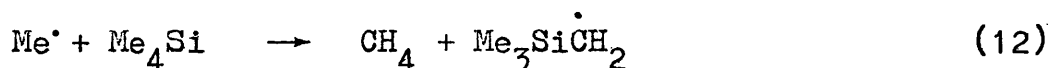


The situation was thus reasonably consistent, the only anomalous feature being the A factor for the silicon-silicon bond rupture in HMDS which was very low for a unimolecular bond fission¹⁰, and in conflict with values obtained from rotating sector experiments¹¹⁻¹².

Further difficulties arose when Gowenlock et al.¹³ studied the thermolysis of tetramethylsilane (4MS) in a linear flow system between 810K and 980K. Ten products were detected, those formed in high yield being methane, trimethylsilane, and 1,1,3,3-tetramethyl-1,3-disilacyclobutane (TMDS). Arrhenius parameters for the formation of methane were given by:

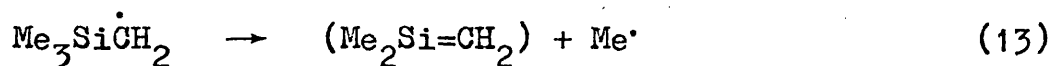
$$\log_{10}(k/s^{-1}) = 14.3 - 282.8 \text{ kJ mol}^{-1}/2.303 \text{ RT}$$

From the thermolysis of HMDS¹ and 3MS⁸ it would be expected that methane should be formed in a non-chain process, reactions (11)-(12).



However, as the activation energy is undoubtedly lower than

D(Me₃Si-Me), it appears that methane is formed in a chain reaction, whilst the production of TMDS indicated that this chain also produced the double bonded intermediate (Me₂Si=CH₂). This is strong evidence for the occurrence of reaction (13) as a chain propagation step.



Thus, if the thermolysis of TMS involves a chain reaction propagated by reaction (13), it would seem likely that a similar mechanism should apply in the cases of HMDS and ZMS. This in turn would imply that the bond dissociation energies for the initial steps in these thermolysis were higher than was previously thought, and that the Arrhenius parameters measured in previous studies related not the initial dissociation steps, but to chain or other processes.

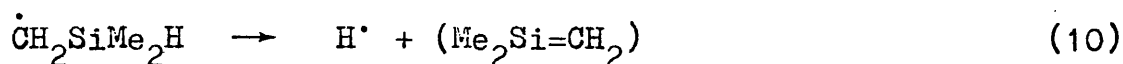
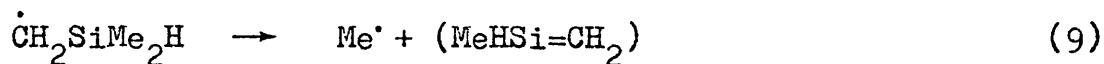
In view of this Davidson and Howard^{14,15}, reinvestigated the thermolysis of HMDS. In a very detailed study, conducted in a stirred-flow system between 770K and 872K, they measured the Arrhenius parameters for the formation of all products, both in presence and absence of a chain inhibitor. They were able to advance a radical chain mechanism that satisfactorily explained all their results and those of previous studies. The details of this mechanism are discussed in Chapter 6 when it is subjected to a computer simulation using the methods described in Chapter 4. In the presence of a chain inhibitor the Arrhenius parameters for the silicon-silicon bond rupture can be deduced from the rate of formation of trimethylsilane given by:

$$\log_{10}(k/\text{s}^{-1}) = 17.2 \pm 336.6 \text{ kJ mol}^{-1}/2.303 \text{ RT}$$

The A factor is now of the correct magnitude, whilst the

activation energy can be identified with $D(\text{Me}_3\text{Si-SiMe}_3)$, now close to the value of $D(\text{H}_3\text{Si-SiH}_3)^{16}$ which seems reasonable. Using this value and electron impact results¹⁷, $D(\text{Me}_3\text{Si-H})$ can be calculated as 368 kJ mol^{-1} , in good agreement with a direct determination from the rate of iodination of 3MS by Walsh and Wells^{18,19} of $376 \pm 11 \text{ kJ mol}^{-1}$.

This higher value for $D(\text{Me}_3\text{Si-H})$ clearly indicated that the activation energy for the production of hydrogen, found by Davidson and Lambert⁸ in thermolysis of 3MS, related to a chain reaction and not to the initial rupture of the silicon-hydrogen bond. Similarly, the activation energy for the production of methane in this case must relate to a chain process, and $D(\text{Me}_2\text{HSiMe})$ must be considerably greater than the activation energy of 320 kJ mol^{-1} . It can be calculated as greater than 350 kJ mol^{-1} ¹⁵ and a recent value based on electron impact data²⁰ is $355 \pm 17 \text{ kJ mol}^{-1}$. Reactions (9)-(10) now seem reasonable as chain propagation steps and the radical disproportionation reactions (6)-(8) now appear much less likely to occur.



A detailed mechanism for the thermolysis of 3MS is suggested in Chapter 6, it is subjected to computer analysis and the results compared with the experimental values of Davidson and Lambert⁸.

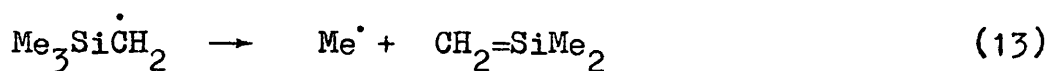
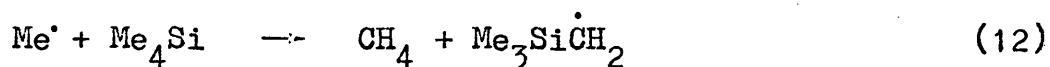
It was then decided that a detailed study of the thermolysis of tetramethylsilane should be undertaken in order to elucidate the mechanism of the chain reaction found by Gowenlock et al¹³, to account for the different Arrhenius parameters for the formation of methane from 4MS and from 3MS, and in

particular to determine the silicon-methyl bond dissociation energy in 4MS.

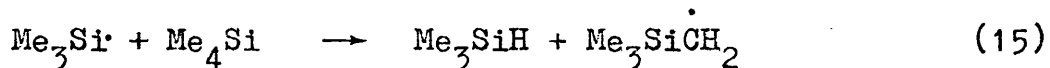
The initial step in the reaction mechanism was almost certain to be reaction (14)



Methane, it was known was formed in a chain process; reactions (12) and (13) being a reasonable choice for the propagation steps,



However it was thought that trimethylsilyl radicals produced in reaction (14) would participate in a non-chain sequence forming 3MS by reaction (15).



If the $\text{Me}_3\dot{\text{Si}}\text{CH}_2$ radical only undergoes decomposition by reaction (13) or termination reactions to form stable products the Arrhenius parameters for the formation of 3MS could be identified with reaction (14), the initial rupture of the silicon-methyl bond. The results of this study are described in Chapter 5 and discussed in conjunction with the mechanisms for the thermolysis of HMDS and 3MS in Chapter 6.

1.2 Computer Modelling

The thermolysis of $\text{Me}_6\text{Si}_2^{15}$ was found to be a short chain reaction, involving several radicals and other intermediates, which cannot be analysed by conventional steady-state methods without drastic, and possibly fallacious, simplification. Similar mechanisms are likely to operate in the thermolysis of 3MS and 4MS, and it is therefore necessary to develop a satisfactory method for the analysis of kinetic schemes of this type. By means of a recent computer program written by Gear²¹, a complete numerical solution of a set of differential equations, corresponding to any given mechanism, can be calculated. This has facilitated the comparison of complex reaction schemes with experimental results in cases which would otherwise be insoluble. The use of the computer program for the solution of systems of ~~of~~ kinetic differential equations is discussed in Chapter 4, and its application to the thermolysis of HMDS, 3MS and 4MS are discussed in Chapter 6.

1.3 The Experimental Method

For the experimental work on 4MS a pulsed stirred flow system²² was used as in the study of HMDS by Davidson and Howard¹⁵. Prior to this work the accuracy of the method was checked by inert tracer methods^{23,24}, and the investigation of a well known reaction²⁵, the thermal isomerisation of cyclopropane. The results of these experiments, which demonstrates the validity and considerable advantages of this method, are given in Chapter 5 with the results of the study on 4MS. The theory underlying the method is summarised in Chapter 3.

CHAPTER TWO

APPARATUS AND EXPERIMENTAL PROCEDURE

APPARATUS AND EXPERIMENTAL PROCEDURE

All the experimental results presented in Chapter 5 were obtained from a novel type of stirred-flow system, in which a pulse of reactant vapour was injected into a carrier gas stream, carried into a stirred flow reactor where it was partially converted into products, and then directly into a gas chromatograph. The apparatus is described in two sections, the flow system and the sampling system which are connected by the sampling valve. The experimental procedure and analysis of data are then discussed. Finally, experiments are described which check the validity of the assumptions necessary for the derivation of the equations governing reaction in this system, as presented in Chapter 3.

2.1 The Flow System

The flow system is shown diagrammatically in Fig. 2.1. Pure nitrogen gas at a controlled pressure and flow rate was passed, in turn, through the sampling valve, reaction vessel, trap, G.L.C. column, and gas density detector. A pulse of reactant vapour, injected into the gas stream using the sampling valve, was carried into the vessel where it is partially converted to products. The products and undecomposed reactant flowed out of the reactor continuously until it was "empty", i.e., contained nothing but carrier gas, and were collected in the trap. The trap was then warmed and the compounds flowed through the column to be individually recorded by the detector.

2.1.1 The Reaction Vessel (Fig. 2.2, 2.3)

The reaction vessels were of the stirred-flow type designed to achieve perfect mixing within the reactor, thus ensuring that the concentration of any species is spatially uniform. The fused quartz vessels were based on the design of Mulcahy and Williams²⁶, developed from the combustion apparatus of Langwell and Weiss²⁷. They were spherical with narrow inlet and outlet pipes, the gas entered radially from a small, central, perforated sphere and flowed out tangentially.

Two different sizes of reactor were used. The reaction space was taken to be the volume of bulb less the volume of the inlet pipe where no reaction is assumed to occur. This is a reasonable assumption since the pulse of reactant vapour spends an extremely short time in the inlet tube, similarly very little

Key to FIG. 2.1

- | | |
|--|---|
| a) Pressure controller | h) Stirred flow reaction vessel |
| b) Molecular sieve column | j) Trap |
| c) Rotameter | k) Diaphragm tap Fig. 2.7 |
| d) 'Oxy' trap | l) G.L.C. system Fig. 2.6 |
| e) To sampling vacuum line,
Fig. 2.10 | m) Two-way greased tap |
| f) To vacuum pumps
Fig. 2.10 | n) Soap bubble flowmeter |
| g) Sampling valve | o) Vent to atmosphere through
glass wool |
| | p) Furnace |

FIG. 2.1 The Flow System

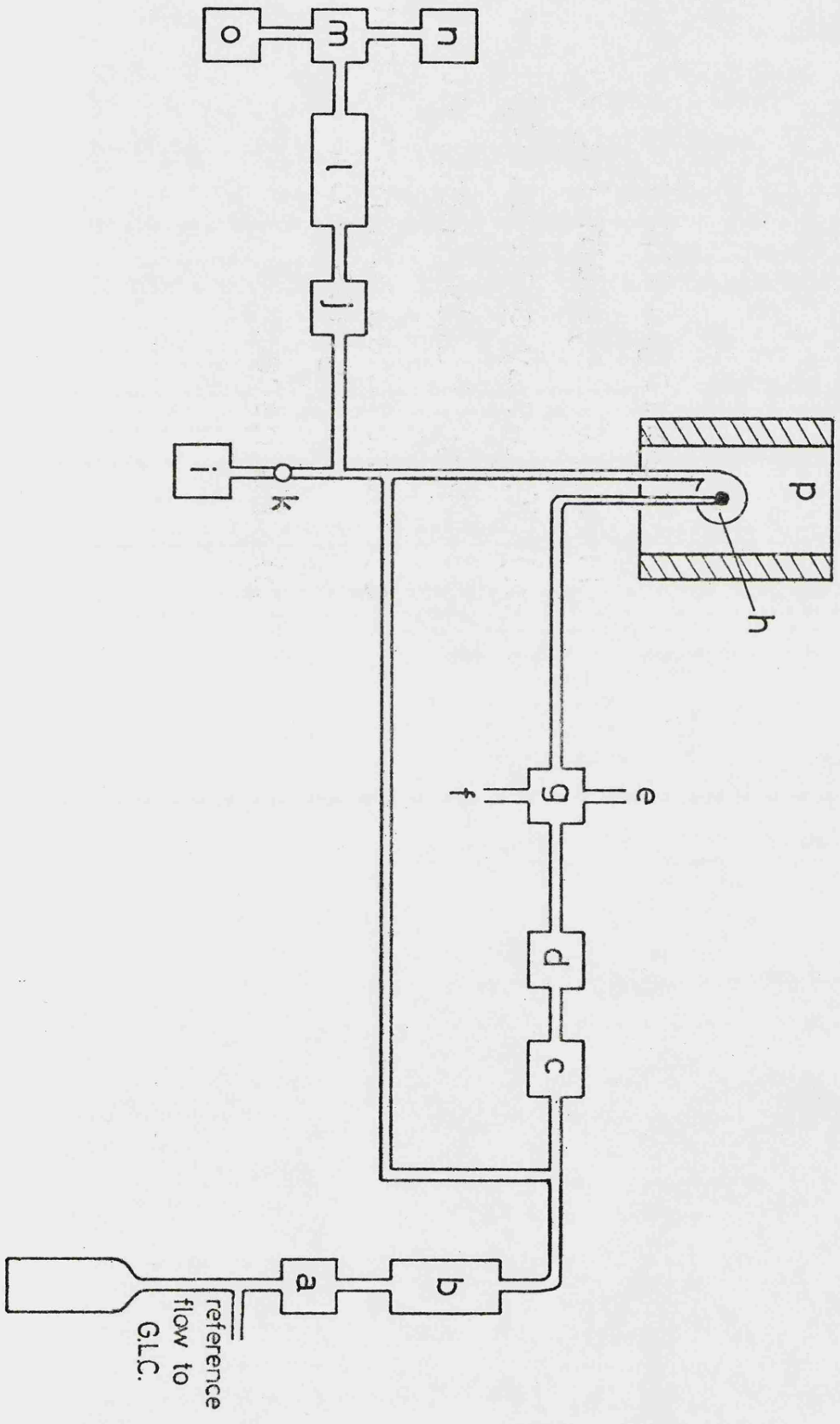


FIG. 2.2 Photograph of Reaction Vessels

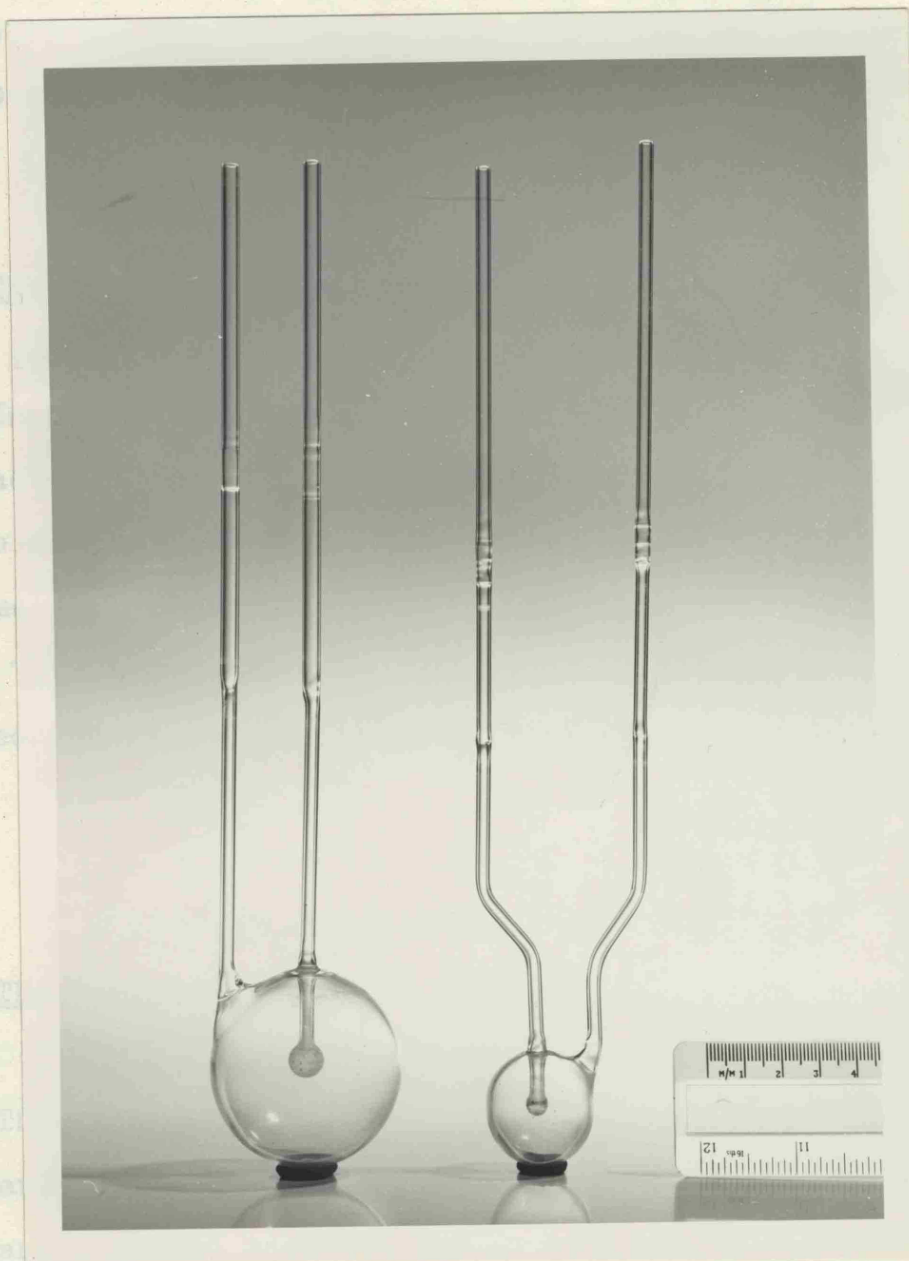
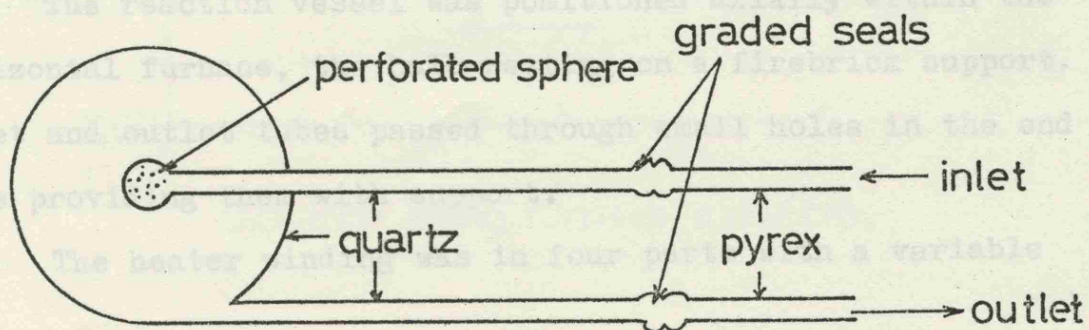


FIG 2.3 Diagram of a Reaction Vessel



reaction occurs in the outlet tube as the gases rapidly cool as they leave the heated area. The volumes of the reactors used were 10.4 cm^3 , 11.7 cm^3 , 51.6 cm^3 and 60.2 cm^3 .

2.1.2 The Packed Reaction Vessel

In order to investigate the effect of surface reactions one reactor was used packed with quartz wool, to increase the surface to volume ratio. This vessel was 5 cm in diameter, had a volume of 55.1 cm^3 and contained 0.7g of fine quartz wool, radius $7.5 \times 10^{-4} \text{ cm}$. The surface to volume ratio of the unpacked vessel was 1.2 cm^{-1} and that of the packed vessel 12.2 cm^{-1} .

2.1.3 The Furnace

The furnace consisted of a stainless steel tube (8 cm in diameter, 25 cm in length) wrapped with a thin layer of asbestos board and a graded nichrome heater winding. This was covered with a second layer of asbestos board and soft asbestos pipe lagging 5 cm thick. The ends of the furnace were syndanyo plugs 1 cm thick which were attached to syndanyo plates used to support the furnace.

The reaction vessel was positioned axially within the horizontal furnace, the bulb resting on a firebrick support. The inlet and outlet tubes passed through small holes in the end wall thus providing them with support.

The heater winding was in four parts with a variable

FIG. 2.4 Furnace Wiring Diagram.

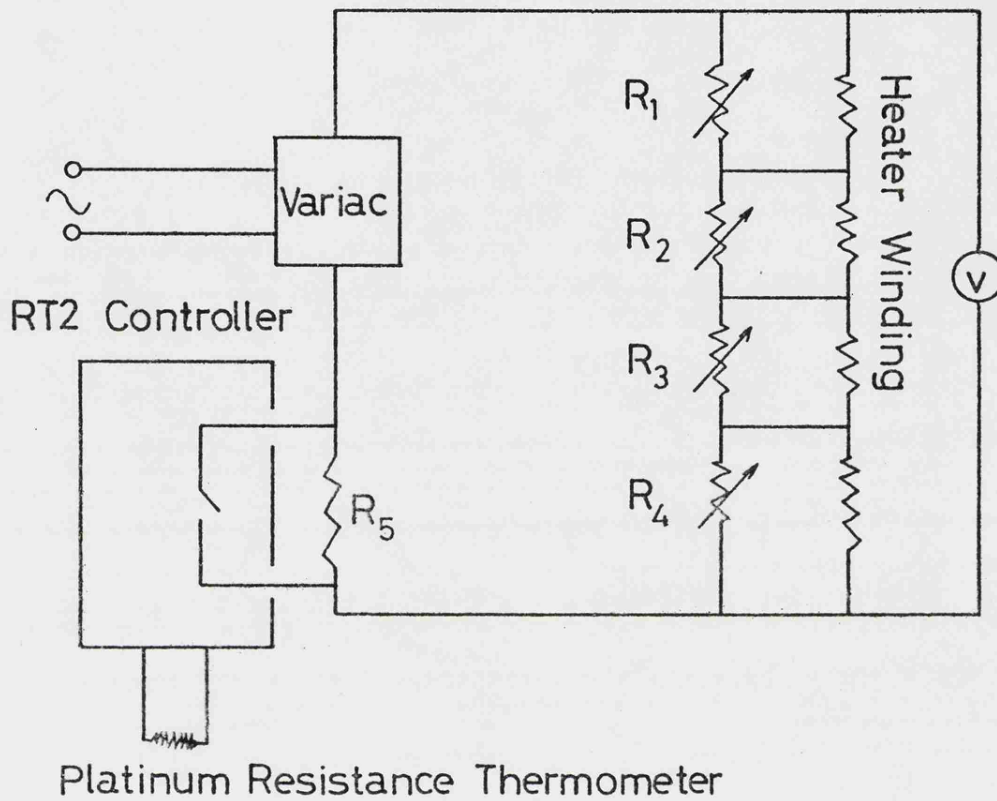
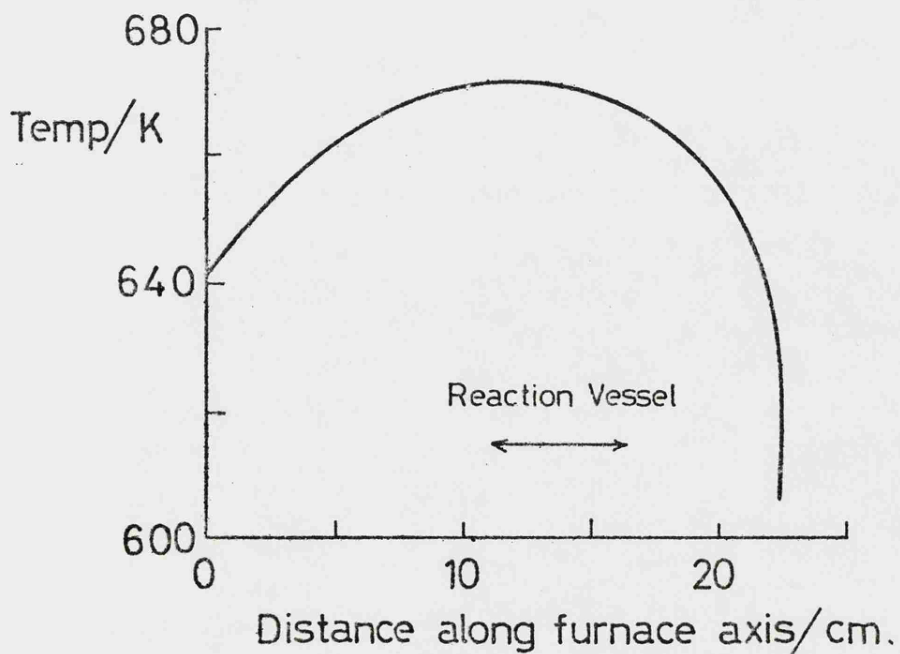


FIG. 2.5 Furnace Temperature Profile



resistance in parallel with each (Fig. 2.4). The values of these resistances (R1 - R4) were adjusted to achieve a fairly constant temperature along the furnace length. A temperature profile is given in Fig. 2.5. Power input was adjusted using a 'variac' variable transformer. Temperature control was achieved by switching the resistance R5 in and out of the circuit. This was done using a Sunvic RT2 controller which utilised a platinum resistance thermometer, situated next to the reaction vessel, as its sensing element.

The reactor temperature was measured using a platinum/platinum-rhodium thermocouple situated in a quartz pocket adjacent to the vessel.

2.1.4 Control and Measurement of the Flow Rate of Carrier Gas

(Fig. 2.1)

For a given vessel the reaction time is determined by the flow rate of carrier gas which must, therefore, be controlled at a constant measurable value. This was achieved by means of a B.O.C. pressure controller (a) fitted to the nitrogen cylinder, and a sensitive flow controller (a) ('Flowstat Major' manufactured by G.A. Platon, Croydon). The carrier gas emerged from the system at the exit of the gas density detector mixed with the chromatographic reference. The flow rate was measured using a 50 cm³ soap bubble flow meter with the reference gas stream switched off, subsequent measurement of the total flow rate gave the reference flow by difference. The temperature and pressure at which the measurements were made was noted so that the flow rate at the reactor exit could be calculated from a knowledge of the temperature and pressure there (see Chapter 3).

The pressure at the reactor exit was measured with a mercury manometer (i).

The flow of carrier gas was found to be sensitive to the temperature of the trap (j), thus, all measurements were made with the trap at the temperature used during the 'reaction' stage of the experiment (see Section 2.1.7).

2.1.5 Purification of Carrier Gas (Fig. 2.1)

Previous studies on the thermal decomposition of organo-silicon compounds have been found to be extremely susceptible to traces of oxygen and water, which were thought to enhance surface reactions^{28,29,30}. Therefore, care was taken to remove any trace of these impurities from the carrier gas, which was B.O.C. oxygen free nitrogen. The pressure regulator (a) was of a special type, fitted with a non-permeable stainless steel diaphragm (B.O.C. model 19 - for special gases), to remove the slight possibility of atmospheric oxygen permeating into the gas stream. Before reaching the reaction vessel, the gas was passed through a cylindrical column (2.5 cm O.D. and 92 cm in length) packed with dehydrated molecular sieve, to remove traces of water, and an 'oxy-trap' (Alltech Associates) to remove traces of oxygen. The 'oxy-trap' was regenerated by reduction with hydrogen and the molecular sieve dehydrated at regular intervals.

2.1.6 The Sampling Valve (Fig. 2.1 and Fig. 2.6)

The flow system and the sampling system were connected by a stainless steel rotary valve, based on the design of Pratt and Purnell³¹. It consisted of a central key fitted with six 'O' rings, of which four were sloping, and an outer barrel containing six parts. Various parts could be interconnected by rotation of the central key. Parts 3 and 4 were connected externally with a piece of stainless steel tubing to form a 'sample loop'. Two such loops were used, with volumes 2.6 cm^3 and 5 cm^3 , to provide an increased range of initial concentrations of reactant. By operation of the valve the 'sample loop' could be evacuated, filled with reactant vapour, or flushed out with carrier gas.

2.1.7 The Gas Chromatograph and Trap

When a pulse of reactant enters the reactor, products and undecomposed reactant immediately begin to flow out. It is shown in Chapter 3 that 99% of the pulse will have left the reactor after a time 4.85τ , where τ is the time constant of the reactor. If the products are allowed to flow directly into the gas chromatograph column a product with a retention time less than 5τ will not be quantitatively detected. Products with retention times $\geq 5\tau$ give normal G.L.C. peaks, with slight tailing and loss of resolution if the retention time is $< 10\tau$. This can cause difficulties if the reaction products are of widely differing types as conditions which give retention times $> 5\tau$ for the least retained compound result in unacceptably long

FIG. 2.6 The Sampling Valve

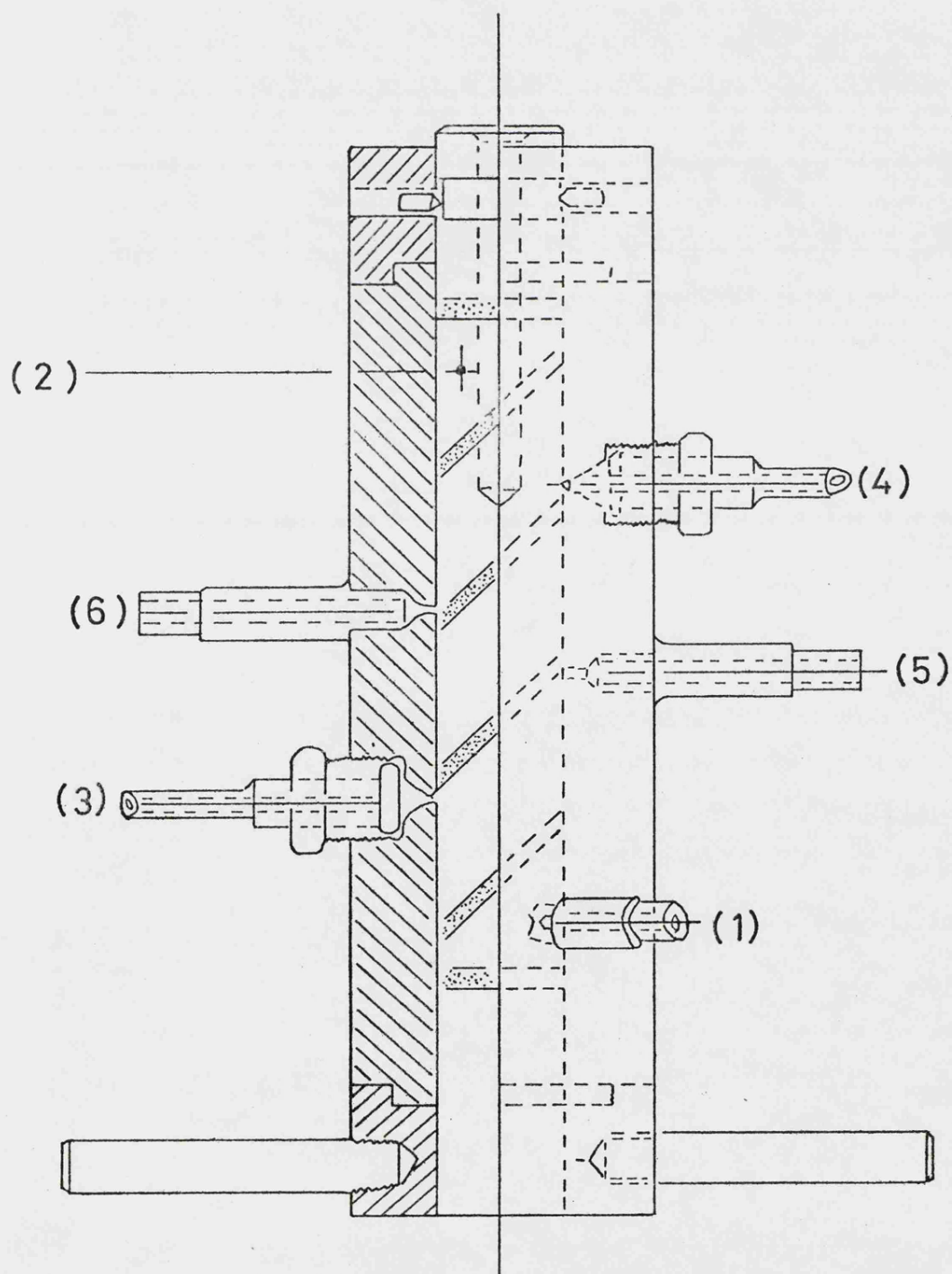
18

(Courtesy of Mr. C. Masters)

Inlet ports connections:-

- (1) To vacuum system. (2) To sampling system.
- (3) & (4) Connected by the sample loop.
- (5) Nitrogen carrier gas in.
- (6) Nitrogen and sample vapour carried to reaction vessel.

 Part of 'O' rings shown thus.



retention times for others. This can be overcome by means of a trap between the reactor and the column.

Two types of trap were used. The first was a coil of stainless steel (0.32 cm O.D. and 2 m in length) (Fig. 2.8) containing a small amount of embacel packing. This was cooled to 90K by immersion in liquid oxygen to trap all the products and undecomposed reactant. By allowing the coil to warm to room temperature the various compounds evaporated off in order of their volatility. This is an adaptation of a technique known as fractional co-distillation³² and enabled compounds of widely differing volatility to be analysed on a single G.L.C. column.

The second trap (Fig. 2.8) was a length of copper tubing (0.64 cm O.D. and 60 cm in length) packed with porapak-Q, a very retentive G.L.C. packing. This was wound with heating tape which could raise its temperature quickly to about 150°C. At room temperature this trap acted similarly to the 'cold trap', the products can then be evaporated off in order of volatility by heating. Both traps were used successfully, the liquid oxygen cooled trap gave improved resolution and overall shorter retention times, whereas the heated column was easier to use.

The gas chromatograph consisted of a single column and a Gow-Mac Gas Density Detector housed in an oven. The column was a copper tube 3m long and 0.64 cm O.D. packed with 10% w/w squalane on embacel (60-100 mesh acid washed).

The oven consisted of an aluminium box (61.0 cm x 25.4 cm x 30.5 cm), divided into two compartments by a wall of marinite, (2.5 cm thick), and encased in marinite. The column was situated in one compartment, and the detector was rigidly mounted in the other, which was filled with sand for increased thermal stability. Chromalox heaters (manufactured by G. Bray and Co., Leeds) were

FIG. 2.7 The G.L.C. System

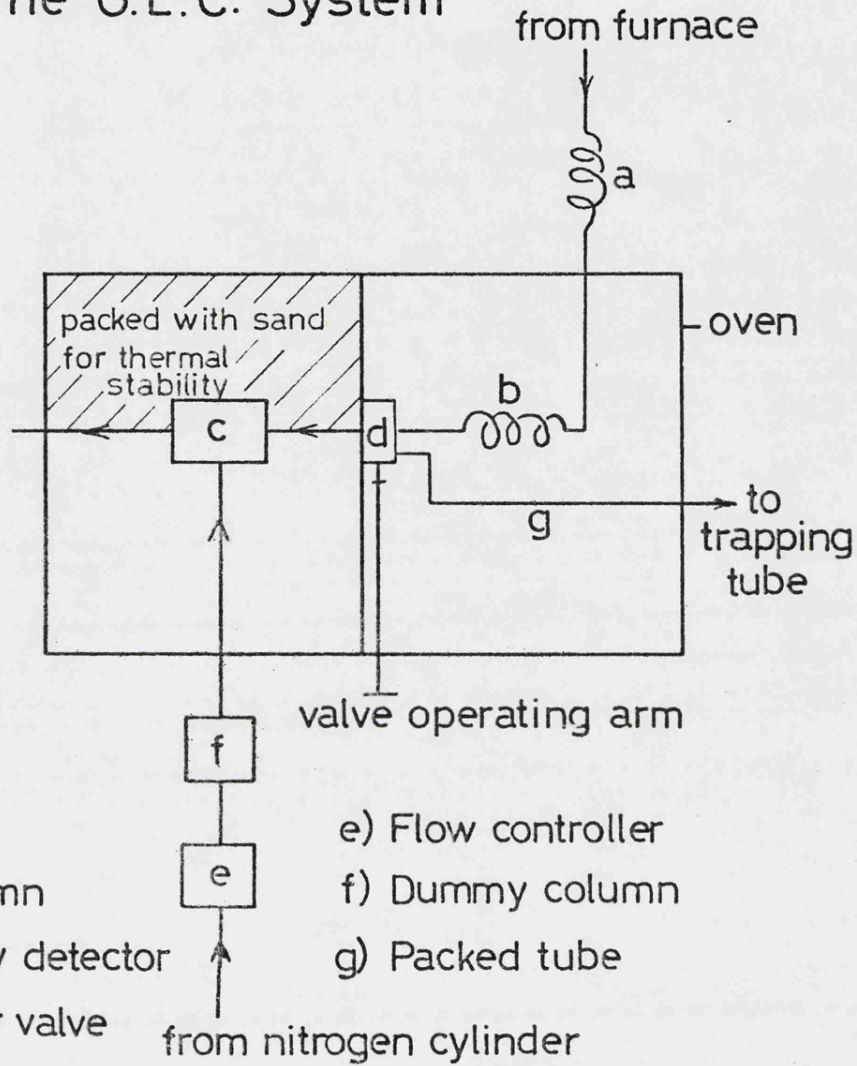
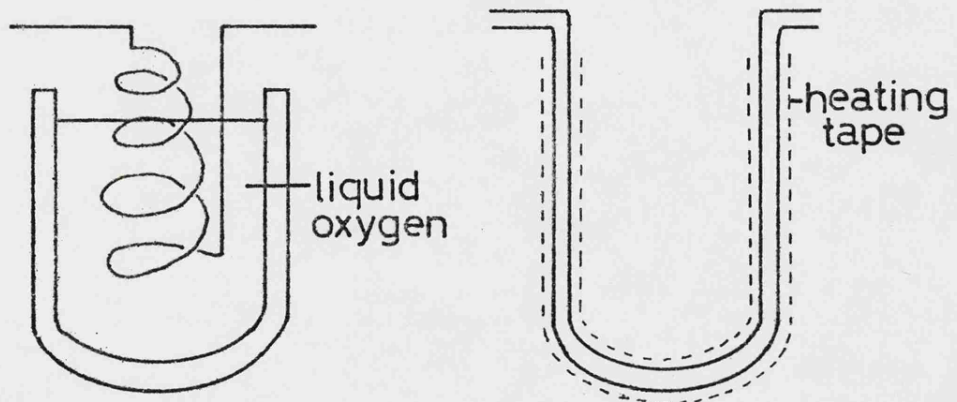


FIG. 2.8 The Traps



0.32 cm. O.D s/steel, 2m. long

0.64 cm. OD copper
60cm long

fitted to the walls, base and lid of each compartment. Power supply was from a 'variac' variable transformer. Temperature control was achieved by using a contact thermometer and relay switch to cut a resistance in and out of series with the heater bank. Both compartments were supplied and controlled separately at 80°C.

2.1.8 The Detector (Fig. 2.7 and Fig. 2.9)

The gas density detector was a Gow-Mac model 373, fitted with thermistor elements (F and G), which were wired in a Wheatstone bridge. Changes in the balance of the bridge were recorded on a Kipp and Zonen Micrograph (BDS-686E) chart recorder.

As the theory behind the operation of gas density detectors has been discussed in detail elsewhere^{33,34,35}, only a brief account will be given here. The flow of nitrogen from the column enters the gas density detector at B and is split into two streams, BCE and BDE, whilst the flow of nitrogen from the reference side enters the gas density detector at A and is split into two streams, ACE and ADE. If the stream of nitrogen from the column is free from any other compound, then the flow of nitrogen on the sides AC and AD will be identical, the elements will be equally cooled and the bridge will be balanced. If the nitrogen flow from the column contains a compound with a molecular weight greater than nitrogen, more of this compound will flow along AD than AC. This results in a greater increase in the pressure of gas at D so reducing the flow rate of AD. In a similar way, the flow rate of AC is increased. If the nitrogen flow contains a compound with a molecular weight less than

nitrogen then the reverse will occur. The change in flow rate will affect the relative temperature of the two elements which, in turn, will cause an imbalance in the bridge.

The peak area produced can be shown^{34,35} to be proportional to the molar quantity of sample present:-

$$A = \frac{N_s (M_s - M_c)}{Y \cdot Z} \quad (2.1)$$

where:- A = Peak area (chart paper)

N_s = Molar quantity of sample

M_s = Molecular Weight of sample

M_c = Molecular Weight of carrier gas

Z is a constant representing the sensitivity of the detector under given operating conditions. This will depend upon the detector dimensions and temperature, nature of carrier gas, reference and column flow rates, and the chart speed and sensitivity of the recorder.

Y is a constant representing the relative sensitivity at any other chart speed and amplification of the recorder.

Transposing equation (2.1) gives:-

$$N_s = \frac{A}{(M_s - M_c)} Y Z \quad (2.2)$$

Hence, for constant operating conditions of the detector, the molar ratio (R_{ij}) of compounds i and j is given by:-

$$R_{ij} = \frac{N_{si}}{N_{sj}} = \frac{\frac{A_i}{(M_{si} - M_c)} \cdot Y_i}{\frac{A_j}{(M_{sj} - M_c)} \cdot Y_j} \quad (2.3)$$

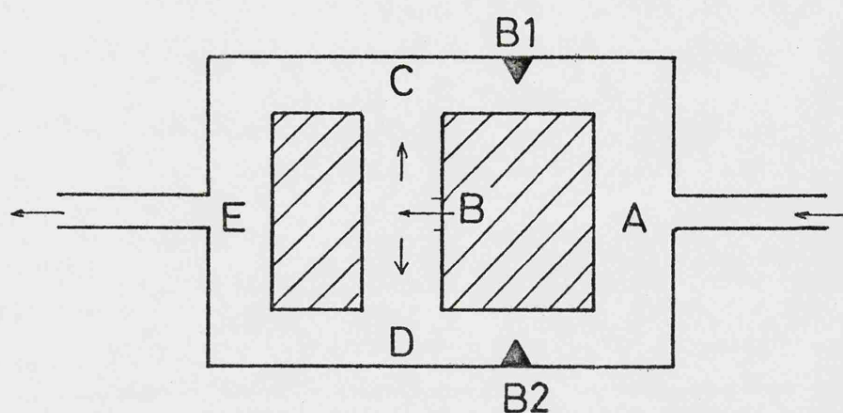
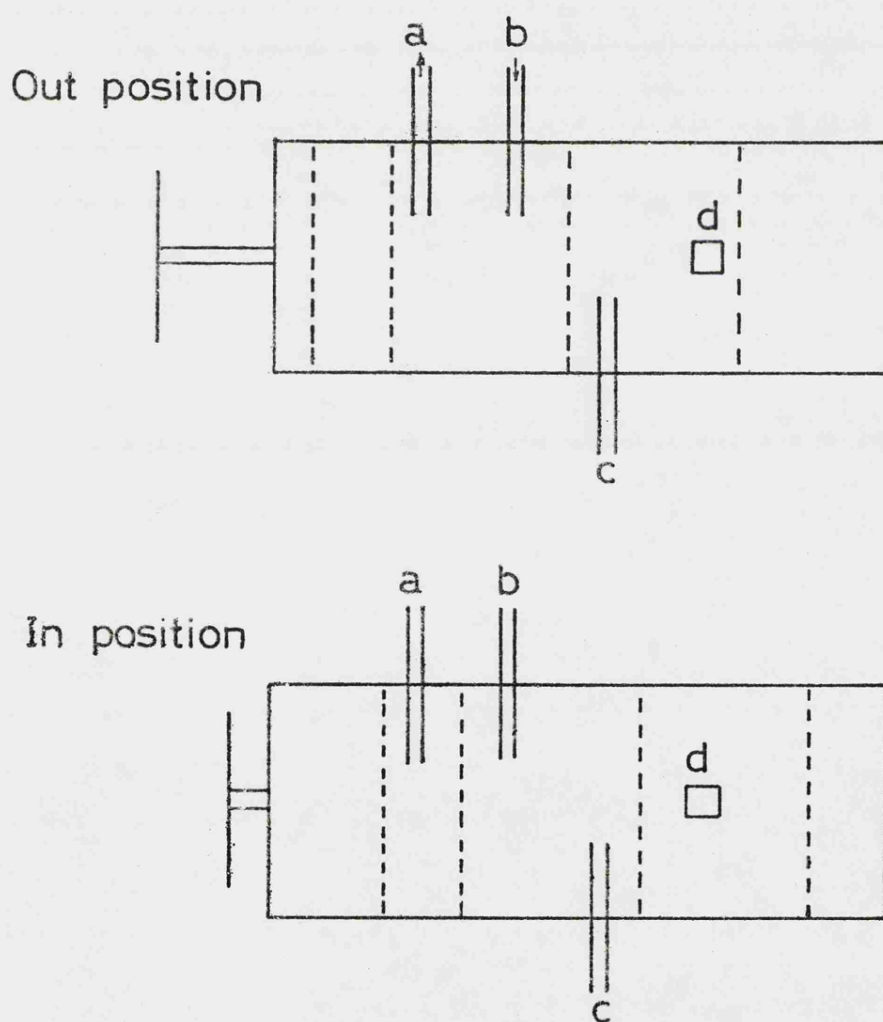


FIG.2.11

The trapping valve



- a Flow of nitrogen to gas density detector
- b Flow of nitrogen from G.L.C. column
- c Exit leading to tube containing amberlite resin cooled in liquid nitrogen
- d Closed

Thus, molar ratios can be obtained directly from peak areas, with a knowledge of molecular weights and recording conditions. In order to determine absolute molar quantities, the detector must be calibrated under normal operating conditions. However, with a gas density detector, this can be done using one suitably volatile known compound (see Appendix 1).

2.1.9 The Trapping Valve (Fig. 2.11)

The trapping valve enabled individual products to be analysed mass spectrometrically, once they have passed through the G.L.C. column. The valve (Mechanism Change-Over Valve, Mechanism Ltd., Croyden.) is mounted inside the oven adjacent to the detector and operated remotely by a metal rod. By movement of the central key various parts can be interconnected. In position (1), the nitrogen stream flows from the G.L.C. column (b) into the gas density detector (a). In position (2) the nitrogen stream flows from the G.L.C. column (b) through the exit (c) down a narrow bore tube packed with embacel to the exterior of the oven. Thus, from a knowledge of its retention time, any given product can be diverted from the detector by operation of this valve.

Outside the oven the stream of nitrogen carrying the product was passed through a small (2 mm I.D. and 25 mm long) quartz tube packed with 80-100 mesh Amberlite XAD-4 resin (Rohm and Haas Ltd.) which had previously been heated under vacuum³⁶. The compound was absorbed onto the resin, and analysed on an A.E.I. MS9 mass spectrometer, by inserting the tube containing the resin directly into the source.

2.2 The Sampling System

A conventional vacuum system was used to evacuate the sampling valve loop and fill it with reactant vapour at a known pressure.

2.2.1 The Pumping System

Pumping was performed by a Genevac single-stage rotary pump and a mercury diffusion pump, which were protected from contamination by a liquid nitrogen cooled trap at 77K.

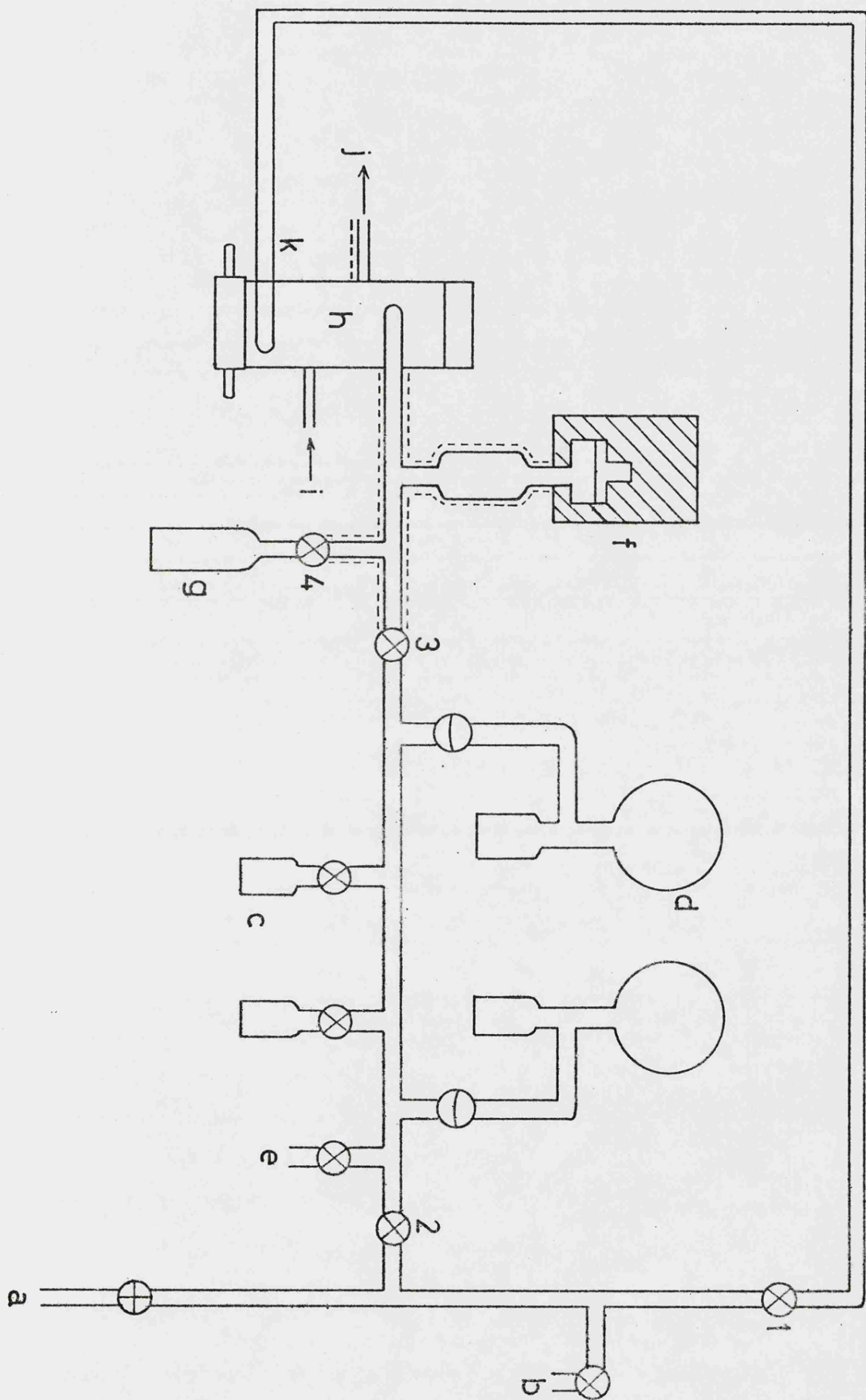
2.2.2 Pressure Measurement

Measurement of the residual gas pressures were made using a Pirani gauge (Genevac type DR 3/3), the system normally being evacuated to 5×10^{-5} torr. Sample vapour pressures were measured using a pressure transducer (Bell and Howell type 4-327-0003), which had previously been calibrated against a mercury manometer (see Appendix 2). In order to obtain consistent results the transducer was thermostatted at 330K. The resistance elements were wired in a wheatstone bridge, imbalance in which was recorded on a chart recorder (Honeywell Brown sensitivity 1 mv F.S.D.).

KEY to FIG. 2.10

- a) To pumps and liquid nitrogen trap
 - b) To manometer
 - c) Storage flasks - liquids
 - d) Storage bulbs - gases
 - e) Sample inlet
 - f) Pressure transducer in thermostat jacket
 - g) Sample reservoir
 - h) Sampling valve (sample loop not shown)
 - i) Nitrogen stream FIG. 2.1
 - j) To reaction vessel FIG. 2.1
 - k) Vacuum line to evacuate sample loop
-
- ⊗ Youngs greaseless stopcock
 - ⊖ Diaphragm tap
 - ⊕ Ground glass greased tap

FIG. 2.10 The Sampling System



2.2.3 Storage of Samples

Because of the problem associated with the presence of trace quantities of oxygen and water all reactant samples were thoroughly degassed and stored over dehydrated molecular sieves. Gases were stored in 5 dm³ bulbs each equipped with a cold finger, and sealed with a Springham diaphragm tap, while liquids were stored in small flasks sealed with Young's greaseless stopcocks. All taps which came in contact with samples were of the greaseless type.

2.3 Experimental Procedure

The experimental procedure is described in three parts:-

- 1) Setting up the apparatus prior to performing experiments.
- 2) Obtaining experimental data.
- 3) Various methods of analysing the data obtained.

2.3.1 Setting Up

Measurements were made at the start of each day, and subsequently if necessary, to determine the flow rate of carrier gas through the system with the trap at operating (trapping) temperature. The flow meter reading was also noted as a convenient visual check on consistency. When allowance was made for varying atmospheric temperature and pressure, the flow rates were found not to vary significantly over periods of several weeks.

2.3.2 Obtaining Experimental Data

The collection of experimental data can best be illustrated by describing a 'typical run'.

The following procedure was followed (Fig. 2.10):-

- (i) Taps 1, 2, 3 and 4 were opened and the system evacuated through a.
- (ii) Tap 2 was shut and reactant vapour was distilled from the storage bulbs, c, to the sample reservoir, g.
- (iii) Tap 3 was shut and the required pressure of reactant was

evaporated into the sampling line. Tap 4 was then shut.

- (iv) The trap was prepared at its 'trapping' temperature. (see Section 2.1.7)
- (v) The sampling valve was rotated to 'sample', whereupon reactant vapour entered the sampling loop.
- (vi) The sampling valve was rotated to 'inject', and the reactant was flushed into the vessel.
- (vii) The products and undecomposed reactant were flushed from the vessel and accumulated in the trap.
- (viii) After a time appropriate for the collection of all products (about 5τ) the trap was warmed and the mixture evaporated off, was resolved by the G.L.C. column, and its components were detected and recorded on the chart recorder. The sensitivity of the recorder was adjusted as appropriate to suit each peak.
- (ix) The peaks were analysed to determine their area as described in Section 2.3.3. A typical chromatogram is shown in Fig. 2.12 and some typical chromatographic data are listed in Table 2.1.

2.3.3 Analysis of Data

Two methods were used:-

- a) Peak Weighing.
- b) Data Logging and Numerical Integration.

FIG. 2.12 A typical chromatogram

Time axis shortened between peaks. For retention times see Table 2.1.

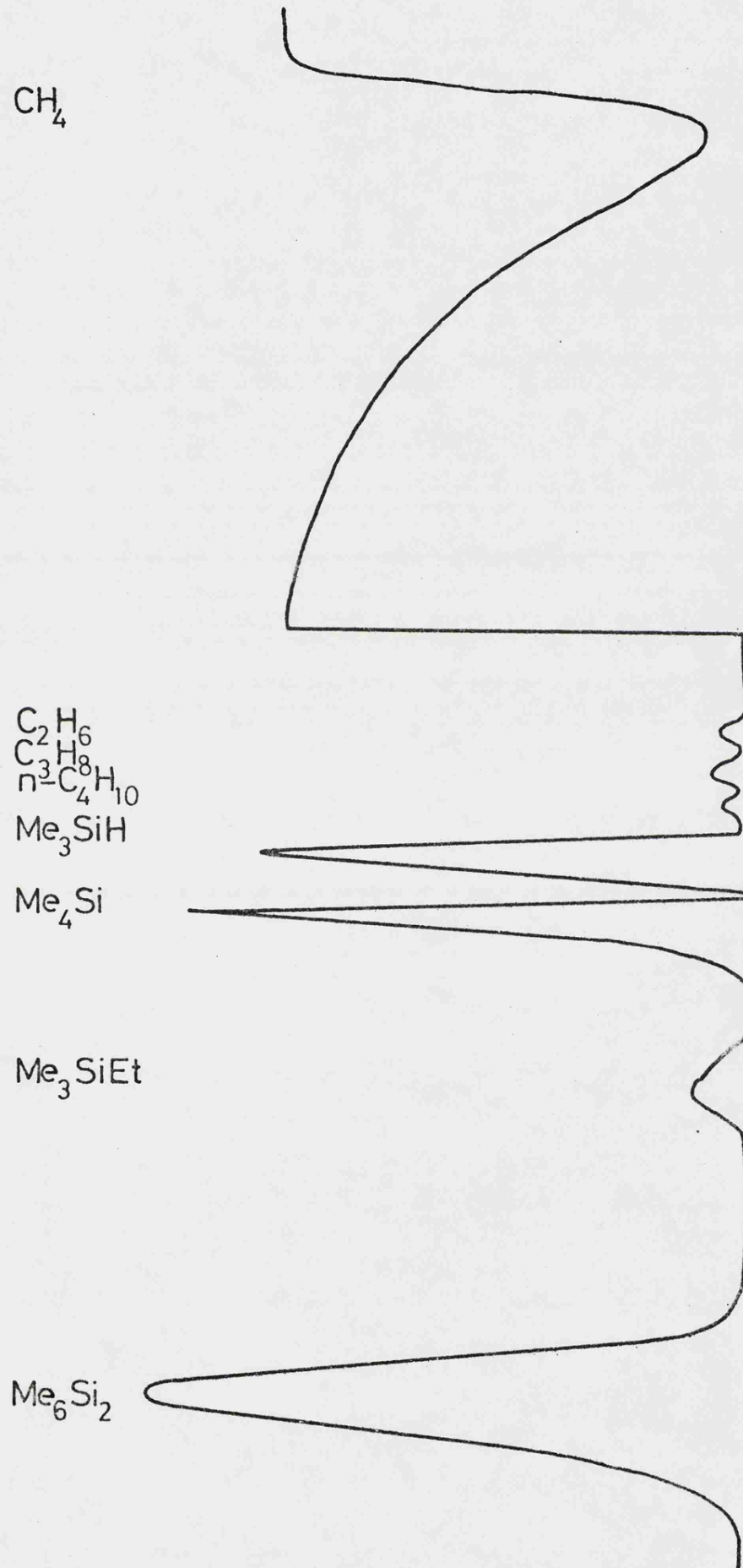


Table 2.1 Some Typical Chromatographic Data

Nitrogen Flow; Sample Side	1.22 cm ³ s ⁻¹
Nitrogen Flow; Reference Side	0.76 cm ³ s ⁻¹
G.L.C. column temperature	80°C
G.L.C. detector temperature	80°C

Retention Time and Sensitivities of Various Products

Compound	Retention time/minutes	Molecular Weight factor
CH ₄	0	12.09
C ₂ H ₆	6.5	2
C ₃ H ₈	7.5	16
n-C ₄ H ₁₀	8	30
Me ₃ SiH	9	46
Me ₄ Si	10	60.19
Me ₃ SiEt	15	74
Me ₆ Si ₂	24	118
$\begin{array}{c} \text{Me}_2\text{Si} \begin{array}{l} \diagup \text{CH}_2 \diagdown \\ \diagdown \text{CH}_2 \diagup \end{array} \text{SiMe}_2 \end{array}$	50	116
Me ₃ SiCH ₂ SiMe ₃	64	132

2.3.3a Peak Weighing

The chromatograms were photostatted and the peaks produced cut out and weighed. The paper weight was found to be constant to within $\pm 1.5\%$, thus these weights were a good representation of the peak areas.

All peak weights were corrected to the same chart speed (10 mm min^{-1}) and sensitivity (2 mV F.S.D.), and divided by their appropriate molecular weight factor (see Section 2.1.8). For a peak recorded at 20 mV F.S.D. and chart speed 5 mm min^{-1} ($Y = 10 \times 2$):-

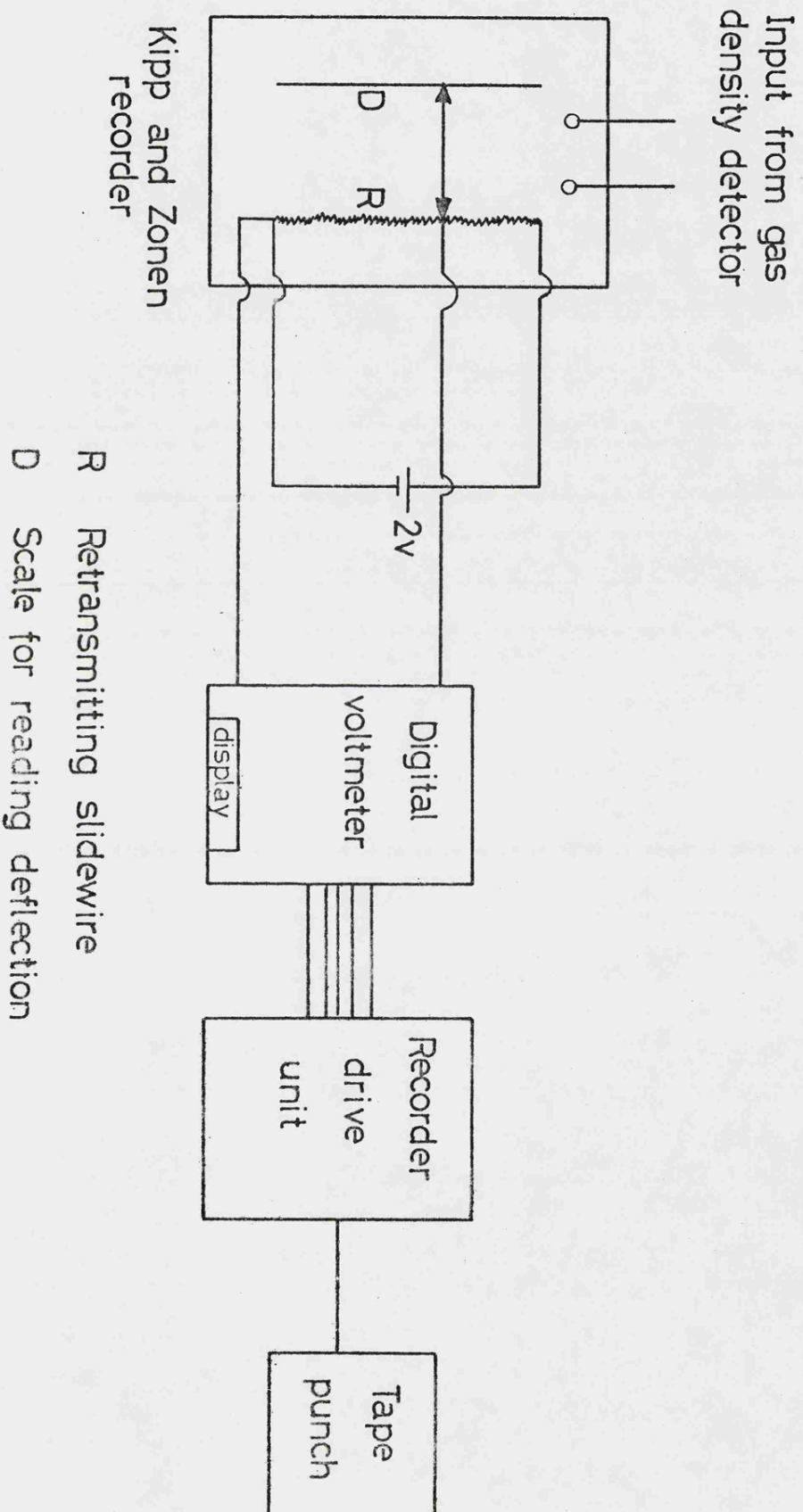
$$\text{'Corrected Weight'} = \frac{\text{Weight}}{(M_s - M_c)} \times (20 \times 2) \quad (2.4)$$

The 'corrected weights' are directly proportional to the molar quantity of each compound, and so can be used for the evaluation of first order rate constants, (see Chapter 3). For rate constants of order other than 1 the absolute molar quantities must be known and the 'corrected weights' must be used with the calibration factor for detector sensitivity (see Appendix 1).

2.3.3b Data Logging and Numerical Integration (Fig. 2.13)

The Kipp and Zonen recorder has a retransmitting slide wire which was used to pass a voltage, proportional to the deflection of the recorder, to a Solatron Schlumberger digital voltmeter. Readings from the digital voltmeter were recorded on paper tape by a Facit tape punch at 1 second intervals. The

FIG. 2.13 Apparatus used for data logging of G.L.C. peaks.



digital voltmeter was switched on just before the appearance of the peak and switched off just after the peak has disappeared, this enables the base line of the peak to be determined. A complete program, compiled in BASIC on a digital P.D.P. 11 computer, performs this calculation from the first and last points on the tape and integrates the remaining values numerically using Simpson's Rule (see Appendix 3). This method was at least as accurate as the peak weighing method. The peak areas so calculated were corrected for recorder sensitivity and molecular weight as were the weighed peaks.

2.4 An Experiment to Test the Validity of the Assumptions of 'Perfect Mixing' and 'Perfect Pulse Behaviour'

It is shown in Chapter 3, that the derivation of usable equations governing behaviour in this system, depends upon the assumptions of 'perfect mixing' and 'perfect pulse behaviour' (see Section 3.2). An experiment was devised to test the validity of these assumptions directly. A good deal of indirect evidence exists to show that the type of reactor used produces perfect mixing. Mulcahy and Williams³⁷, Sullivan and Hauser³⁸, and Lambert^{8,29} have studied known reactions and measured rate constants, independent of the residence time, in good agreement with the accepted values. It is extremely unlikely that the degree of mixing, if not perfect, would be independent of residence time.

However, it was thought desirable to test the assumptions directly using the actual experimental apparatus. In a pulsed system, not operating at steady state, imperfections in mixing or pulse behaviour are manifested as time dependent phenomena. Thus, the apparatus was slightly modified to measure time dependent concentrations at the exit of the reactor.

2.4.1 Modifications to the System (Fig. 2.14 and Fig. 2.15)

A gas chromatographic detector (Gow-Mac, Thermal Conductivity Cell Model 30-5) was mounted as close as possible to the exit of the reactor followed by a needle valve to simulate the effect of the chromatographic column. Pulses of methane were then injected, using the sampling valve, at a furnace temperature

FIG. 2.14 Modification the system for time dependent measurements.

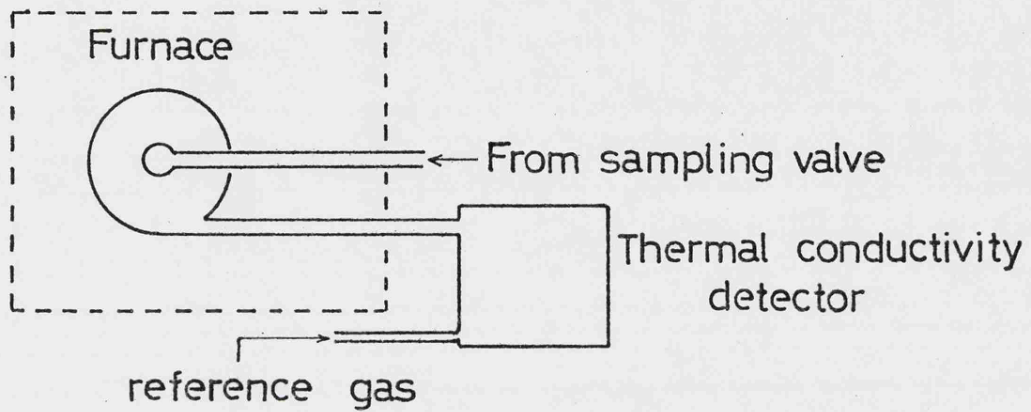
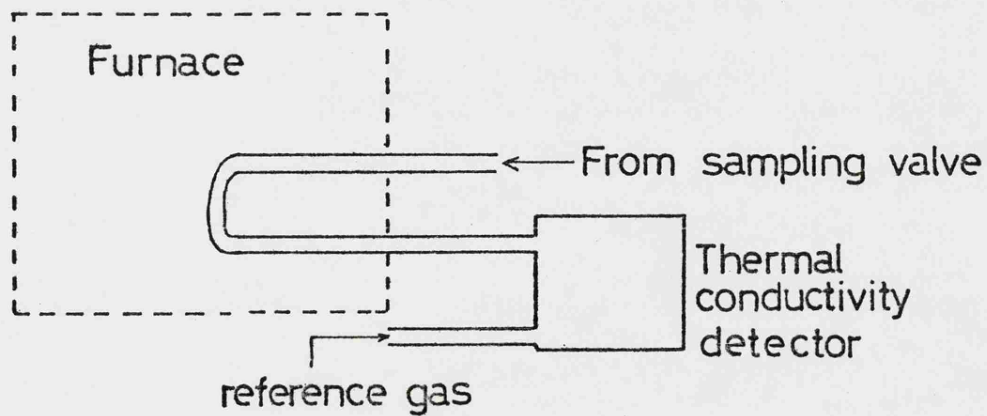


FIG 2.15 System used for time delay measurements.



at which no decomposition occurred. This was done for various sizes of pulse and at various flow rates of carrier gas corresponding to residence times from 20 s to 120 s. The detector response, which was recorded on the Kipp and Zonen chart recorder, was a measure of the concentration of methane at the exit of the reactor, and could be compared with that predicted by the equations of Chapter 3. To do this accurately the time zero of the system must be known. This means that the time the pulse spends in the tube between the valve and the vessel, and the vessel and the detector must be known. This was achieved by removing the reactor, connecting the inlet and outlet tubes directly together, and measuring the time interval between injection of the pulse and its arrival at the detector.

CHAPTER THREE

THE THEORY OF THE

PULSED STIRRED-FLOW TECHNIQUE

THE THEORY OF THE PULSED STIRRED-FLOW TECHNIQUE

In general, two types of flow reactor are used for the study of thermolysis reactions. These are the linear flow reactor and the continuously stirred flow reactor, which are distinguished by the degree of mixing of the reactant. In the stirred flow reactor the reactants, products, and carrier gas if any are considered to be 'perfectly mixed', that is uniformly distributed throughout the reactor^{40,41}. Conversely, in the linear flow reactor no mixing is assumed to take place as the reactants flow along the reactor. In theory this situation cannot be realised as mixing occurs due to radial and axial diffusion of products and reactants, although this may be minimised by careful design^{42,43}. Alternatively this diffusional mixing may be intensified by bulk stirring of the reactants to fulfill the theoretically possible criterion of perfect mixing^{40,44}.

Bulk stirring results in very fast thermal equilibration of reactants when entering, and eliminates temperature gradients and 'dead-space' within the reactor. In the linear flow reactor, on the other hand, all the reactant molecules are assumed to spend the same time in the tube, and reach the reaction temperature immediately on entering. This is an idealised flow situation, and is in many cases not realised in practice. Mulcahy⁴² has shown by heat and mass transfer calculations that these errors can be very large. Thus, a stirred flow reactor offers distinct advantages over a linear flow reactor for the study of thermolysis reactions.

Our novel method of operation offers still further advantages which are summarised at the end of this chapter.

Preceding this the kinetic equations for the system are derived and examined.

3.1 Time-Dependent Response of a Pulsed Stirred-Flow Reactor

In a conventional flow technique, steady state conditions prevail in which reactant continuously flows into the reactor inlet, whilst products and undecomposed reactant continuously flow from the outlet. The steady state conditions in the reactor may be monitored spectroscopically or by sampling, while products may be accumulated for analysis downstream from the reactor^{45,46,47}. In our pulsed system steady state conditions do not exist and thus new equations governing its behaviour must be derived. As will be shown later, time-dependent concentrations are not needed to determine rate constants, but a knowledge of them is necessary to the understanding of behaviour in the system.

3.1.1 Time-Dependent Response of a Non-Reactive Pulse

Consider first the time-dependence of concentration in the reactor resulting solely from the pulsed method of operation, without any chemical reaction. For any material in a reaction system, the general mass balance is⁴⁸:-

$$\text{input} - \text{output} = \text{accumulation within reactor} - \text{generation} \quad (3.1)$$

For the injection of an inert pulse, the derivation of an expression for the time-dependence of concentration in the reactor is simple if the following two conditions are fulfilled:-

(i) "Perfect pulse behaviour": the pulse is of small volume relative to the reactor, entering it and being dispersed through-

out it almost instantaneously.

(ii) "Perfect mixing": the dispersal of the pulse throughout the reactor is spatially uniform.

The mass balance is then:-

$$u[A_i(t)] - u[A_o(t)] = \frac{d}{dt} v[A_o(t)] - 0 \quad (3.2)$$

where u is the volumetric flow rate of carrier gas through the reactor (see Section 3.3.1); $[A_i(t)]$ and $[A_o(t)]$ are the concentrations of the injected compound A at the inlet (i) and outlet (o) of the reactor at any time t ; and v is the volume of the reactor. It is a consequence of perfect mixing that $[A_o(t)]$ is also the concentration of A at any point within the reactor.

From (3.2),

$$[A_i(t)] - [A_o(t)] = \tau \frac{d}{dt} [A_o(t)] \quad (3.3)$$

where $\tau = \frac{u}{v}$, the time constant for the reactor. In a reactor operating at steady state τ is the residence or reaction time⁴⁸. Its significance in the pulsed system will become apparent at the end of this derivation.

Assuming "perfect pulse behaviour" it has been shown by Baldwin, Davidson and Howard⁵⁰ that (3.3) may be solved explicitly by means of a Laplace transform⁵¹. Alternatively the equation may be reduced to an integrable form by setting $[A_i(t)] = 0$ for $t > 0$ and assuming the initial concentration of A in the reactor is $[A_o(0)]$. Both approaches yield

$$[A_o(t)] = [A_o(0)] \exp(-t/\tau) \quad (3.4)$$

or
$$[A_o(t)] = \frac{(A_o)}{v} \exp(-t/\tau) \quad (3.5)$$

where (A_o) = amount of A collected at the exit, in moles. This is an important result as it shows that the rate of loss of any species from the reactor obeys a first order law with a "rate constant" of $1/\tau$.

3.1.2 Time-Dependent Response of a Reactive Pulse Undergoing a First Order Reaction

If A also undergoes a first order reaction $A \rightarrow B$ with rate constant k , the mass balance equation (3.1) becomes:-

$$u[A_i(t)] - u[A_o(t)] = \frac{d}{dt} v[A_o(t)] + k_1 v[A_o(t)]$$

which may be solved⁵⁰ as before to give

$$[A_i(t)] = [A_o(0)] \exp -t(k_1 + 1/\tau) \quad (3.6)$$

or
$$[A_o(t)] = \frac{(A_i)}{v} \exp(-t(k_1 + 1/\tau)) \quad (3.7)$$

where (A_i) is the amount of A injected. Thus

$$(A_i) = (A_o) + (B) \quad (3.8)$$

where (B) = amount of B formed. In this derivation it has been assumed for simplicity that one molecule of B is formed from each molecule of A decomposed. If the stoichiometry differs from this, an appropriate stoichiometric factor must be included in equations (3.6) to (3.8) and all subsequent similar equations.

Similarly the mass balance for B is:

$$u[B_o(t)] = \frac{d}{dt} v[B_o(t)] - k_1 v[A_o(t)] \quad (3.9)$$

Substituting for $[A_o(t)]$ from equation (3.7) and integrating gives:

$$[B_o(t)] = \frac{(A_i)}{v} \exp(-t/\tau) [1 - \exp(-k_1 t)] \quad (3.10)$$

The implications of equations (3.5), (3.7) and (3.10) are shown graphically in figures 3.1 and 3.2 as plots of concentration against time.

FIG. 3.1 Graph of Reactant Concentration within the Reactor against Time.

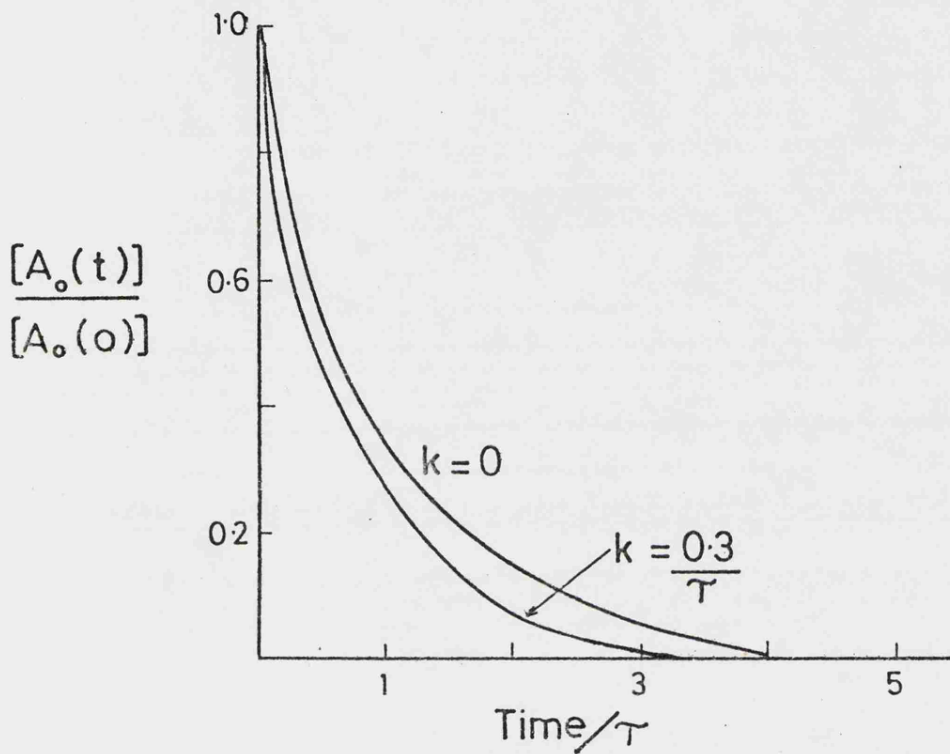
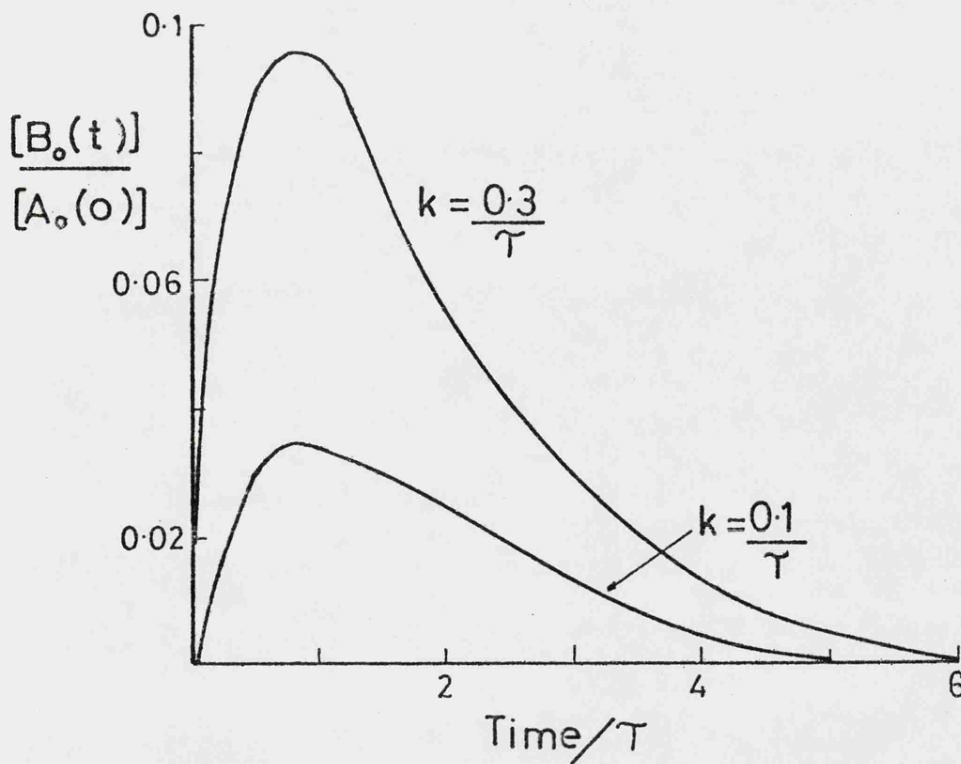


FIG. 3.2 Graph of Product Concentration within the Reactor against Time.



3.2 Derivation of Rate Constants in Terms of Experimentally Accessible Parameters

In a reactive situation, where many different chemical species are leaving the reactor simultaneously, time-dependent concentrations cannot conveniently be measured. The action of the G.L.C. column in resolving the various product species is to "integrate" the concentrations so that the only information readily available is the molar amount of each product formed, and the molar amount of reactant undecomposed. Thus, it is necessary to derive equations relating the rate constants to these measurable quantities.

Again, consider the reaction $A \rightarrow B$, with order n and rate constant k , then an overall mass balance on B is:-

$$\text{amount of B found within reactor} = \text{amount of B measured at outlet} \quad (3.11)$$

Assuming "perfect mixing" this becomes:

$$\int_0^{\infty} k v [A_0(t)]^n dt = (B) \quad (3.12)$$

where (B) = number of moles of B measured at the outlet.

The various solutions of equation (3.12) are considered separately for different values of n .

3.2.1 First Order Reaction

Equation (3.12) may be solved exactly when $n=1$, because the time-dependence of A in a first order reaction obeys the same

mathematical law as the time-dependence of the sweeping-out of A from the reactor, as given by equation (3.5). Thus for $n=1$,

$$\int_0^{\infty} k v [A_0(t)] dt = (B) \quad (3.13)$$

However, the amount of A measured at the outlet,

$$(A_0) = \int_0^{\infty} u [A_0(t)] dt. \quad \text{Substitution in equation (3.13) gives:}$$

$$k = \frac{(B)}{(A_0) \tau} \quad (3.14)$$

This is an exact expression independent of the degree of conversion of A to B, the only necessary condition being that of "perfect mixing". The form of equation (3.14) is a familiar one in kinetics. It shows that the ratio of the rate constants for the two first order processes, k and $1/\tau$, is proportional to the ratio of the products formed in each process, B and A lost from the reactor.

3.2.2 Reactions of Order Other Than One

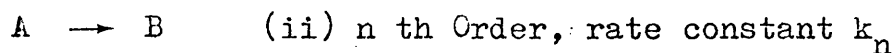
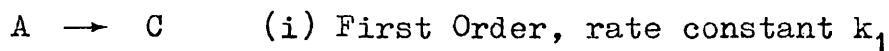
Equation (3.12) can only be solved if the overall time-dependence of A in the reactor is known. When $n \neq 1$ this time-dependence is not amenable to calculation, but the problem can be overcome by arranging the experimental conditions so that the percentage conversion of A to B is small. The change in concentration of A in the reactor due to reaction may then be ignored relative to the change due to sweeping out, and the left hand side of equation (3.12) can be evaluated from the time-dependence of equation (3.5). Hence

$$k = \frac{(B) v^{(n-1)}_n}{(A_0)^n \tau} \quad (3.15)$$

For $n=1$ equation (3.15) reduces to equation (3.14) as would be expected.

3.2.3. Minor Reactions of Order Other Than One Concurrent With a Major First Order Reaction

If the major decomposition route is by a first order reaction, rate constants for minor routes of order other than one can be determined, even at high percentage decomposition, as follows. Consider the reactions



If reaction (i) is predominant, reaction (ii) may be neglected in the mass balance resulting in the time-dependence of A as given by equation (3.7), which when substituted into equation (3.12) and integrated gives

$$(B) = \frac{k_n}{v^{(n-1)}} (A_i)^n \frac{1}{n(k_1 + 1/\tau)} \quad (3.16)$$

But $(A_i) = (A_0) + \text{amount of A converted to C}$
 $= (A_0) + k_1(A_0)\tau$ from equation (3.14)

$$k_n = \frac{(B)v^{(n-1)}_n}{(A_0)^n \tau (1+k_1\tau)^{(n-1)}} \quad (3.17)$$

3.3 Application of Derived Equations in Practice

The preceding equations are simple to use in practice. Orders and rate constants for reactions can be easily calculated from a knowledge of the amount of product formed, the amount of reactant remaining and the time constant for the reaction as described in the following sections.

3.3.1 Calculation of τ

Throughout the preceding derivations it has been assumed that τ was an experimental observable, or more correctly, since $\tau = u/v$, that u could be measured, v being known. The flow rate of carrier gas can only be conveniently measured at the exit of the gas density detector and it is important to realise that the volumetric flow rate here is not the same as that at the reactor exit, u . However, since the mass flow rate must be constant these two volumetric flow rates can be related by the ideal gas law provided the pressure and temperature of the carrier gas at the point of measurement and the exit to the reactor are known. If u_m represents the measured flow rate then:

$$u = u_m \frac{P_A \cdot T}{T_A \cdot (P_A + P)}$$

where P_A = atmospheric pressure

T_A = atmospheric temperature

T = reactor temperature

P = pressure difference between reactor and
atmosphere

3.3.2 Treatment Of Experimental Data

The treatment of experimental data is extremely simple due to the nature of the kinetic equations. Examination of the appropriate equation (3.14, 3.15, 3.17) shows that a plot of $\log(\text{product})$ against $\log(\text{reactant})$ will be a straight line of slope n , where n is the order with respect to the reactant, for the formation of that product. Once the order has been determined the rate constants can be obtained by substitution in the appropriate equation; number 3.14 for first order reactions and either 3.15 or 3.17 for non first order reactions.

3.4 Advantages of the Pulsed Stirred Flow System

The relative merits of flow and static systems for the study of thermolysis reactions are well documented^{52,53}, the principal advantage of flow systems is their ability to produce short reaction times accurately. As discussed previously, a stirred flow system offers significant advantages over a linear flow system in terms of potential accuracy, due to the greater validity of the assumptions used in deriving the kinetic equations. Our pulsed technique embodies all of these advantages over conventional steady state stirred-flow systems in using much simpler equipment, and being far more economical in reactants.

CHAPTER FOUR

COMPUTER MODELLING

COMPUTER MODELLING

Two of the primary aims in a kinetic study are the formulation of a mechanistic model of the reaction process, and the determination of unknown reaction rate constants. From any given model, consisting of a series of elementary reaction steps, a set of simultaneous ordinary differential equations may be derived. One equation may be written for each chemical species in the model, relating the rate of change of concentration of that species to a sum of terms involving the product of rate constants and concentrations of species present. By solving this set of equations either analytically, numerically or by approximation the implications of the model in terms of experimentally observable parameters can be determined.

The various methods for the solution of sets of kinetic differential equations are summarised below. By far the most powerful of these is the complete numerical solution by means of a computer program, using a linear multi-step method. The mathematical background to this method is described and its advantages and limitations discussed.

4.1 Approximate Solutions - The Steady-State Approach

In general, apart from the most simple system of three or four species⁵⁴, analytical solutions of sets of kinetic differential equations are not possible. The classical method of overcoming this problem is the application of the steady-state approximation, in which the concentrations of intermediates in the reaction scheme are assumed to be constant, and therefore their differential rate equations can be reduced to algebraic equations. This approach has been very widely used, particularly in the study of chain reactions, where the intermediates are very reactive and present in small quantities.

In the system of differential equations for a chain reaction equating the derivatives of the intermediate concentrations to zero enables the remaining differential equations to be rearranged into a form suitable for comparison with experiment. Unfortunately, due to the nature of the equations, this can only be done in cases where there is only one, or one predominant, termination step. Systems with several termination steps of similar rates cannot be solved by this method.

Recently, attention has been focused on the validity of the steady-state approximation under various different conditions. This has been done by solving sets of differential equations by an advanced numerical technique (see Section 4.3) and comparing the results with those predicted by a steady-state analysis. Also, since a numerical solution gives the concentration-time profiles of all species, the existence of a steady state in any particular species can be checked directly. The results are difficult to generalise. In some cases,

particularly in relatively simple organic free radical systems, the detailed comparison has verified the existence of a steady state over a limited time regime⁵⁵. Examples have been found⁵⁶ where although a steady state does not appear to exist, the results of a steady state analysis do not conflict greatly with the numerical solutions. In general however, for complex reaction systems with large numbers of intermediates steady-state methods are either not applicable, or are subject to serious doubts as to their accuracy⁵⁷.

4.2 Numerical Solutions

It is useful, at this point, to formulate the problem mathematically before discussing the various methods available for the solution of systems of ordinary differential equations. The system can be written as:-

$$\dot{y} = f(y, t)$$

or, more specifically,

$$\frac{dy_i}{dt} = f_i(y_1(t), \dots, y_n(t), t)$$

where y , \dot{y} , and f are vectors of length N . Here y_1 is the concentration of species 1 and f_i is a function of the concentrations of species in the system involving the rate constants for specific reactions in the system.

Given an initial value of the vector,

$$y(t_0) = y_0,$$

that is the concentration of each species at time t_0 , the required solution is $y(t)$ for $t_0 \leq t \leq T$. All numerical methods proceed by calculating approximate solution values at $t = t_0, t_1, t_2, \dots, T$, where $t_n = t_{n-1} + h$, with same step size h . These fall into two categories;⁵⁸ explicit methods in which the solution y_n is computed explicitly from solution values at previous points, and implicit methods in which y_n is found from an expression involving the unknown $f(y_n)$ as well as previous solution values. Implicit methods therefore also require the numerical solution of a set of generally non-linear equations.

4.2.1 Explicit Methods

Given a computed solution $y_n = y(t_n)$ at time $t = t_n = nh$, where $h =$ step size, an explicit method gives the solution y_{n+1} in terms of previous solutions. For example, the Euler method⁵⁸ is

$$y_{n+1} = y_n + hf(y_n)$$

and the fourth order Runge-Kutta⁵⁸ is

$$y_{n+1} = y_n + \frac{1}{6}(k_0 + 2k_1 + 2k_2 + k_3)$$

where $k_0 = hf(y_n)$

$$k_1 = hf(y_n + \frac{1}{2}k_0)$$

$$k_2 = hf(y_n + \frac{1}{2}k_1)$$

$$k_3 = hf(y_n + \frac{1}{2}k_2)$$

The accuracy of these methods is governed by the size of h , in general the smaller h the more accurate the solutions obtained. Unfortunately with certain sets of differential equations, now referred to as stiff systems⁵⁸, explicit methods generally fail in one of two ways. If a constant step size is used widely oscillating or infinite solutions are often obtained, whereas if a variable step size governed by an accuracy criterion is used, the solution advances so slowly in real time that the computation is not practicable even on very high speed computers. Sets of kinetic differential equations are almost entirely of this type, this is normally ascribed to large differences in rate that exist between fast radical reactions and the relatively slow overall reaction⁵⁹.

One approach to overcoming this problem has been to

incorporate the steady-state hypothesis into a numerical method⁶⁰. Here specific species are considered to be in steady state and the differential equations for these species are reduced to algebraic equations

$$f_i(y, t) = 0$$

where i represents species in steady-state. This eliminates most of the fast processes from the system and enables a solution to be obtained. However Farrow and Edelson⁵⁷, using a more exact numerical method discussed later, have concluded that this procedure can lead to completely spurious solutions and that there is no way to predict a priori when this will happen.

4.2.2 Implicit Methods

Implicit methods express the solution y_{n+1} in terms of previous solutions and the function value $f(y_{n+1})$. For instance the trapezium rule is

$$y_{n+1} = y_n + h [f(y_n) + f(y_{n+1})] / 2$$

In these cases y_{n+1} cannot be evaluated directly because $f(y_{n+1})$ is not known, so the equation only implicitly defines the value of y_{n+1} . Thus, at each integration time step a series of simultaneous equations must be solved. In a system of kinetic equations these will be nonlinear and will require an iterative numerical solution. This results in long computational times, but allows much larger step sizes (h) than explicit methods. This helps to overcome the problem of stiffness as the

reduced time steps necessary for stable solutions, are still within the bounds of computational practicability.

4.3 Gears Method For The Solution of Systems of Ordinary Differential Equations

A major advance in the development of implicit methods was made by Gear⁶¹ based on the earlier work of Nordsieck⁶². The procedure, now known as Gear's Method, utilises a multi-step, implicit, predictor-corrector formula. Its prime advantage is its ability to solve stiff systems, which it does by varying the step size throughout the problem to maximise the efficiency of computation. The method is widely agreed⁶³ to be the most accurate and efficient available for the solution of stiff systems, and has been successfully used in several kinetic studies^{64,65,66}.

The algorithm has been extensively discussed, and so only a brief description will be given here.

4.3.1 Mathematical Formulation of Gear's Method and the Problem of Stiffness

A system of ordinary differential equations is called stiff if it involves both very rapidly and very slowly changing terms, all of a decaying nature. More precisely, if the eigenvalues λ_i of the Jacobian,

$$J = \frac{\partial f}{\partial y} = \left(\frac{\partial f_i}{\partial y_j} \right)_{i,j=1}^N$$

all have negative real parts, but the time constants,

$T_i = 1/ \text{Re}(\lambda_i)$ are widely varying, then the system is stiff.

This property is local; a problem may be stiff in some regions

of t but not in others. It is also relative, the ratio $\max T_i / \min T_i$ being a measure of the stiffness.

The difficulty with stiff problems is that conventional methods for solving differential equations require incremental values of t commensurate with $\min T_i$, while the size $|T - t_0|$ of the problem range is commensurate with $\max T_i$. As a result the problem cannot be run to completion in a reasonable number of steps. With Gear's method, however, the increment h is restricted to small values, by the requirements of accuracy, only where the solution is relatively active. By definition, the system is not stiff in such regions and accuracy is achieved at minimum cost. Then in regions of stiffness, where the solution is inactive, Gear's method has the property of "stiff stability", which ensures that h is no longer restricted by the small time constants, unless or until the corresponding rapidly varying terms become active again.

Gear's method uses the implicit formula

$$y_n = \sum_{j=1}^q \alpha_j y_{n-j} + h \beta_j y_{n-j} \quad (4.1)$$

where y_k is an approximation to $y(t_k)$, \dot{y}_k is an approximation to $\dot{y}(t_k) = f(y_k, t_k)$. The α_j and β_j are constants associated with the method⁶⁷, and q is an integer called the order of the method. This is also variable throughout the program under an accuracy criterion and basically reflects the number of terms needed in equation (4.1) for a sufficiently accurate solution. Equation (4.1) represents a set of nonlinear simultaneous equations, these are solved iteratively using a standard method⁶⁸. The initial value of y_n used in the iteration is predicted by an explicit method using previous solution points.

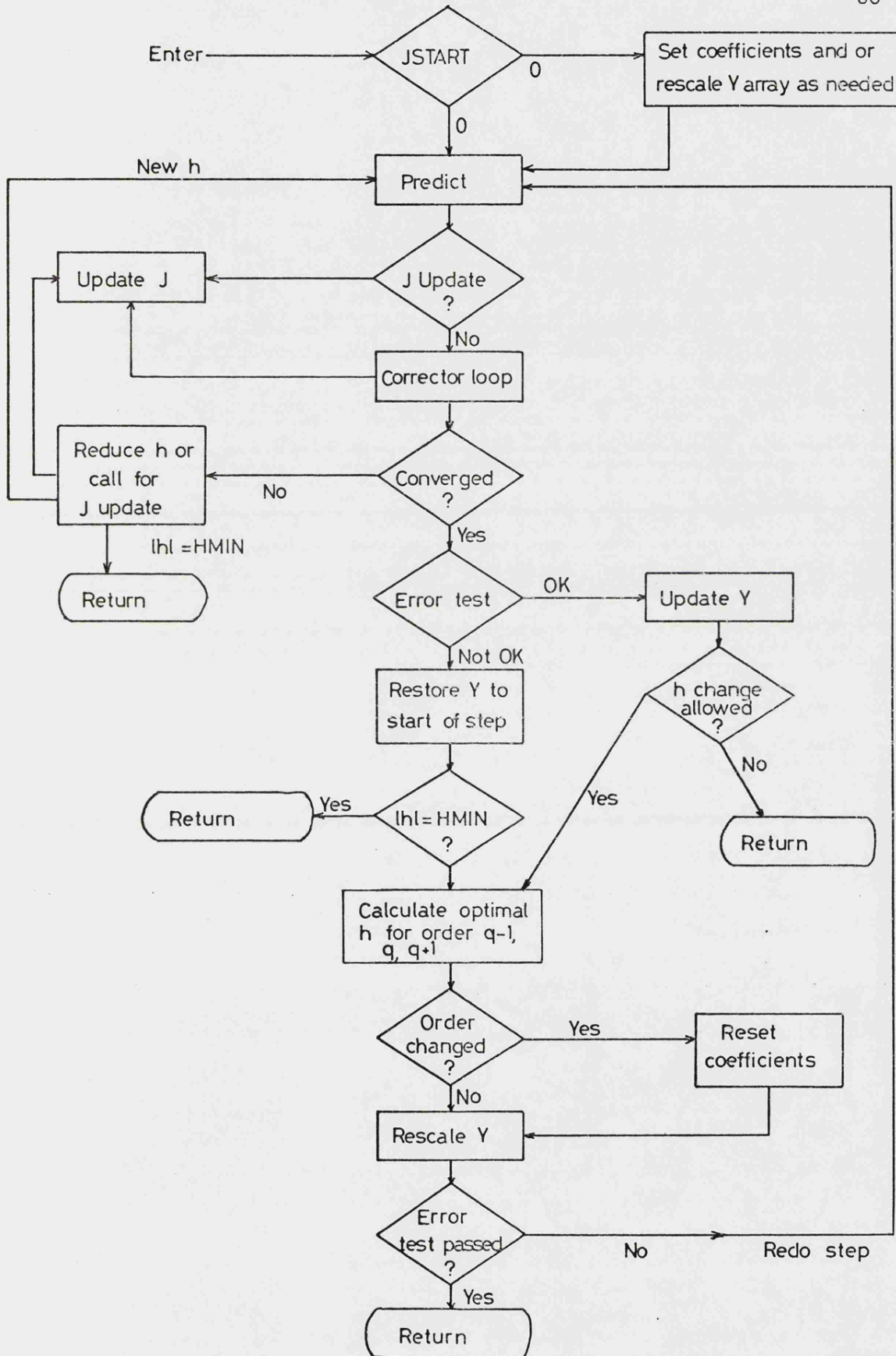


FIG. 4.1 Macroscopic flowchart of D02LF1-A Subroutine to implement Gear's Method

4.3.2 Use of Gear's Method

The computer program used to implement Gear's method was written by A.C. Hindmarsh⁶³ based on an improved version of Gear's algorithm. It was written in Fortran IV and a complete listing has been published⁶⁹. A macroscopic flow chart of the method is shown in Fig. 4.1. It is used as a subroutine called DO2LF1 in a specially written program, this program defines the problem and the time scale, and checks for numerical errors. The subroutine is called repeatedly returning a set of solution points, that is concentrations, at the chosen time intervals. This time interval does not represent h which is controlled by DO2LF1. The control program is listed and described in Appendix 4.

In use the program computes a complete concentration time profile for all the species in a given reaction mechanism. To do this it requires the rate constant for each individual reaction step, which may or may not be known accurately. Unknown rate constants may be estimated and the results of the computed model compared with experiment, they may then be adjusted to bring the two models into agreement. The accuracy with which this may be done is determined by the model, the types of reaction for which the rate constants are unknown, and the amount of information available from experiment.

CHAPTER FIVE

EXPERIMENTAL RESULTS

EXPERIMENTAL RESULTS

The pulsed stirred-flow system, described in Chapter 2, was thoroughly tested to determine the validity of the assumptions, made in Chapter 3, when deriving the equations governing behaviour in the system. The derived equations were tested directly by means of a time dependent inert tracer technique, and by the measurement of a known reaction, the isomerisation of cyclopropane to propene.

The thermolysis of tetramethylsilane (4MS) was then studied using the pulsed stirred-flow system at temperatures between 840K and 1055K. The reaction was carried out in a stream of nitrogen carrier gas at a pressure of approximately 2 atmospheres, initial concentrations of 4MS were low, in the range 1.0×10^{-3} to 1.0×10^{-4} mol dm⁻³ at most temperatures. To facilitate measurements over such a wide range of temperatures, residence times of between 13 s and 120 s were used. This variation in residence times was achieved by altering the size of the reaction vessel and the flow rate of carrier gas (see Chapter 3). The reaction was thus studied between approximately 2% and 97.5% conversion of reactant to products.

The possibility of heterogeneous reactions occurring was investigated by using a reaction vessel packed with quartz wool, and thus having a surface to volume ratio approximately 10 times that of the normal vessels.

5.1 Inert Tracer Experiments

Meaningful kinetic parameters can be obtained from the pulsed stirred-flow system only if the conditions of 'perfect mixing' and 'perfect pulse behaviour', as described in Chapter 3, are fulfilled. Using an approach originally suggested by Denbigh²⁴, and developed by Mason and Piret²⁵, this can be done by monitoring the time-dependent response of the system to a pulse of an inert tracer material. Equation (3.5), plotted as Fig. 3.1, gives the theoretical concentration time profile, and this may be compared with an experimental one obtained as described in Section 2.4.

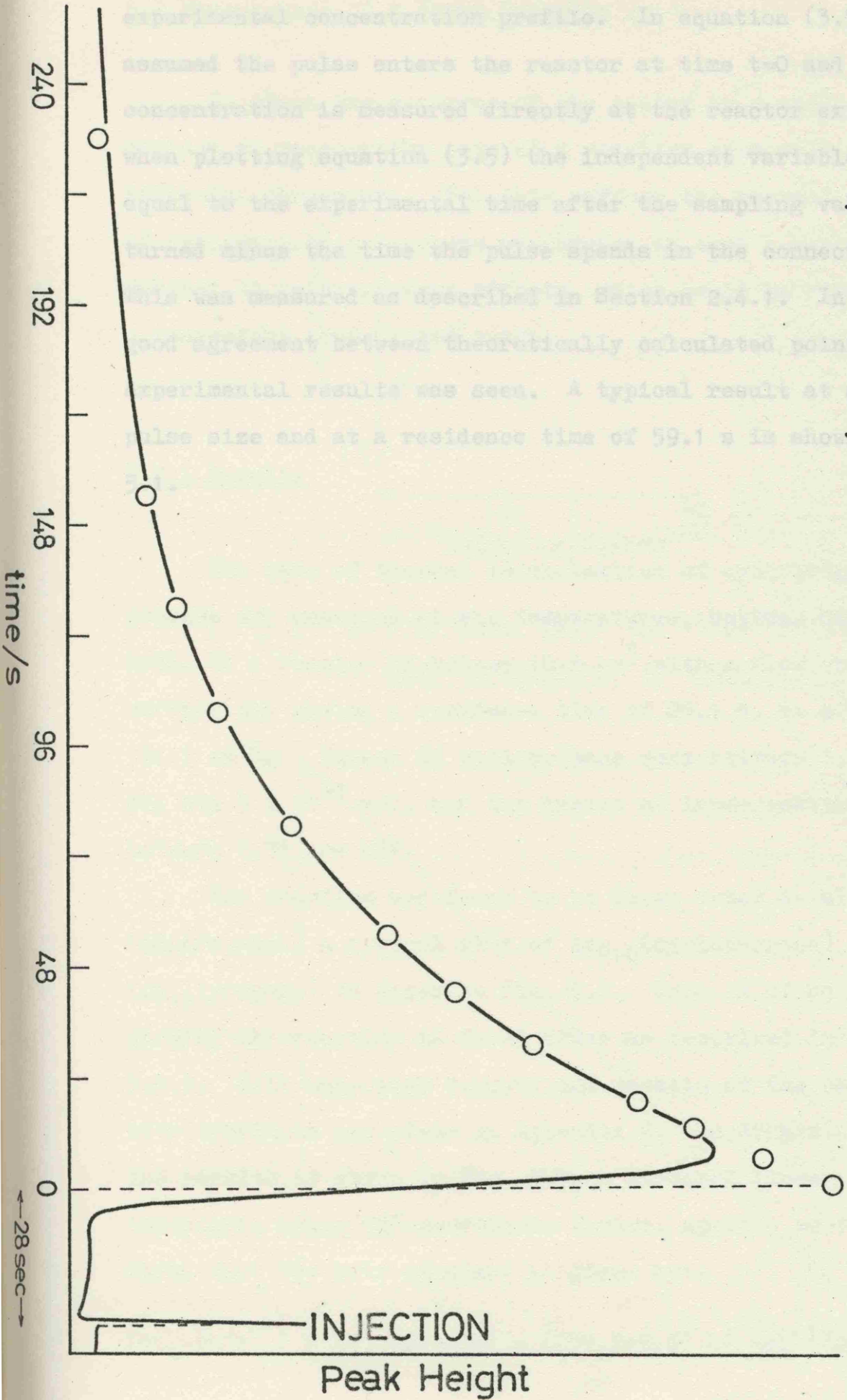
5.1.1 Results

Concentration time profiles were measured using a reactor of volume 54.58 cm³ at various flow rates of carrier gas corresponding to residence times of 19.8 s, 59.1 s and 101.6 s. The reaction vessel was at a temperature of 811K and methane, which is thermally stable at this temperature, was used as the tracer material. Several different sized pulses of tracer were used for each residence time. Points calculated according to equation (3.5) were plotted superimposed on the experimental chart records.

$$\left[\frac{A_o(t)}{v} \right] = \frac{(A_o)}{v} \exp(-t/\tau) \quad (3.5)$$

v and τ are known from independent measurements and (A_o) is the total amount of tracer used which is given by the area under the

FIG 5.1 Comparison of experimental response curve and calculated points for injection of an inert pulse.



experimental concentration profile. In equation (3.5) it is assumed the pulse enters the reactor at time $t=0$ and that the concentration is measured directly at the reactor exit. Thus, when plotting equation (3.5) the independent variable t is equal to the experimental time after the sampling valve is turned minus the time the pulse spends in the connecting pipes. This was measured as described in Section 2.4.1. In all cases good agreement between theoretically calculated points and experimental results was seen. A typical result at an average pulse size and at a residence time of 59.1 s is shown in Fig. 5.1.

5.2 Measurement of a Known Reaction

To check the accuracy of the system as a whole it was decided to measure the rate of a reaction with well established Arrhenius parameters. For this purpose the thermal isomerisation of cyclopropane to propene was chosen as such a reaction, not subject to heterogeneous effects, which could be studied over a convenient temperature range.

5.2.1 Results

The rate of thermal isomerisation of cyclopropane to propene was measured at six temperatures, between 801K and 868K, in a reactor of volume 10.4 cm^3 with a flow rate of carrier gas giving a residence time of 20.1 s, at a pressure of 134.3 cm Hg. Pulses of cyclopropane were between 1.2×10^{-4} mol and 5×10^{-4} mol, and the degree of isomerisation was between 6.7% and 63%.

The reaction was found to be first order at all temperatures, a typical plot of $\log_{10}(\text{cyclopropane})$ against $\log_{10}(\text{propene})$ is shown in Fig. 5.2. This is of unit slope showing the reaction is first order as described in Section 3.3.2. Full numerical results and details of the calculation of rate constants are given in Appendix 5. An Arrhenius plot of the results is given in Fig. 5.3, a standard linear regression technique, using 95% confidence limits, applied to these results shows that the rate constant is given by:-

$$\log_{10}(k/s^{-1}) = (15.76 \pm 0.36) - (279.2 \pm 5.6) \text{ kJ mol}^{-1} / 2.303RT$$

FIG. 5.2 Plot of $\log(\text{cyclopropane})$ against $\log(\text{propene})$

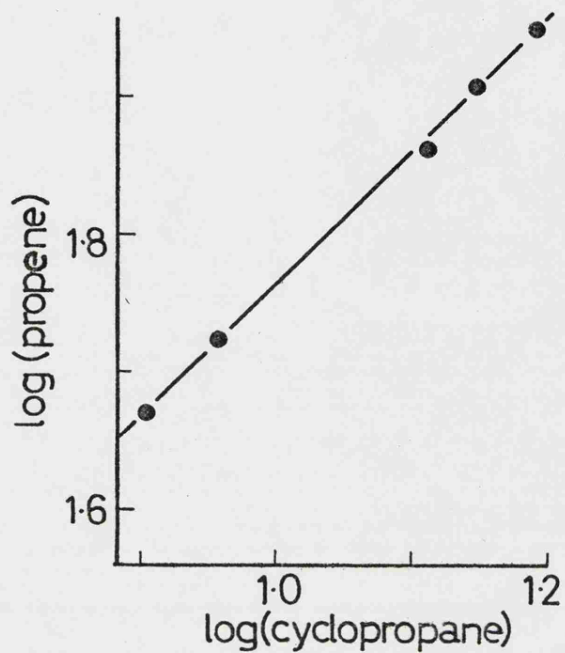
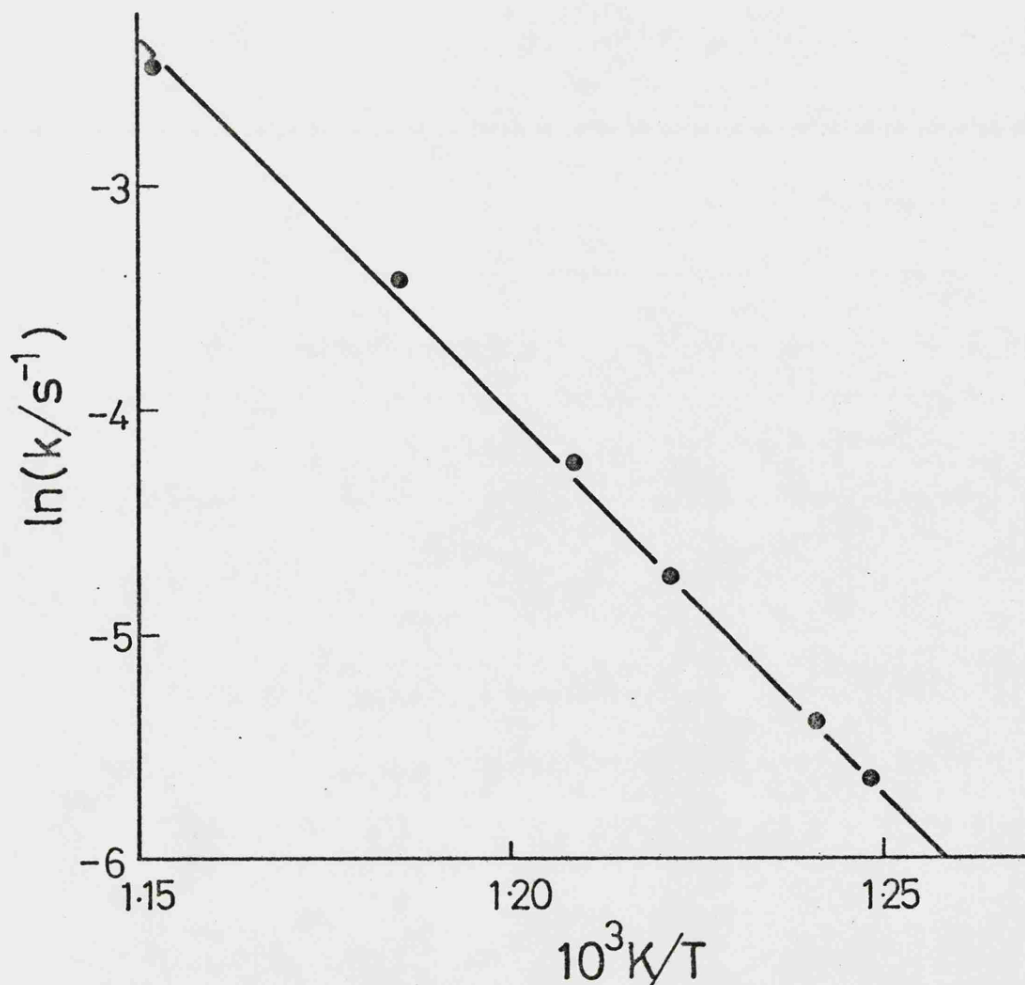


FIG. 5.3 Arrhenius plot for the thermal isomerisation of cyclopropane



5.3 Thermolysis of Tetramethylsilane

The thermolysis of 4MS was investigated under the conditions described above. The reactant used (see Appendix 7) contained no impurities detectable by G.L.C. or mass spectrometry. Several reaction vessels were used, including one packed with quartz wool, most required approximately ten thermolysis; to be carried out within them before consistent results could be obtained.

5.3.1 Thermolysis Products and their Identification

The main product was methane, with the following other products; 1,1,3,3-tetramethyl-1,3-disilacyclobutane, trimethylsilane, ethyltrimethylsilane, hexamethyldisilane, and small quantities of bis-trimethylsilylmethane, ethane, propane, and n-butane. Ethyltrimethylsilane and bis-trimethylsilylmethane were identified by their mass spectra (see Section 2.1.9), all other products by comparison of their retention times with authentic samples (see Appendix 7). The relative yields of product were affected by temperature, the main feature being that the proportion of methane to other products increased with temperature. Another significant feature was that 1,1,3,3-tetramethyl-1,3-disilacyclobutane was not formed at temperatures below 870K. Some typical product distributions at 908K and 980K are shown in Table 5.1.

Table 5.1 Typical Product Distributions

Product	Molar % of products at	
	908K	980K
CH ₄	67.3	93.1
C ₂ H ₆	4.6	2.59
C ₃ H ₈	2.3	0.32
n C ₄ H ₁₀	0	0.03
Me ₃ SiH	4.43	1.20
Me ₃ SiEt	5.0	0.09
Me ₆ Si ₂	4.71	0.99
$ \begin{array}{c} \text{CH}_2 \\ \diagup \quad \diagdown \\ \text{Me}_2\text{Si} \quad \text{SiMe}_2 \\ \diagdown \quad \diagup \\ \text{CH}_2 \end{array} $	11.5	1.68

5.3.2 Kinetic Measurements

Kinetic measurements were made on methane and trimethylsilane and are listed in full in Appendix 6. The formation of methane was first order over the entire temperature range from 840K to 1055K, typical order plots (see Section 3.3.2) at 898K and 1013K are shown in Fig. 5.4. However, the Arrhenius parameters were found to vary as can be seen from the Arrhenius plot, Fig. 5.6. In the unpacked reaction vessels first order

FIG 5.4 Order plots of data obtained from unpacked reaction vessels

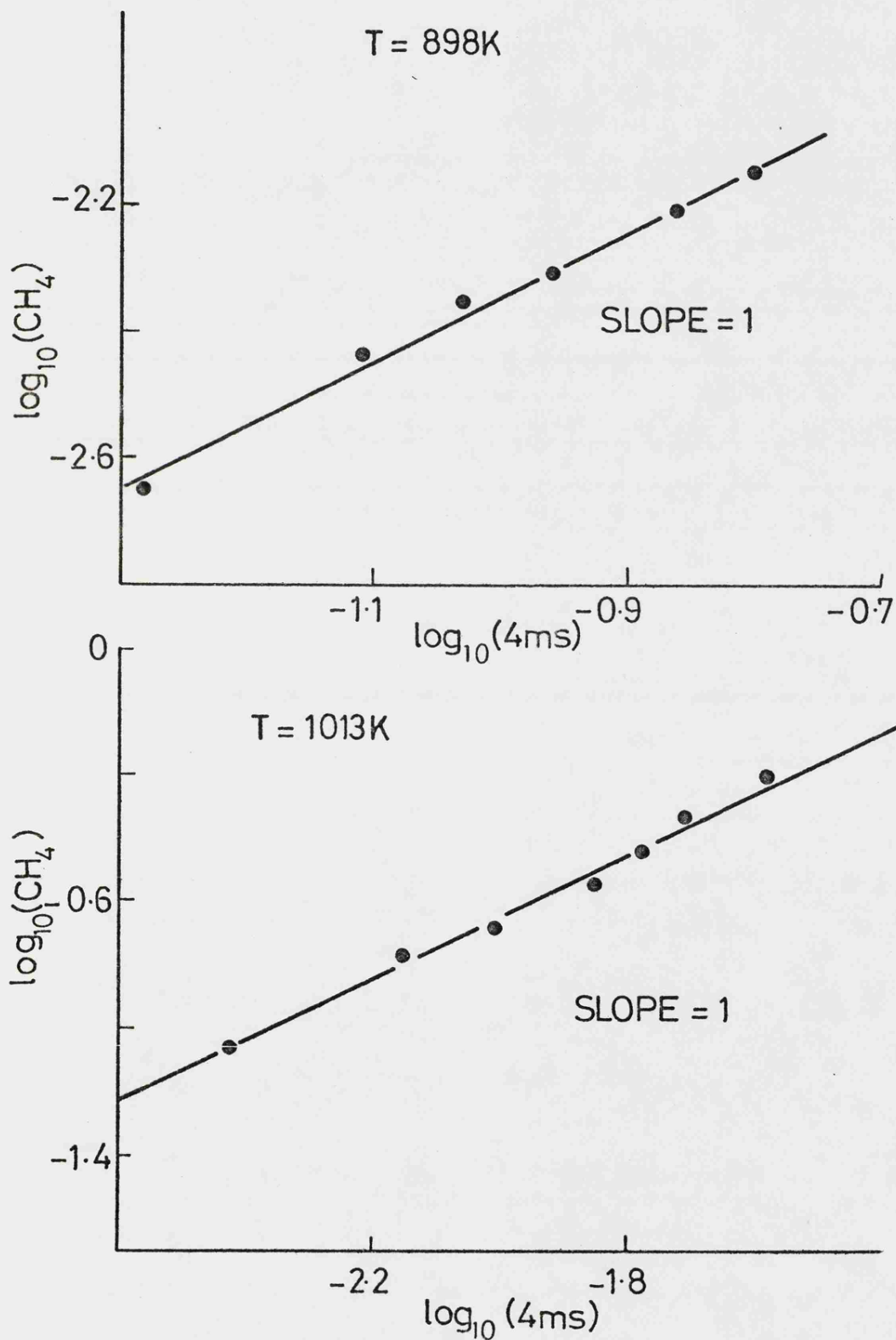


FIG. 5.5 Order plots of data obtained from packed reaction vessel

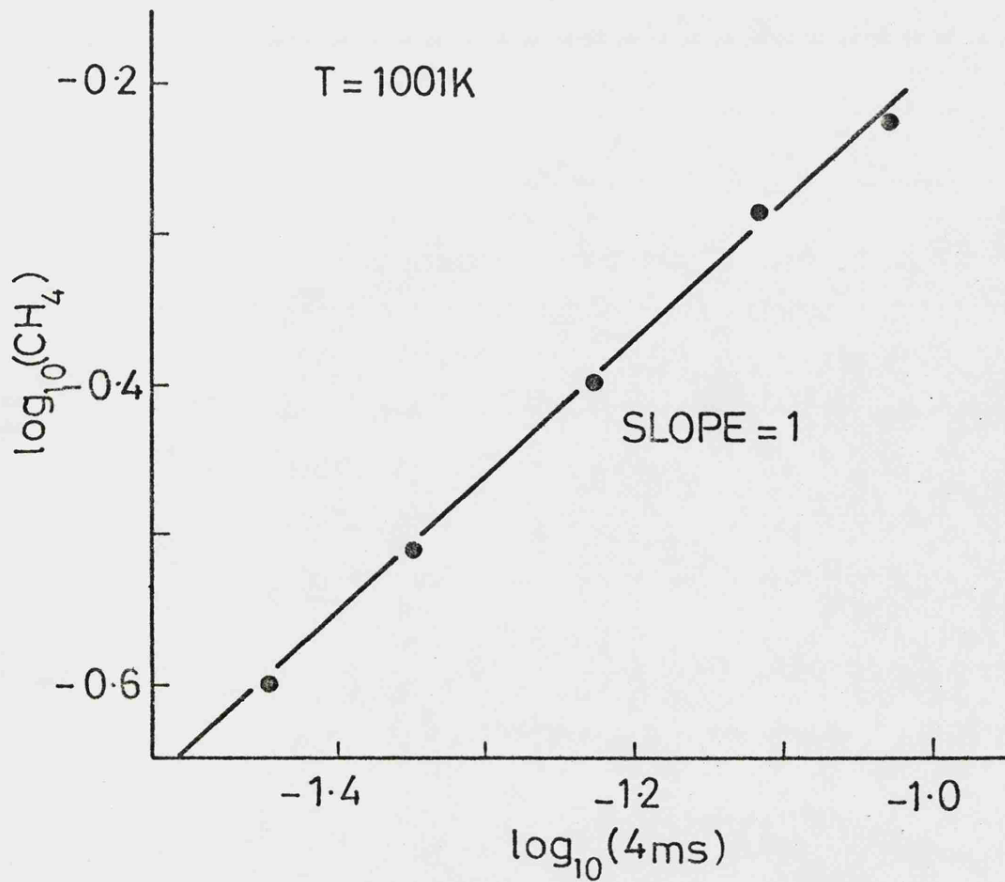
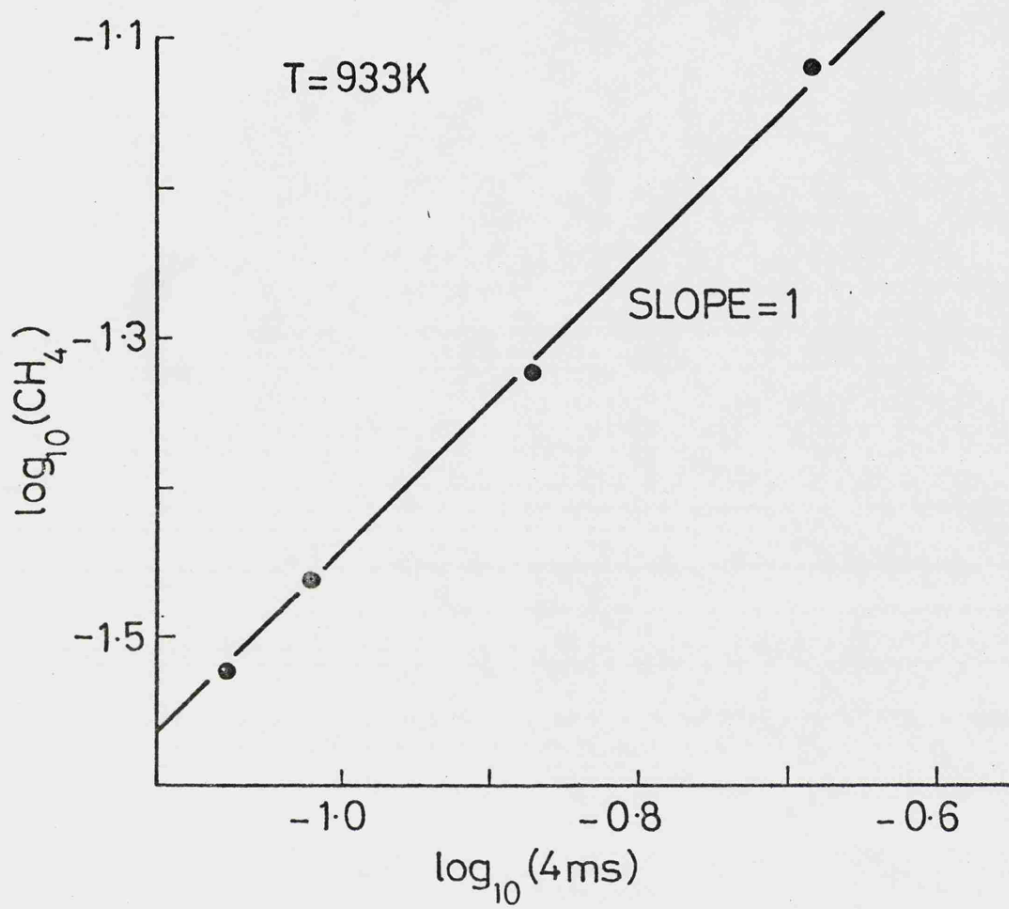


FIG. 5.6 Arrhenius plot for the formation of methane in the thermolysis of tetra-methylsilane.

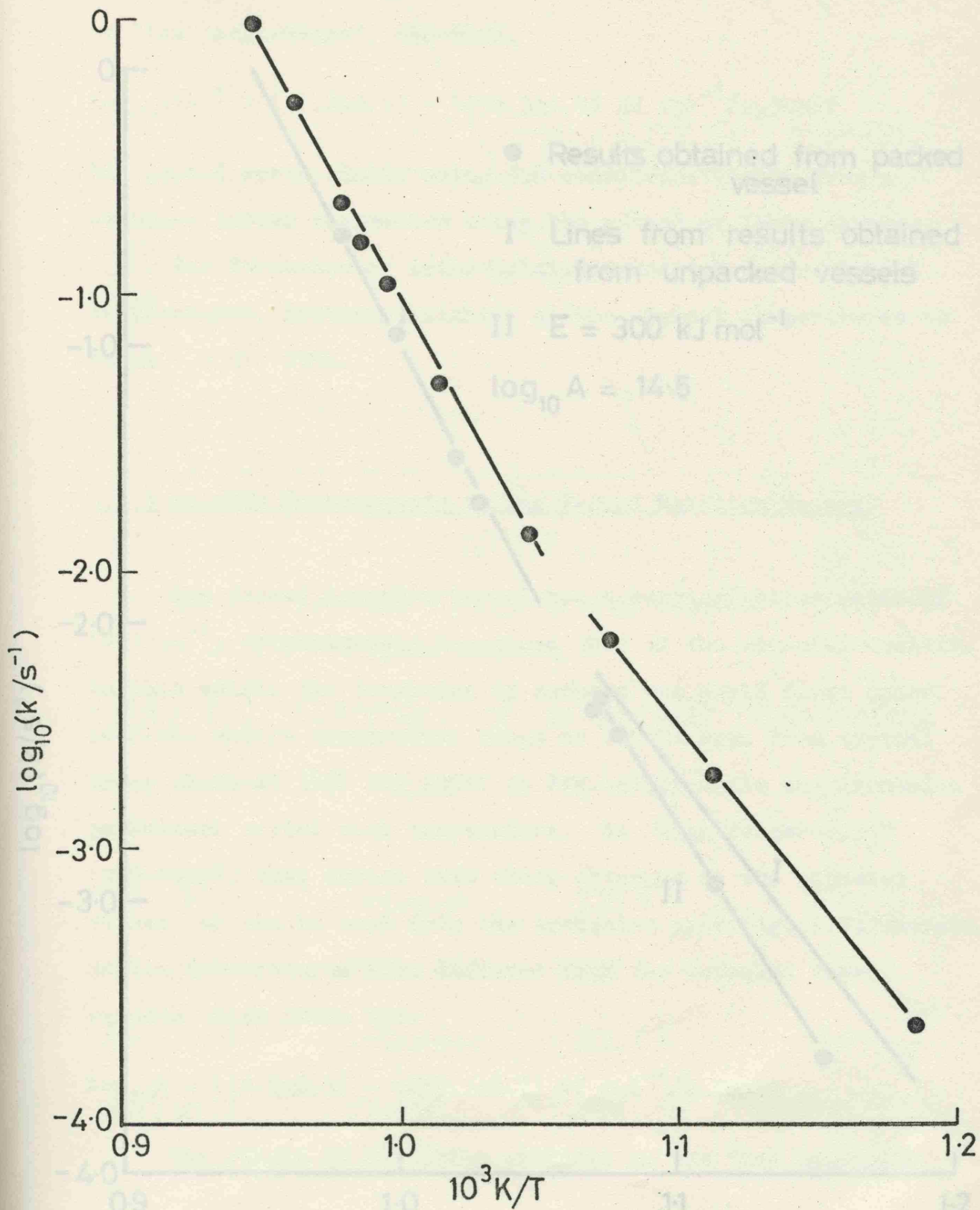
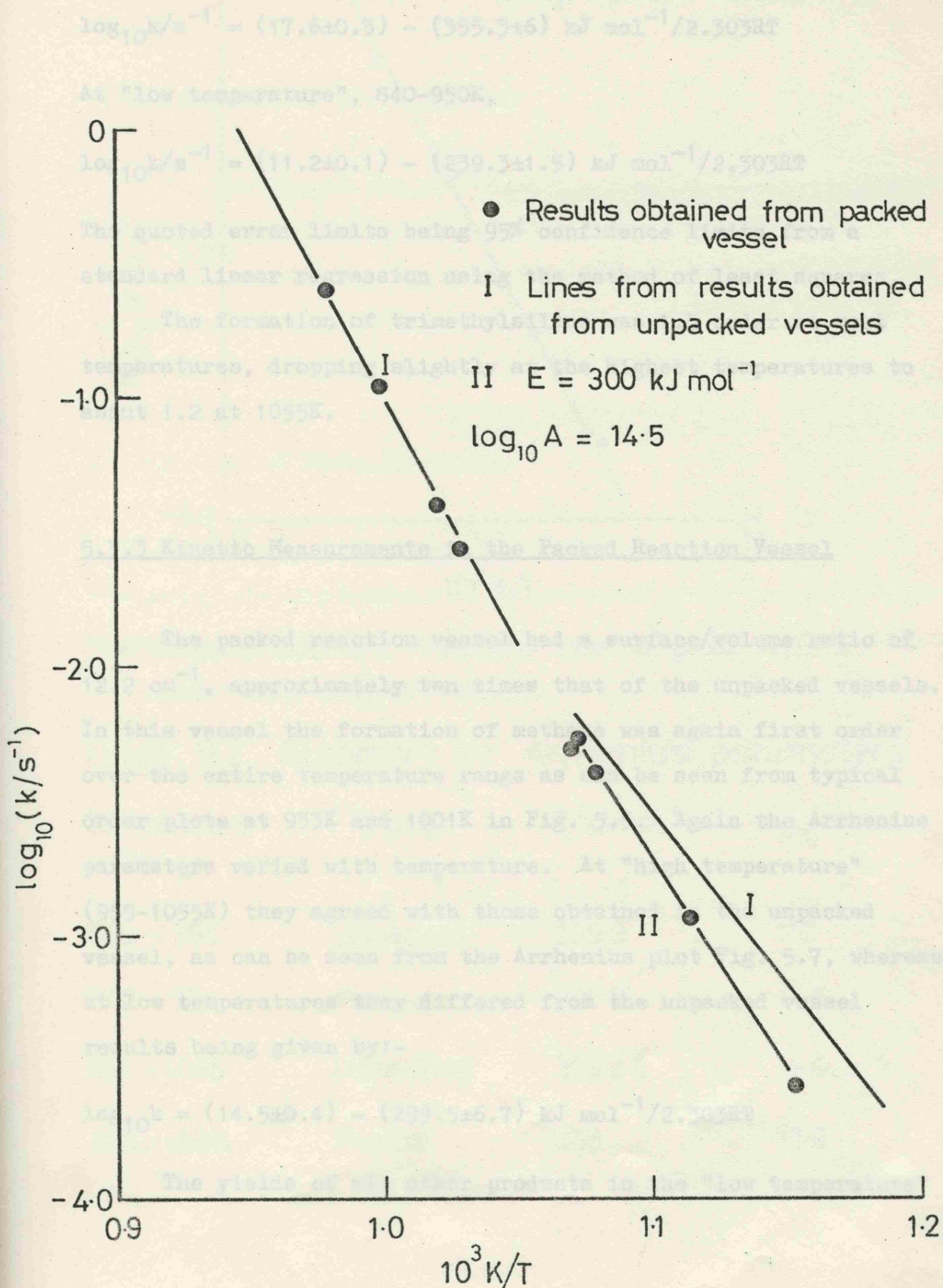


FIG. 5.7 Arrhenius plot for the formation of methane in the thermolysis of tetramethylsilane in a packed vessel.



rate constants for the formation of methane were as follows:-

At "high temperature", 955-1055K,

$$\log_{10} k/s^{-1} = (17.6 \pm 0.3) - (355.3 \pm 6) \text{ kJ mol}^{-1} / 2.303RT$$

At "low temperature", 840-950K,

$$\log_{10} k/s^{-1} = (11.2 \pm 0.1) - (239.3 \pm 1.5) \text{ kJ mol}^{-1} / 2.303RT$$

The quoted error limits being 95% confidence limits from a standard linear regression using the method of least squares.

The formation of trimethylsilane was 1.5 order at most temperatures, dropping slightly at the highest temperatures to about 1.2 at 1055K.

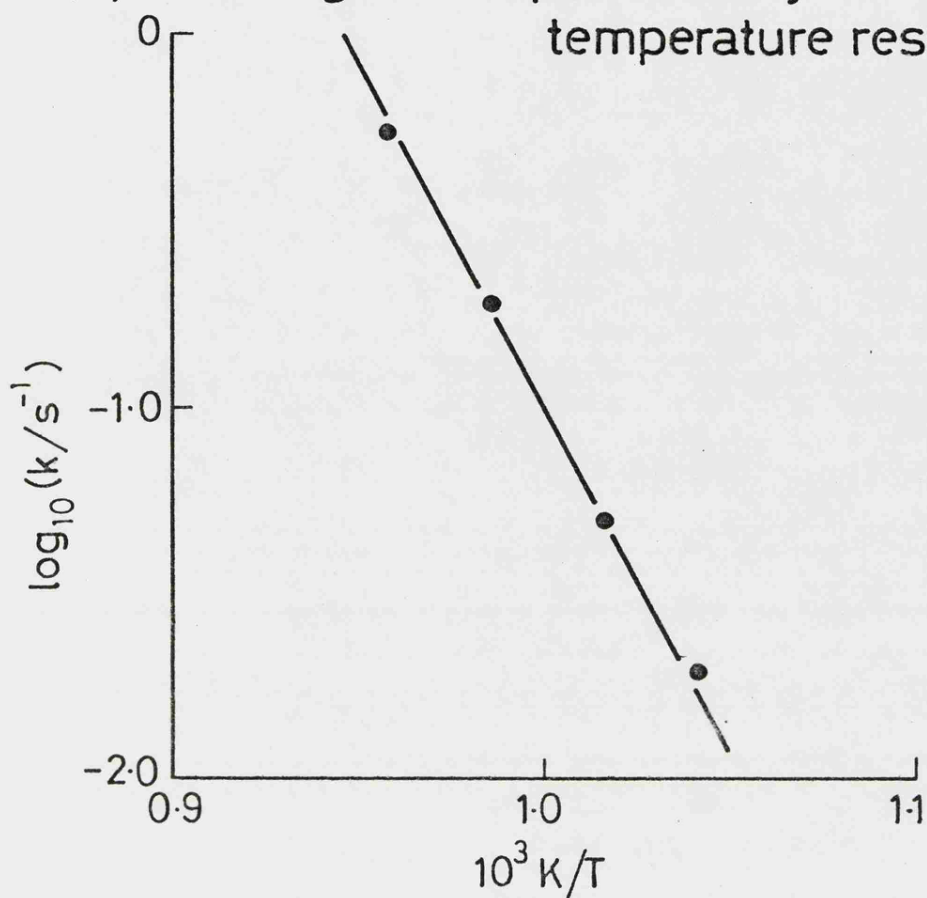
5.3.3 Kinetic Measurements in the Packed Reaction Vessel

The packed reaction vessel had a surface/volume ratio of 12.2 cm^{-1} , approximately ten times that of the unpacked vessels. In this vessel the formation of methane was again first order over the entire temperature range as can be seen from typical order plots at 933K and 1001K in Fig. 5.5. Again the Arrhenius parameters varied with temperature. At "high temperature" (955-1055K) they agreed with those obtained in the unpacked vessel, as can be seen from the Arrhenius plot Fig. 5.7, whereas at low temperatures they differed from the unpacked vessel results being given by:-

$$\log_{10} k = (14.5 \pm 0.4) - (299.5 \pm 6.7) \text{ kJ mol}^{-1} / 2.303RT$$

The yields of all other products in the "low temperature"

FIG. 5.8 Arrhenius plot for the formation of methane in the thermolysis of tetramethylsilane, showing the reproducibility of the high temperature results. ⁷⁵



- Results obtained 6 months after original results
Line from original results.

Table 5.2. Summary of Arrhenius parameters

Temperature Range	Vessel	$E/kJmol^{-1}$	$\log_{10} A$
840 - 955	Unpacked	239.3	11.2
840 - 955	Packed	299.5	14.5
955 - 1055	Unpacked	355 ± 6	17.6 ± 3
955 - 1055	Packed	355	17.6

region were reduced compared to those in the unpacked reaction vessels.

5.3.4 Reproducibility of Results

To investigate the reproducibility of the "high temperature results" some subsequent experiments were performed 6 months after the original series. These results are compared with the measured Arrhenius parameters in Fig. 5.8.

5.3.5 Action of Chain Inhibitors

Attempts were made to inhibit any chain reaction by conducting the thermolysis in an excess of known chain inhibitors. Propene and m-xylene were used, no change in rate of formation of any product was detected.

CHAPTER SIX

DISCUSSION

DISCUSSION

The experimental results presented in Chapter 5 are examined and discussed in this chapter. In addition, the results of the computer simulation of some complex reaction schemes are described. The use of the numerical integration technique described in Chapter 4 has facilitated the analysis of schemes which would have otherwise proved intractable. Following a discussion of the expected accuracy of the numerical results for the thermolysis of tetramethylsilane, based on the study of the isomerisation of cyclopropane, the mechanistic implications of these results are considered in the light of current ideas on the thermolysis of methylsilanes.

It was originally thought⁷ that the thermolysis of organosilanes did not proceed by means of chain reactions of the Rice - Herzfeld type common in hydrocarbons, due to the inability of silicon to form $p_{\pi} - p_{\pi}$ bonds. Thus, the characteristic propagation step in these chain reactions in which a radical decomposes to an unsaturated π bonded species and another radical could not occur. Subsequently it became clear that "double bonded" intermediates, $>Si=CH_2$, could exist in the gas phase and played an important part in the thermolysis of methylsilanes^{15,19,70}. $Me_2Si=CH_2$ was first discovered by Flowers and Gusel'nikov⁹ as an intermediate in the thermolysis of 1,1-dimethyl-1-silacyclobutane, where it dimerised to form 1,1,3,3-tetramethyl-1,3-disilacyclobutane. In the presence of water or ammonia dimerisation was inhibited and products consistent with a species containing a silicon - carbon double bond were obtained. Walsh⁸² originally estimated the π -bond energy of $Me_2Si=CH_2$ as lying between 119 and 158 kJ mol^{-1} on the

basis of this work and the thermolysis of trimethylsilane⁸. In the light of recent upward revisions of silicon-carbon bond dissociation energies these figures have also been revised¹⁹ to $(200 \pm 20) \text{ kJ mol}^{-1}$ which is about 80% of the π -bond energy in olefins.

A chain mechanism is advanced, consistent with that previously established for the thermolysis of hexamethyldisilane,¹⁵ which satisfactorily accounts for the experimental results on the thermolysis of tetramethylsilane. This in turn enables a satisfactory re-interpretation of the results obtained some years ago on the thermolysis of trimethylsilane to be made, in terms of a similar chain reaction.

6.1 The Numerical Accuracy of the Experimental Results

In the inert tracer experiments good agreement was observed at all residence times and pulse sizes between the experimental concentration-time profiles and those predicted by the equations derived in Chapter 3 (see Fig. 5.1). This is good evidence that the assumptions made in deriving the equations are fulfilled experimentally, and that the system should be capable of yielding accurate experimental results.

The thermal isomerisation of cyclopropane was investigated and the first order rate constant was found to be given by

$$\log_{10}(k/s^{-1}) = (15.76 \pm 0.36) - (279.2 \pm 5.6) \text{ kJ mol}^{-1}/2.303RT$$

This reaction has been extensively studied by many groups of workers, and it is widely agreed^{25,71,72} that the high pressure first order limiting rate constant over the experimental temperature range is given by⁷³

$$\log_{10}(k/s^{-1}) = 15.45 - 274.6 \text{ kJ mol}^{-1}/2.303RT$$

This is in good agreement with the experimental results, the experimental rate constant at the mid point of the temperature range (830K) is within 6% of the accepted value.

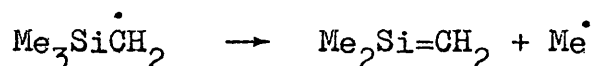
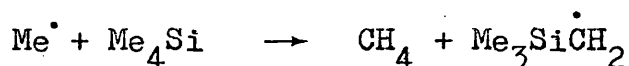
The statistical error limits quoted above, 0.36 log units in the A factor and 6 kJ in the activation energy are a good indication of the precision with which unknown rate constants may be measured. However, they do not take any account of possible systematic errors, but the good agreement between the experimental and accepted values for the rate constant for thermal isomerisation of cyclopropane indicates that no systematic errors are present.

6.2 The Mechanism of Thermolysis of Tetramethylsilane

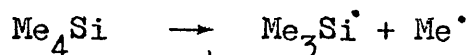
The thermolysis of tetramethylsilane was previously investigated by Gowenlock and his co-workers¹³ in linear flow systems between 810 and 980K, as has been described in Chapter 1. They obtained first order rate constants for the formation of methane given by:-

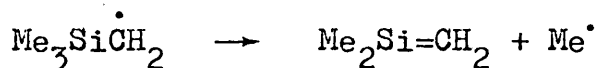
$$\log_{10}(k/s^{-1}) = (14.3 \pm 0.23) - (283 \pm 3) \text{ kJ mol}^{-1}/2.303RT$$

As they pointed out, this activation energy was significantly lower than any reasonable estimate of $D(\text{Me}_3\text{Si-Me})$, thus indicating that a chain mechanism operates. In the work described in this thesis attention was initially focused on the formation of trimethylsilane which had not previously been measured. A chain sequence involving methyl radicals to form methane could easily be visualised as follows.



However, there was no obvious chain sequence in which trimethylsilyl radicals would participate. Therefore, trimethylsilane might be a non-chain product, formed at a rate determined by the initial dissociation of the silicon-carbon bond in tetramethylsilane, as follows





In this case, formation of trimethylsilane should be first order. Unfortunately this was not so, the order being 1.5 at most temperatures and significantly greater than one at all temperatures, indicating that trimethylsilane is probably also formed in a chain process. If the trimethylsilane results from hydrogen abstraction by trimethylsilyl radicals from tetramethylsilane, as seems likely, then the trimethylsilyl radical concentration must be half order in tetramethylsilane. The decrease in order for the production of trimethylsilane at the highest temperatures is due to the fact that at these temperatures a significant amount of that produced subsequently decomposes. Thus, attention was redirected to the formation of methane in an attempt to elucidate the mechanism of the chain reaction.

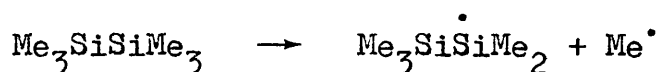
6.2.1 Formation of Methane

The Arrhenius plot for the formation of methane (Fig. 5.6) and the error limits quoted for the Arrhenius parameters in Section 5.3.2 clearly indicate that this plot is not curved but consists of two distinct straight lines of different slope at "high" and "low" temperature. The Arrhenius parameters for the "high" temperature region agree well with those to be expected for reaction (1):



Davidson and Howard¹⁵ calculate a value of $10^{10.6} \text{ dm}^3 \text{ mol}^{-1} \text{ s}^{-1}$, by the geometric mean rule, for the A factor for the reverse of

reaction (1), the combination of a methyl and a trimethylsilyl radical, using an estimate for the rate constant for the combination of trimethylsilyl radicals and the well established rate constant for the combination of methyl radicals. From a recent value of the entropy change for reaction (1), A_1 may then be estimated as $10^{17.6} \text{ s}^{-1}$. An estimate for E_1 is provided by the value of $D(\text{Me}_3\text{SiMe}_2\text{Si-Me})$ which Davidson and Howard¹⁵ obtained from the rate of production of methane resulting from the following reaction:-



The reaction was only measured at one temperature but the value of 350 kJ mol^{-1} may be regarded as a lower limit for $D(\text{Me}_3\text{Si-Me})$. The most recent estimate of $D(\text{Me}_3\text{Si-Me})$ is $356 \pm 17 \text{ kJ mol}^{-1}$, obtained from electron impact experiments combined with thermochemical calculations.

In the "low" temperature region a chain mechanism almost certainly operates, and this must be initiated by reaction (1). If reaction (1) has the Arrhenius parameters given by the "high" temperature results for the formation of methane, then the point at which the two lines on the Arrhenius plot intersect represents the temperature at which the rate of the chain reaction equals the rate of the initiation step, i.e. the temperature at which the chain length is unity. As the temperature is lowered from this point the rate of initiation decreases faster than the rate of the chain reaction, as the former has a larger activation energy, and the chain length increases above unity. Conversely, as the temperature is increased the rate of initiation becomes greater than the rate of the chain reaction, and the reaction becomes non-chain, rate determined by reaction (1). Thus, if a

reasonable chain sequence can be found, initiated by reaction (1) with the Arrhenius parameters given by the "high" temperature results for the formation of methane, which reproduces the experimental rate for the chain production of methane then $D(\text{Me}_3\text{Si-Me})$ may be identified with the activation energy for reaction (1).

6.2.2 Chain Reaction for the Formation of Methane

Any reasonable chain sequence for the thermolysis of tetramethylsilane must involve several termination steps, all of which would be expected to have similar rates, and thus the scheme would not be suitable for conventional steady-state analysis. It was therefore necessary to use the numerical methods described in Chapter 4 to analyse possible mechanisms for comparison with the experimental results. In setting up the differential equations describing the rate of change of concentration of each type of molecule and radical present in the reaction scheme, account had to be taken of the fact that the reaction was conducted in a pulsed stirred-flow system, in which all species in the reactor are swept from it with a first order "rate constant" of $1/\tau$, where τ is the time constant of the reactor (see Section 3.1.1). This was done by including the term $\{-(\text{concentration of species})/\tau\}$ in each differential equation. For a given mechanism with estimates of the Arrhenius parameters for each step the computer program calculated the concentration within the reactor of all species and tabulates them at any selected time intervals. This can be done for any temperature and initial concentration of tetramethylsilane.

However, the experimental results were calculated from the total amount of a product formed and the total amount of reactant undecomposed over the entire period of the experiment, concentrations in the reactor at any time being unknown. To simulate this the computer program also integrates numerically the concentrations of selected species with respect to time to yield these quantities from which rate constants may be calculated exactly as in the experiments.

A simple initiation and propagation sequence, reactions (1) to (4) in Table 6.1, followed by dimerisation of $(\text{Me}_2\text{Si}=\text{CH}_2)$, reaction (5), and by all possible radical termination reactions, (7) to (12), formed the basis of the most likely chain reaction scheme. With the Arrhenius parameters listed in Table 6.2 either from the literature or from reasonable estimates it was found that this scheme did not reproduce the experimental results satisfactorily. The rate of formation of methane was too slow and the formation of trimethylsilane was first order with respect to tetramethylsilane instead of 1.5, implying that the model underestimated the concentration of trimethylsilyl radicals and that there should be another reaction forming them. Whilst there is evidence that $(\text{Me}_2\text{Si}=\text{CH}_2)$ is a polar double-bonded molecule⁷⁰, it would initially be formed in reaction (4) as a biradical and might react as such before reorganising itself into a π bonded entity. Accordingly an abstraction reaction of $(\text{Me}_2\text{Si}=\text{CH}_2)$ was included, reaction (6). The Arrhenius parameters for this reaction were assumed to be the same as those for reaction (2), which are well established. Thus the reaction is assumed to be a simple hydrogen abstraction by a silicon centred radical and unaffected by the biradical structure. At the present time this is the best estimate that can be made.

Table 6.1 Mechanism of Thermolysis of Tetramethylsilane

Reaction

Number

- 1 $\text{Me}_4\text{Si} \rightarrow \text{Me}_3\text{Si}^\cdot + \text{Me}^\cdot$
- 2 $\text{Me}^\cdot + \text{Me}_4\text{Si} \rightarrow \text{CH}_4 + \text{Me}_3\text{Si}\dot{\text{C}}\text{H}_2$
- 3 $\text{Me}_3\text{Si}^\cdot + \text{Me}_4\text{Si} \rightarrow \text{Me}_3\text{SiH} + \text{Me}_3\text{Si}\dot{\text{C}}\text{H}_2$
- 4 $\text{Me}_3\text{Si}\dot{\text{C}}\text{H}_2 \rightarrow \text{Me}_2\text{Si}=\text{CH}_2 + \text{Me}^\cdot$
- 5 $2\text{Me}_2\text{Si}=\text{CH}_2 \rightarrow \text{Me}_2\text{Si} \begin{array}{l} \diagup \text{CH}_2 \\ \diagdown \text{CH}_2 \end{array} \text{SiMe}_2$
- 6 $\text{Me}_2\text{Si}=\text{CH}_2 + \text{Me}_4\text{Si} \rightarrow \text{Me}_3\text{Si}^\cdot + \text{Me}_3\text{Si}\dot{\text{C}}\text{H}_2$
- 7 $2\text{Me}_3\text{Si}^\cdot \rightarrow \text{Me}_6\text{Si}_2$
- 8 $\text{Me}_3\text{Si}^\cdot + \text{Me}_3\text{Si}\dot{\text{C}}\text{H}_2 \rightarrow \text{Me}_3\text{SiCH}_2\text{SiMe}_3$
- 9 $2\text{Me}^\cdot \rightarrow \text{C}_2\text{H}_6$
- 10 $\text{Me}_3\text{Si}\dot{\text{C}}\text{H}_2 + \text{Me}^\cdot \rightarrow \text{Me}_3\text{SiEt}$
- 11 $2\text{Me}_3\text{Si}\dot{\text{C}}\text{H}_2 \rightarrow (\text{Me}_3\text{SiCH}_2)_2$
- 12 $\text{Me}^\cdot + \text{Me}_3\text{Si}^\cdot \rightarrow \text{Me}_4\text{Si}$
- 13 $\text{Me}_3\text{Si}\dot{\text{C}}\text{H}_2 + \text{Wall} \rightarrow \text{Stable Products}$

etc.

Table 6.2 Arrhenius Parameters for the Mechanism of Thermolysis of Tetramethylsilane

Reaction Number	$\log_{10} A$	$E/\text{kJ mol}^{-1}$	Source (see Table 6.3)
1	17.6 ± 0.3	355 ± 6	a
2	8.3 ± 0.2	40 ± 2	b
3	10.5	78	c
4	14.4	212	d
5	~7	~50	e
6	8.3	40	f
7	10	0	g
8	9	0	h
9	10.5	0	i
10	10	0	h
11	9.5	0	h
12	10.6	0	g
13	1.544	0	j
	0.544		k

Arrhenius parameters without error limits are approximate estimates.

First order A factors in s^{-1} , second order in $\text{dm}^3 \text{mol}^{-1} \text{s}^{-1}$.

Table 6.3 Sources of Arrhenius Parameters in Table 6.2

a) This work.

b) Ref. 75.

c) High A factor cf. Ref. 5.

$$E_3 = \Delta H_3 + E_{-3}$$

$\Delta H_3 = 38 \text{ kJ mol}^{-1}$ from dissociation energies in Ref. 15.

$$E_{-3} \approx 40 \text{ kJ mol}^{-1}$$

d) cf. similar reaction in Ref. 15.



e) Estimated (see text).

f) Assumed analogous to reaction (2).

g) Ref. 15.

h) Estimated in accordance with the geometric mean rule.

i) Ref. 76.

j) Pseudo first order rate constant in packed vessel,
empirical value (see text).

k) Pseudo first order rate constant in unpacked vessel,
empirical value (see text).

Since this meant that the concentration of $(\text{Me}_2\text{Si}=\text{CH}_2)$ now became involved in determining the rate of the chain reaction an estimate for the rate of reaction (5) which also affects the concentration is needed. The product of reaction (5) the disilacyclobutane was not observed below 870K, although formation of all other products continued normally down to lower temperatures. The simplest explanation is that reaction (5) requires some activation energy, so that all of the $(\text{Me}_2\text{Si}=\text{CH}_2)$ is lost from the reactor below 870K. The Arrhenius parameters for reaction (5) are approximate "common-sense" estimates which may be greatly in error. This is not a serious problem, however, because the computer model is insensitive to them, the principal process controlling the concentration of $(\text{Me}_2\text{Si}=\text{CH}_2)$ being the unimolecular "sweeping out" with rate constant $1/\tau$.

With the addition of reaction (6) and some minor optimisation of estimated rate constants the mechanism was then satisfactory, giving the correct orders of reaction for the formation of methane and trimethylsilane and reproducing exactly the Arrhenius plot for the formation of methane at "low" temperature.

6.2.3 Effect of Surface/Volume Ratio in the Formation of Methane

In the packed reaction vessel at "low" temperature both the A factor and activation energy for the production of methane were increased, resulting in a reduction in the rate. This effect is inconsistent with heterogeneity in the initiation or termination steps, which would be expected to give a lower activation energy and an increased rate in the packed reaction vessel, but could be explained by loss of a chain carrying radical

to the wall. The most likely radical is $\text{Me}_3\text{Si}\dot{\text{C}}\text{H}_2$ due to its relatively long life. An attempt was made to include this process in the computed mechanism for comparison with the experimental results. Reaction (13) was added to simulate the reaction between $\text{Me}_3\text{Si}\dot{\text{C}}\text{H}_2$ radicals and the wall of the vessel with a pseudo first order rate constant representing the rate constant for the actual reaction multiplied by the concentration of active sites on the surface. A value of this rate constant which brought the results from the computed model into agreement with those obtained experimentally was found empirically. When this rate constant was reduced by a factor of ten, to simulate conditions in the unpacked vessel with a ten fold lower surface to volume ratio, the heterogeneous term became insignificant and the mechanism continued to give the Arrhenius parameters appropriate to the experiments in the unpacked vessel, as it had before the heterogeneous term was introduced.

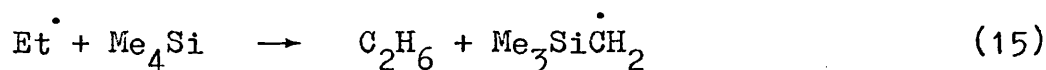
At "high" temperatures packing the vessel had no effect on the rate of formation of methane. This is consistent with the view that at these temperatures the rate of formation of methane is non-chain rate determined by reaction (1), thus the heterogeneous loss of $\text{Me}_3\text{Si}\dot{\text{C}}\text{H}_2$ radicals have no effect on the overall rate.

6.2.4 The Overall Mechanism

The complete mechanism, which thus accounts quantitatively for all the experimental results at "high" and "low" temperatures in packed and unpacked vessels is described with details of the Arrhenius parameters used in the computations in Tables 6.1 to

6.3. All of the products of the reactions in Table 6.1 were observed experimentally, except for the product of reaction (11), 1,2,-bis-trimethylsilylethane. The computer calculations show that this would have been formed in smaller amounts than the bis-trimethylsilylmethane, which was only just detectable under the most favourable conditions in our G.L.C. apparatus. It is not surprising that the less volatile higher molecular weight compound did not give a discernible peak. Of the other minor products not accounted for in the mechanism, hydrogen would be formed mainly by secondary decomposition of trimethylsilane, and propane and n-butane by secondary decomposition of ethane.

The importance of certain other reactions not included in Table 6.1 was investigated, in particular reactions(14)-(15) were considered as possible alternatives to reaction (6).



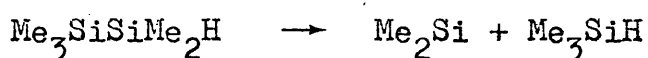
Substantial variations in the rate constants about their expected values produced no effect on the calculated results and the reactions were thus concluded to be unimportant.

The computed results were most sensitive to the values of k_1 and k_4 . There is good evidence from this work that $D(\text{Me}_3\text{Si-Me})$ and hence E_1 is $355 \pm 6 \text{ kJ mol}^{-1}$, but higher values up to ca. 380 kJ mol^{-1} have been suggested¹⁹. It was found that if E_1 was increased beyond the error limits of $355 \pm 6 \text{ kJ mol}^{-1}$ then no other reasonable values of the other rate constants in the mechanism could be found that would reconcile the computed with the experimental results. The mechanism was similarly inconsistent if E_4 differed from 215 by more than $\pm 5 \text{ kJ mol}^{-1}$.

6.2.5 Thermochemistry of Methylsilanes

Thermochemical data on methylsilanes have been unreliable in the past⁷⁰ and current estimates of various heats of formation have been shown to be inconsistent¹⁹. There is good evidence from this study that $D(\text{Me}_3\text{Si-Me})$ is $(355 \pm 6) \text{ kJ mol}^{-1}$ and this enables the calculation of certain other thermochemical quantities for comparison with recent work. $D(\text{Me}_3\text{Si-SiMe}_3)$ has recently been measured¹⁵ as 337 kJ mol^{-1} which in conjunction with a recent literature value⁷⁸ for $\Delta H_f^\circ(\text{Me}_6\text{Si}_2)_g$ of -359 kJ mol^{-1} , gives $\Delta H_f^\circ(\text{Me}_3\dot{\text{Si}})_g = -11 \text{ kJ mol}^{-1}$. Taking $D(\text{Me}_3\text{Si-Me})$ and $\Delta H_f^\circ(\text{Me}_3\dot{\text{Si}})_g$ as above and the well established⁷⁹ $\Delta H_f^\circ(\text{Me}\dot{\text{e}})_g = 149 \text{ kJ mol}^{-1}$, $\Delta H_f^\circ(\text{Me}_4\text{Si})_g = -217 \text{ kJ mol}^{-1}$, which differs significantly from the literature value⁷⁸ of -236 kJ mol^{-1} . The latter, with the above radical heats of formation would give $D(\text{Me}_3\text{Si-Me}) = 374 \text{ kJ mol}^{-1}$. Walsh and Wells¹⁹ have measured $D(\text{Me}_3\text{Si-H})$ as $(376 \pm 17) \text{ kJ mol}^{-1}$ which if used with the literature value⁷⁸ for $\Delta H_f^\circ(\text{Me}_3\text{SiH}) = -156 \text{ kJ mol}^{-1}$ gives $\Delta H_f^\circ(\text{Me}_3\dot{\text{Si}}) = 2 \text{ kJ mol}^{-1}$, on the borderline of compatibility with the value of -11 kJ mol^{-1} derived above. This figure with $\Delta H_f^\circ(\text{Me}_4\text{Si})$ as above gives $D(\text{Me}_3\text{Si-Me}) = 384 \text{ kJ mol}^{-1}$, again not consistent with this work. Clearly further work is required to clarify the situation concerning the heats of formation of these methylsilanes.

Davidson and Matthews⁸⁰ have measured ΔH for the following reaction as 195 kJ mol^{-1} .



Using the above heats of formation $\Delta H_f^\circ(\text{Me}_2\text{Si})_g$ can be calculated as $(66 \pm 10) \text{ kJ mol}^{-1}$ which leads to a value of 216 kJ mol^{-1}

for the second bond dissociation energy in tetramethylsilane. This large drop from first to second bond dissociation energy appears to be a general feature of silicon chemistry, the same trend being apparent⁸¹ with monosilane.

6.3 The Mechanism of Thermolysis of Other Methylsilanes

The thermolysis of hexamethyldisilane¹⁵ has recently been investigated and was successfully interpreted in terms of a short chain reaction similar to that proposed for tetramethylsilane. Despite the occurrence of several termination reactions the mechanism was analysed by means of a steady state approach using some reasonable approximations and the consideration of limiting cases. This mechanism was subjected to a computer analysis in exactly the same way as has been described for tetramethylsilane to provide a more rigorous analysis of the results to be made and to provide a check on the applicability of the numerical method to systems of this type. The results are described below.

The thermolysis of trimethylsilane was investigated some time ago and incorrectly interpreted in terms of a non-chain mechanism⁷⁰. The detailed mechanism developed for tetramethylsilane enabled a similar mechanism to be written for trimethylsilane. This was then subjected to a computer analysis and the results compared with those obtained experimentally. The results are fully described below.

6.3.1 Mechanism of Thermolysis of Hexamethyldisilane:

The thermolysis of hexamethyldisilane was investigated in a pulsed stirred-flow system¹⁵ and complex kinetic behaviour was recorded. Trimethylsilane was the major product, formed in a first order process in the lower part of the temperature range and a 1.5 order process at higher temperatures. This behaviour

was attributed to a short chain reaction in which the relative importance of different termination steps changed with temperature. The mechanism suggested by Davidson and Howard¹⁵ was analysed in exactly the same manner as has been described for tetramethylsilane. The computed results reproduced the transition from first to 1.5 order for the formation of trimethylsilane, in accordance with the experimental results while the computed Arrhenius parameters for the formation of trimethylsilane in the first-order region agreed with the experimental values of $\log_{10} A = 15.3$, $E = 295 \text{ kJ mol}^{-1}$ well within the error limits. This confirms that the original analysis in terms of an approximate steady-state treatment was correct and increases confidence in the ability of the computer program to produce realistic results in systems of this kind.

6.3.2 Mechanism of Thermolysis of Trimethylsilane

The thermolysis of trimethylsilane was investigated by Davidson and Lambert⁸, the experimental details and results being summarised in Table 6.4. Arrhenius parameters were obtained for the two primary products, methane and hydrogen, the activation energies were measured satisfactorily but there is some uncertainty in the values of the A factors, mainly because of fractionation in the sampling system⁸, and also because the measured flow-rate of the carrier gas was not corrected to account for the temperature and pressure of the reactor²⁹. After applying the appropriate correction factor (see Section 3.3.1) to the experimental results²⁹ the first-order rate constants for hydrogen and methane respectively are best

Table 6.4 Experimental Details for the Thermolysis of
Trimethylsilane

System:	Continuous stirred-flow with analysis by mass spectroscopy.
Temperature:	943K to 1031K
Partial pressure of reactant:	2 to 4 mm Hg
Carrier gas:	Nitrogen at 20 mm Hg
Products:	Methane, Hydrogen plus smaller amounts of 1,1,3,3-tetramethyl-1,3-disilacyclobutane 1,1,3-trimethyl-1,3-disilacyclobutane 1,3-dimethyl-1,3-disilacyclobutane disilanes $\text{Si}_2\text{H}_m\text{Me}_{(6-m)}$ $m=0,1,2$ disilamethylenes $\text{CH}_2\text{Si}_2\text{H}_n\text{Me}_{(6-n)}$ $n=1,2$
Kinetic Results:	Methane and hydrogen formed in first order reactions with rate constants given by respectively:-

$$\log_{10}(k/s^{-1}) = 15.9 - 320 \text{ kJ mol}^{-1} / 2.303RT$$

$$\log_{10}(k/s^{-1}) = 15.6 - 336 \text{ kJ mol}^{-1} / 2.303RT$$

given by:-

$$\log_{10}(k/s^{-1}) = (16.1 \pm 0.7) - (336 \pm 2) \text{ kJ mol}^{-1}/2.303RT$$

$$\log_{10}(k/s^{-1}) = (16.4 \pm 0.7) - (320 \pm 2) \text{ kJ mol}^{-1}/2.303RT$$

At the time this work was performed the activation energies agreed well with the best estimates available for $D(\text{Me}_3\text{Si-H})$ and $D(\text{HMe}_2\text{Si-Me})$ and this was taken as evidence for the non-chain formation of hydrogen and methane (see Chapter 1). The above Arrhenius parameters were therefore identified with the unimolecular dissociations, reaction (16)-(17).



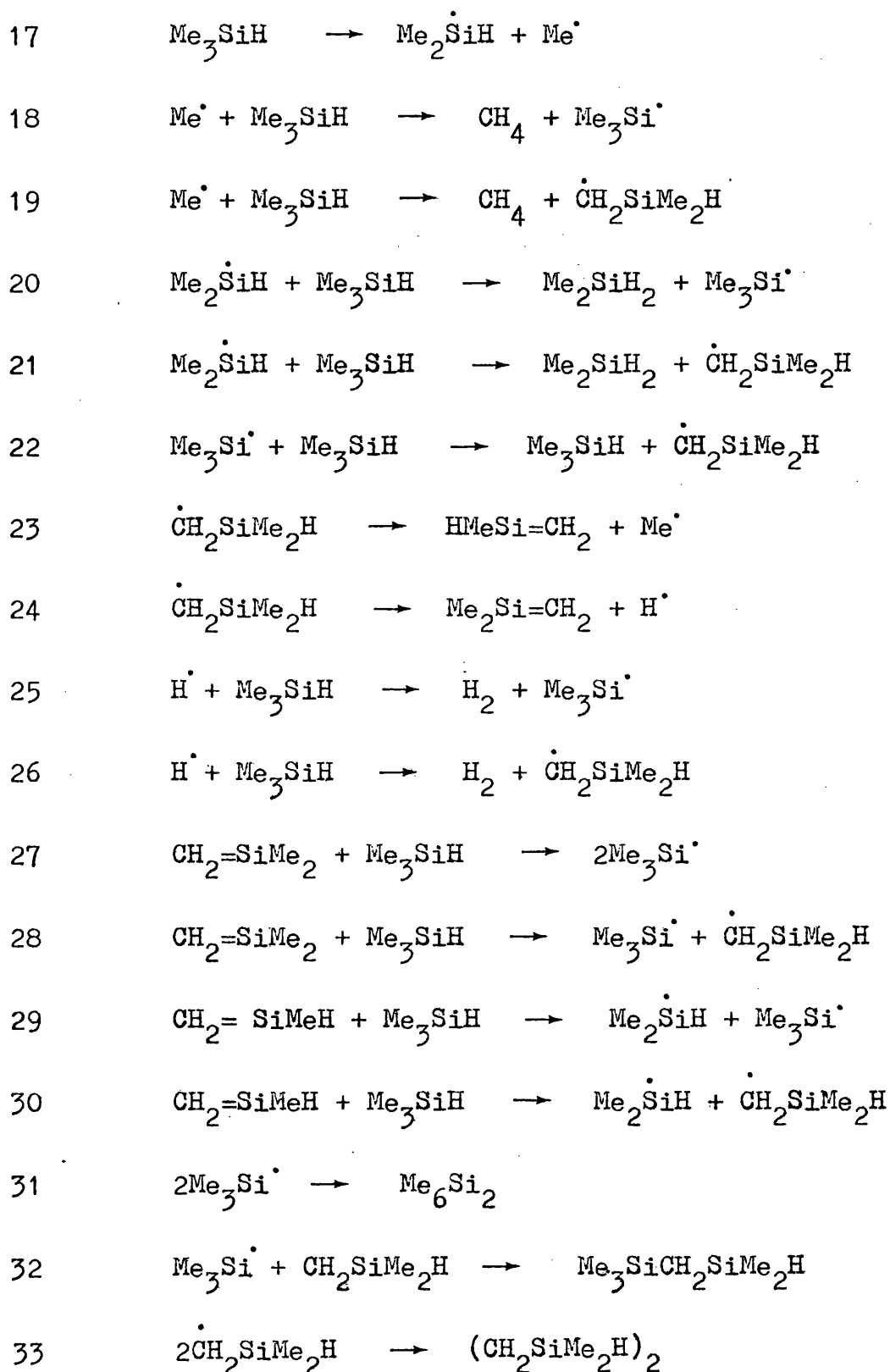
However, it is now clear that the activation energies for reaction (16) and (17) are considerably higher than the experimental figures and that the mechanism almost certainly proceeds by a chain mechanism analogous to that suggested for tetramethylsilane. E_{16} has been recently measured^{18,19} as $375 \pm 11 \text{ kJ mol}^{-1}$, and E_{17} must be ca. 355 kJ mol^{-1} by analogy with tetramethylsilane, $\log_{10}A_{17}$ should similarly be ca. 17.6 whilst $\log_{10}A_{16}$ has recently been calculated⁷⁴ as ca. 14.5. There should be a close parallel between the chain mechanisms for tetramethylsilane and trimethylsilane, although the latter is more complex because trimethylsilane has two types of hydrogen atom (attached to carbon and to silicon) and gives rise to more types of radical.

A mechanism for the thermolysis of trimethylsilane analogous to that for tetramethylsilane is given in Tables 6.5-6.7, along with the sources of the Arrhenius parameters used. Initiation

Table 6.5 Mechanism of Thermolysis of Trimethylsilane

Reaction

Number



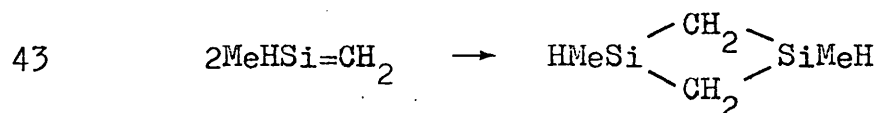
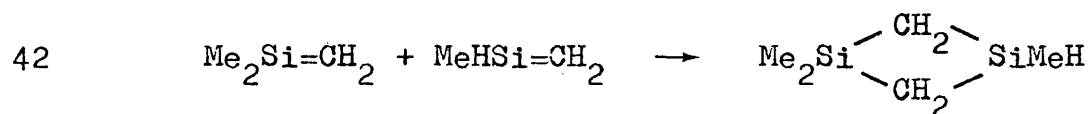
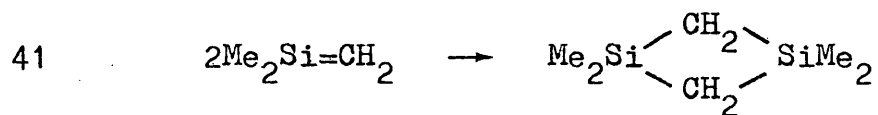
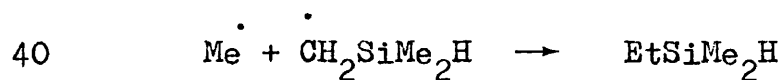
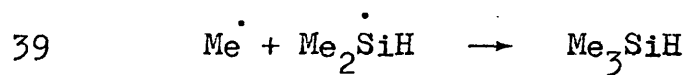
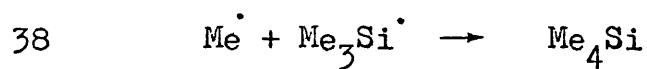
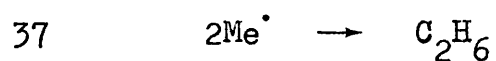
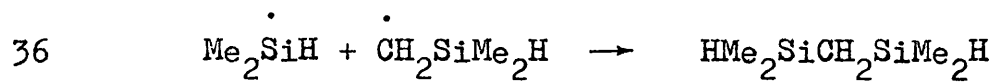
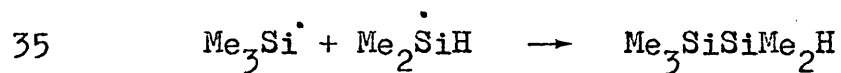
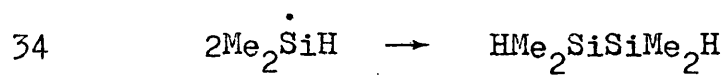


Table 6.6 Arrhenius Parameters for the Mechanism of Thermolysis of Trimethylsilane

Reaction Number	$\log_{10} A$	$E/\text{kJ mol}^{-1}$	Source (see Table 6.3)
17	17.6	355	a
18	8.7 ± 0.3	35 ± 2	b
19	8.3 ± 0.2	40 ± 2	a
20	9.5	50	c
21	10.5	78	a
22	10.5	78	a
23	14.4	212	a
24	13.5	225	d
25	8	10	e
26	9	28	f
27	8.7	35	g
28	8.3	40	h
29	8.7	35	g
30	8.4	40	h
31	10	0	a
32	9.4	0	i

33	8	0	i
34	10	0	j
35	10	0	j
36	9.4	0	k
37	10.5	0	a
38	10.6	0	a
39	10.6	0	l
40	10	0	a
41	~7	~50	a
42	~7	~50	a
43	~7	~50	a

Arrhenius parameters without error limits are approximate estimates.

First order A factors in s^{-1} , second order in $\text{dm}^3 \text{mol}^{-1} \text{s}^{-1}$.

Table 6.7 Sources of Arrhenius Parameters in Table 6.6

- a) From identical or equivalent reactions in the thermolysis of tetramethylsilane (see Tables 6.1-6.3)
- b) Ref. 75.
- c) Estimated, cf. Ref. 5.
- d) $\Delta H_{24} - \Delta H_{23} = 13 \text{ kJ mol}^{-1}$, from (Si-C) and (Si-H) bond dissociation energies; low A factor for loss of H atom, cf. (c) above.
- e) Ref. 77.
- f) Estimated by analogy with H abstraction from branched hydrocarbons.
- g) Assumed analogous to reaction (18).
- h) Assumed analogous to reaction (19).
- i) Estimated in accordance with the geometric mean rule.
- j) Assumed analogous to reaction (31).
- k) Assumed analogous to reaction (32).
- l) Assumed analogous to reaction (38).

is by reaction (17) only, the above estimates for the Arrhenius parameters of reaction (16) gives values for k_{16} which are at least 6×10^3 times smaller than k_{17} over the entire temperature range. Reactions (18) and (21) correspond to reactions (2) and (3). The abstraction reactions (19), (20) and (22) are unique to trimethylsilane because of the existence of an hydrogen atom attached to the silicon atom. It is because of these reactions that the rates of formation of methane in the thermolysis of trimethylsilane and tetramethylsilane have different Arrhenius parameters. Reactions (23) and (24) correspond to reaction (4), while reactions (27) to (30) are included because of the importance of reaction (6) in the case of tetramethylsilane. The other reactions in Table 6.5 are the full range of terminations and dimerisations. Estimated rate constants are based on, and consistent with, those used in the mechanism for the thermolysis of tetramethylsilane.

The mechanism in Table 6.5 was subjected to numerical integration, with initial concentrations of trimethylsilane of the same order as was used experimentally, but covering a wider range. "Sweeping out" terms were not included in the differential equations because the experimental technique to be simulated was continuous and not pulsed flow. Rate constants were calculated directly from the slope of the concentration profiles of products at varying initial concentrations of reactant. Formation of hydrogen and of methane was found to be first order, with rate constants given by respectively:-

$$\log_{10}(k/s^{-1}) = 15.8 - 337 \text{ kJ mol}^{-1}/2.303RT$$

$$\log_{10}(k/s^{-1}) = 16.3 - 320 \text{ kJ mol}^{-1}/2.303RT$$

These agree well with the experimental values, and the mechanism also accounts for all of the products observed experimentally.

The above Arrhenius parameters for the rate of formation of methane result in a rate of production of methane much greater than that observed in the thermolysis of tetramethylsilane. This is due to the possibility of reactions at the silicon-hydrogen bond, reactions (19), (20) and (22). Of these reaction (19) which produces methane directly is obviously the most important. This increased rate of the chain cycle in the thermolysis of trimethylsilane over tetramethylsilane means that at any given temperature the chain length in trimethylsilane is longer, thus, the temperature at which the chain length in trimethylsilane becomes unity is 1406K compared with 955K for tetramethylsilane. To verify the importance of reaction (19) in producing this effect the mechanism in Table 6.5 was subjected to computer analysis with the rate constant for reaction (19) set equal to zero. This resulted in the rate of production of methane being much reduced. At temperatures above 955K the rate of the chain was now less than the rate of initiation and the rate of formation of methane was non-chain with Arrhenius parameters the same as those for the initiation step, reaction (17). At lower temperatures than this the rate of formation of methane was very similar to that observed in the "low" temperature region for tetramethylsilane, confirming that it is reaction (19) which accounts for the increased rate of production of methane in the thermolysis of trimethylsilane compared to that in the thermolysis of tetramethylsilane.

6.4 Summary

It is concluded that the mechanisms presented here for the thermolysis of tetramethylsilane and trimethylsilane, and that previously described for the thermolysis of hexamethyldisilane offer a rational and consistent explanation of the experimentally observed results. Methylsilanes of this type do decompose by chain reactions very similar to the Rice-Herzfeld mechanisms seen in hydrocarbons, due to the existence of species of type >Si=CH_2 as intermediates in the gas phase. These chain reactions are generally of short length and at sufficiently high temperatures may become non-chain due to the rate of the initiation step becoming faster than the overall rate of the chain. This has enabled a direct kinetic determination of $D(\text{Me}_3\text{Si-Me})$ of $355 \pm 6 \text{ kJ mol}^{-1}$ to be made.

APPENDICES ONE AND TWO

CALIBRATIONS

Appendix 1 Calibration of the Gas Density Detector

To determine absolute molar quantities it was necessary to calibrate the detector using a known compound. This was done using 4MS by injecting known volumes into the sample gas stream immediately before the G.L.C. column. The following normal operating conditions were used:-

Reference gas flow rate = $1.22 \text{ cm}^3 \text{ s}^{-1}$

Sample gas flow rate = $0.76 \text{ cm}^3 \text{ s}^{-1}$

Detector temperature = 80°C

Column temperature = 80°C

The resulting G.L.C. peaks were measured, corrected to a sensitivity of 2mV F.S.D., and divided by the molecular weight factor for 4MS. A graph of these corrected areas against molar quantity of 4MS injected gave a straight line, through the origin, of slope $(5.41 \pm 0.05) \times 10^3$ (95% confidence limits), using grams of paper as a measure of the peak area. Thus the sensitivity of the detector is 1.85×10^{-4} moles/gram of paper (corrected) or in terms of the areas produced by the numerical integration program 5.61×10^{-10} moles/numerically integrated area (corrected).

Appendix 2 Calibration of the Pressure Transducer

The pressure transducer was calibrated against a manometer containing fresh mercury, the results are shown in Fig. A.2.1.

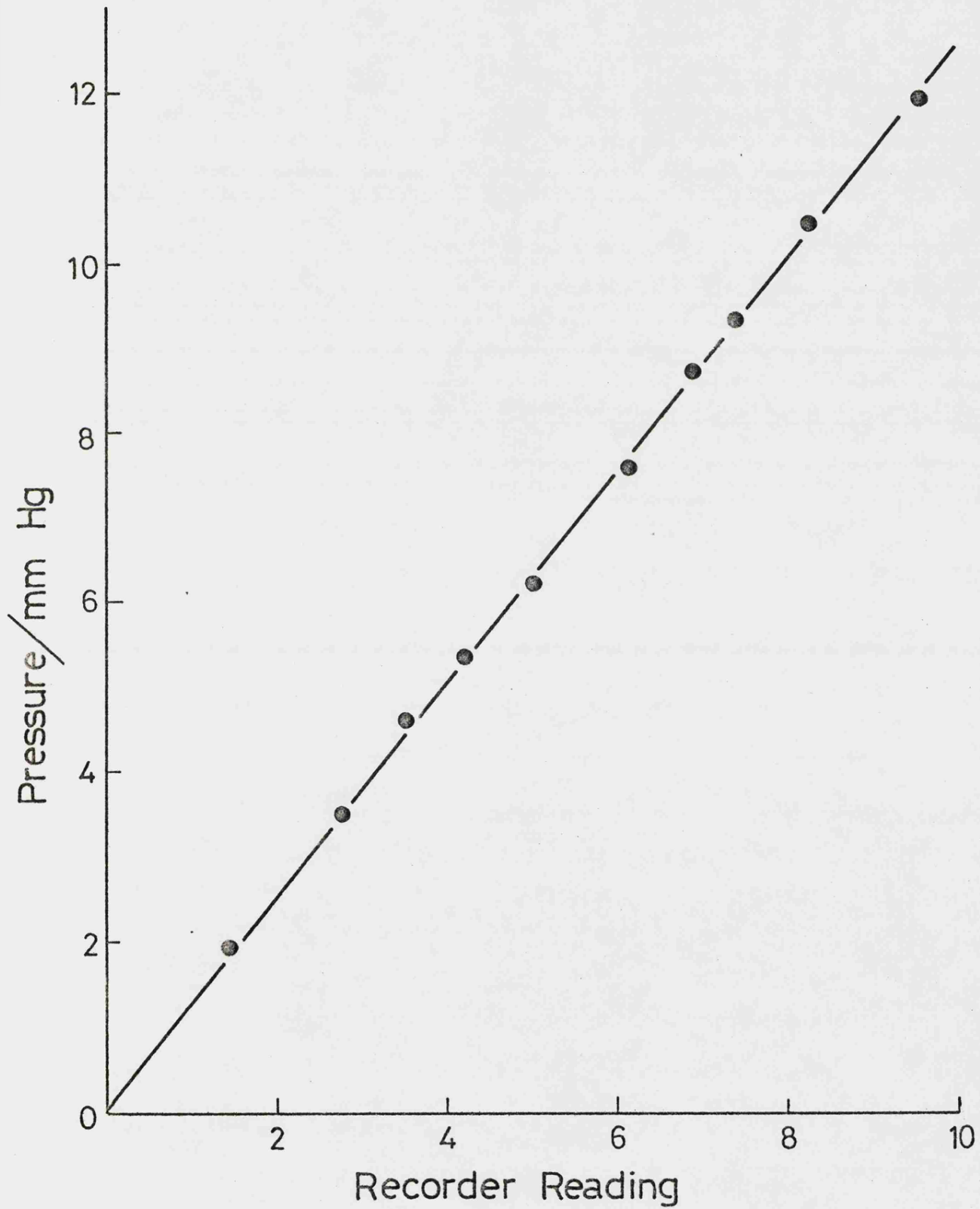
The calibration was carried out at normal operating conditions:-

Transducer temperature = 330 K

Bridge current = 0.3 mA

This results in a value of 12.6 mm of mercury per full scale deflection of the recorder as the calibration factor for the pressure transducer.

FIG. A.2.1 Calibration of the Pressure Transducer



APPENDICES THREE AND FOUR

COMPUTER PROGRAMS

Appendix 3 Computer Program to Calculate the Area of a G.I.C.Peak Using Simpson's Rule.

```
10 CLOSE1
20 DIMY(225)
30 OPEN"KB:"AS FILE1
50 LETN1=225
60 PRINT"VALUES OF POINTS ARE"
70 FORX=1TON1
80 INPUT#1,Y(X)
90 IFY(X)>0GOTO105
100 NEXTX
105 LETN1=X-2
110 LETS1=0:LETS2=0:LETS3=0:LETS4=0
120 LETN=1:LETX=1
130 GOSUB2000
140 LETN=2:LETX=N1
150 GOSUB2000
160 LETC=N*S4-S1*S1
170 LETB=(S2*S4-S1*S3)/C
180 LETA=(N*S3-S1*S2)/C
200 FORX=1TON1
210 LETY=A*X+B
220 LETY(X)=Y(X)-Y
230 NEXTX.
500 LETH1=.3333333
520 LETM1=H1*(Y(1)+(4*Y(2))+Y(3))
540 LETA1=M1+H1*(Y(3)+(4*Y(4))+Y(5))
550 LETA2=H1*(Y(1)+3.875*(Y(2)+Y(5))+2.625*(Y(3)+Y(4))+Y(6))
560 LETM2=A2-H1*(Y(4)+(4*Y(5))+Y(6))
620 FORI=7TON1STEP2
```

```
630 LETM1=A1
640 LETM2=A2
650 LETI8=I-2:LETI7=I-1:LETI6=I+1
670 LETA1=M1+H1*(Y(I8)+(4*Y(I7))+Y(I))
690 LETN4=I-N1
710 IFN4>=0THEN830
730 LETA2=M2+H1*(Y(I7)+(4*Y(I))+Y(I6))
745 NEXTI
780 PRINT"AREA = ";A2
790 GOTO50
830 PRINT"AREA = ";A1
840 GOTO50
2000 LETS1=S1+X
2010 LETS2=S2+Y(X)
2020 LETS3=S3+X*Y(X)
2030 LETS4=S4+X*X
2040 RETURN
2050 END
```

- (a) Lines 10 to 100 are concerned with the input of data.
- (b) Lines 105 to 180 take the first and last numbers and undergo a least squares analysis to obtain the value of the straight line between these points, which is thus taken as the base line.
- (c) Lines 200 to 220 correct the input data with respect to the new base line.
- (d) Lines 230 to 840 contain Simpson's Rule for calculating the area of the peak, which is then printed as output using line 780 or 830.

Appendix 4 Computer Program for the Numerical Solution of
Systems of Differential Equations.

DO2LF1 is a subroutine which solves the initial value problem for a system of first-order ordinary differential equations

$$DY/DT = F(Y,T) , Y = (Y(1),Y(2),..Y(N)).$$

Given values of Y at time T0, DO2LF1 will compute values of Y at time TOUT. Thus DO2LF1 must be called once for each output value of T. Non-stiff systems are solved by Adams methods, stiff systems by Gears method.

The program is based on the Gear package of Alan Hindmarsh, Lawrence Livermore Laboratory, California.

Example of use (e.g. CALL) -

```
CALL DO2LF1(N,TO,HO,YO,YMAX,TOUT,EPS,MF,INDEX,IPRINT,DIFFUN,
PEDERV)
```

PARAMETER LIST -

- N Number of first-order ordinary differential equations N must not exceed 30. N should be set on entry to the first call of DO2LF1; it can be decreased but never increased on entry to subsequent calls.
- TO The initial value of the independent variable T. It need only be set on entry to the first call.
- HO The step-size,H. HO is used on input only for the step-size to be attempted for the first step, on the first call. The sign of H is arbitrary but will not change during a problem. On output, HO is the step-size last used, whether successfully or not.
- YO A vector of length N for the dependent variable Y. On input,YO is the vector of initial values, and is

used only on the first call. On output, YO is the vector of values of Y at T=TOUT.

YMAX A vector of weighting factors, with which the estimated local errors in Y are compared (see EPS). On input to the first call, YMAX(I) should normally be set equal to ABS(YO(I)) unless YO(I) is zero, in which case YMAX(I) should be set to 1.0. However other choices may be useful, and the only restriction is that YMAX(I) must be positive. The weight factors are automatically updated as the program continues and so do not have to be reset.

TOUT The next output value of T. TOUT is used for input on every call. On output, TOUT is unchanged if reached successfully (it is altered slightly if INDEX=2 on input), and is the farthest value of T reached otherwise.

EPS The local error tolerance parameter. It is used only for input, and used only on the first call, unless INDEX=-1. Estimates of the single-step error in Y(I), divided by YMAX(I), are kept less than EPS in root-mean-square norm. EPS should typically be of the order of 0.001.

MF The method flag. It is used only for input, and used only on the first call, unless INDEX=-1. The allowed values of MF are 10,11,12,13,20,21,22,23. MF has two decimal digits, METH and MITER :

$$MF = 10 * METH + MITER$$

METH is the basic method indicator, with the

following values and meanings :

- 1 For implicit Adams methods
- 2 For Gears stiffly stable methods

MITER is the corrector iteration method indicator, with the following values and meanings :

- 0 For functional iteration
- 1 For chord method with user supplied Jacobian from PEDERV.
- 2 For chord method with Jacobian generated internally.
- 3 For chord method with diagonal approximation to Jacobian.

The novice user is recommended to set MF=12 normally, and to set MF=22 if the equations are known to be stiff.

INDEX

An integer flag used for both input and output.

On input, it indicates the type of call to D02LF1, with the following values and meanings :

- 1 For the first call for the problem.
- 2 For a call other than the first, with integration to continue so as to hit $T=TOUT$ exactly, and not to interpolate for output values; this assumes TOUT is beyond the current value of T.
- 0 For a call other than the first, for normal continuation.
- 1 For a call other than the first, in which the user has reset N, EPS, and/or MF.
- 3 For a call other than the first, with control to return to the calling program after one

step; TOUT is ignored on input and set to the current value of T on output.

On output, INDEX indicates the results of the last call with the following values and meanings :

- 0 Integration completed successfully as requested.
- 1 Integration halted after failing to pass error test even after reducing step-size H by a factor of 10^{10} from initial value.
- 2 Integration halted after some initial success either by repeated error test failures or by direct test indicating EPS too small.
- 3 Integration halted after failing to achieve corrector convergence even after reducing H by a factor of 10^{10} from initial value.
- 4 Input value found to be illegal; either $EPS.LE.0.0$, $N.LE.0$, $(T0-TOUT)*H0.GE.0.0$, or input value of index was illegal... or else some $YMAX(I)$ was not positive.
- 5 If INDEX was -1 on input, but TOUT was not beyond the current value of T; the desired changes of parameters were therefore not made; to continue, simply reset TOUT and INDEX and call D02LF1 again.

Notice that since normal output value of INDEX is 0, it need not be reset for a normal continuation.

IPRINT A non-negative integer used on input to control printing within D02LF1. If IPRINT=J, a positive integer, then diagnostic messages are written by

DO2LF1 to TAPE J. If IPRINT=0, then all printing within DO2LF1 is suppressed.

DIFFUN A subroutine, to be provided by the user, which computes the function $YDOT=F(Y,T)$, the right-hand side of the ODE. Its heading must be of the form :

```
SUBROUTINE DIFFUN(N,T,Y,YDOT)
  DIMENSION Y(N),YDOT(N)
```

PEDERV A subroutine, to be provided by the user, which computes the N by N Jacobian matrix of partial derivatives and stores it in PD as an NO by NO array. PD(I,J) is to be set to the partial derivative of YDOT(I) with respect to Y(J). PEDERV is called only if MITER=1. Otherwise a dummy routine can be substituted. The subroutine heading must be of the form :

```
SUBROUTINE PEDERV(N,T,Y,PD,NO)
  DIMENSION Y(N),PD(NO,NO)
```

Remember DIFFUN and PEDERV must appear in an external statement in the program that calls DO2LF1.

Error indicators - see INDEX in above parameter list.

Other routines used -

- D021A Solves linear system $AX=B$ after D021B has been called to decompose A
- D021B Performs an LU decomposition on a matrix
- D021C Interpolates to get the output values at $T=TOUT$
- D021D Computes and processes the Jacobian matrix $J=DF/DY$
- D021E Sets coefficients for use in the integrator D021F
- D021F Is the integrator. It performs a single step and the associated error control

The following program calls D02LF1 repeatedly to provide solutions of a set of differential equations at given times.

```
1      PROGRAM INT(INPUT,OUTPUT,TAPE5=INPUT,TAPE6=OUTPUT)
2      EXTERNAL DIFFUN,PEDERV
3      DIMENSION YO(14),YMAX(14),Y(6),YM(100),YT(100),
4      1AM(100),AT(100)
5      DO 40 K=1,6
6      Y(1)=1.0E-04
7      Y(2)=2.0E-04
8      Y(3)=4.0E-04
9      Y(4)=6.0E-04
10     Y(5)=8.0E-04
11     Y(6)=1.0E-03
12     N=14
13     TQ=0.0
14     HO=0.01
15     TOUT=0.0
16     DO 30 I=2,N
17     YO(I)=0.0
18     YMAX(I)=Y(K)
19     30 CONTINUE
20     YMAX(1)=YMAX(2)
21     YO(1)=YMAX(1)
22     EPS=1.0E-06
23     MF=22
24     INDEX=1
25     IPRINT=6
26     DO 10 I=1,100
27     IF(I.EQ.1)GOTO20
```

```
27      TOUT=TOUT+5.0
28      CALL DO2LF1(N,TO,HO,YO,YMAX,TOUT,EPS,MF,INDEX,
      1 IPRINT,DIFFUN,PEDERV)
29      20 CONTINUE
30      WRITE(6,100)TOUT,(YO(J),J=1,8)
31      200 FORMAT(1P,7E13.5)
32      100 FORMAT(1P,9E13.5)
33      WRITE(6,200)TOUT,(YO(J),J=9,14)
34      YT(I)=YO(1)
35      YM(I)=YO(4)
36      10 CONTINUE
37      NDIM=95
38      H=5.0
39      CALL DO1LF1(H,YT,AT,NDIM)
40      CALL DO1LF1(H,YM,AM,NDIM)
41      DO 50 L=1,95
42      WRITE(6,300)AT(L),AM(L)
43      300 FORMAT(1P,2E13.5)
44      50 CONTINUE
45      40 CONTINUE
46      STOP
47      END

1      SUBROUTINE DIFFUN(N,T,Y,YDOT)
2      DIMENSION Y(N),YDOT(N)
3      Z1=3.371E-05
4      Z2=4.365E05
5      Z3=4.4700E05
6      Z4=17.951
```

$$7 \quad Z5=3.258E03$$

$$8 \quad Z6=3.347E04$$

$$9 \quad Z7=1.0E10$$

$$10 \quad Z8=1.0E09$$

$$11 \quad Z9=3.162E10$$

$$12 \quad Z10=1.0E10$$

$$13 \quad Z11=3.162E09$$

$$14 \quad Z12=0.0$$

$$15 \quad Z13=0.0$$

$$16 \quad Z14=1.791E10$$

$$17 \quad ZT=0.0166$$

$$18 \quad YDOT(1)=-Z1*Y(1)-Z2*Y(1)*Y(3)-Z3*Y(1)*Y(2)$$

$$1-Z6*Y(1)*Y(7)+Z14*Y(3)*Y(2)-ZT*Y(1)$$

$$19 \quad YDOT(2)=Z1*Y(1)-Z3*Y(1)*Y(2)+Z6*Y(1)*Y(7)-2.0*Z7*$$

$$1Y(2)*Y(2)-Z8*Y(2)*Y(5)+Z12*Y(12)-Z14*Y(3)*Y(2)$$

$$1-ZT*Y(2)$$

$$20 \quad YDOT(3)=Z1*Y(1)-Z2*Y(1)*Y(3)+Z4*Y(5)-2.0*Z9*Y(3)*$$

$$1Y(3)-Z10*Y(5)*Y(3)-Z14*Y(3)*Y(2)-ZT*Y(3)$$

$$21 \quad YDOT(4)=Z2*Y(1)*Y(3)-ZT*Y(4)$$

$$22 \quad YDOT(5)=Z2*Y(1)*Y(3)+Z3*Y(1)*Y(2)-Z4*Y(5)+Z6*Y(1)*$$

$$1Y(7)-Z8*Y(2)*Y(5)-Z10*Y(5)*Y(3)-2.0*Z11*Y(5)*Y(5)$$

$$1+Z13*Y(14)*Y(1)-ZT*Y(5)$$

$$23 \quad YDOT(6)=Z3*Y(1)*Y(2)-ZT*Y(6)$$

$$24 \quad YDOT(7)=Z4*Y(5)-2.0*Z5*Y(7)*Y(7)-Z6*Y(1)*Y(7)-ZT*Y(7)$$

$$25 \quad YDOT(8)=Z5*Y(7)*Y(7)-ZT*Y(8)$$

$$26 \quad YDOT(9)=Z7*Y(2)*Y(2)-ZT*Y(9)$$

$$27 \quad YDOT(10)=Z8*Y(2)*Y(5)-ZT*Y(10)$$

$$28 \quad YDOT(11)=Z9*Y(3)*Y(3)+Z13*Y(14)*Y(1)-ZT*Y(11)$$

$$29 \quad YDOT(12)=Z10*Y(5)*Y(3)-Z12*Y(12)-ZT*Y(12)$$

$$30 \quad YDOT(13)=Z11*Y(5)*Y(5)-ZT*Y(13)$$

```
31      YDOT(14)=Z12*Y(12)-Z13*Y(14)*Y(1)-ZT*Y(14)
32      RETURN
33      END
```

```
1      SUBROUTINE PEDERV(N,T,Y,PD,NO)
2      DIMENSION PD(NO,NO),Y(NO)
3      RETURN
4      END
```

The program listed above is for the thermal decomposition of 4MS in a pulsed stirred-flow system. The differential equations and rate constants are defined in subroutine DIFFUN. In the main program solution points are calculated for all concentrations at 5 second intervals, those for methane and 4MS are stored and integrated by subroutine D01LF1 using Simpson's rule. The procedure is repeated for a range of initial concentrations of 4MS.

APPENDIX FIVE

EXPERIMENTAL RESULTS - CYCLOPROPANE

Appendix 5 Numerical Results for the Thermal Isomerisation of Cyclopropane

In the thermal isomerisation of cyclopropane it was necessary only to measure the ratio of the peak areas of propene and cyclopropane. A constant recorder sensitivity was used and the molecular weight factor (see Section 2.1.8) for each compound was the same as they are isomers. A constant ratio independent of peak size indicates that the reaction was first order (see eqn.(3.14); Section 3.2.1) with a rate constant given by this ratio divided by the time constant.

The peak area ratios tabulated in Table 5.1 were measured using a Du Pont 301 curve resolver. At each temperature at least a five fold range of initial concentrations of cyclopropane was used.

Table 5.1 Numerical Results for the Thermal Isomerisation of Cyclopropane

Volume of vessel = 10.4 cm^3

$\tau = 20.1 \text{ s}$

Initial Concentrations of Cyclopropane = 1×10^{-4} to 5×10^{-4}
mol cm^{-3}

Temperature/K	Ratio of Peak Areas Propene/Cyclopropane	Rate Constant /s ⁻¹
801	.072	3.58×10^{-3}
	.072	3.58×10^{-3}
	.070	3.48×10^{-3}
	.072	3.58×10^{-3}
	.073	3.63×10^{-3}
	.073	3.63×10^{-3}

806	.093	4.62×10^{-3}
	.089	4.41×10^{-3}
	.092	4.58×10^{-3}
	.088	4.37×10^{-3}
	.089	4.41×10^{-3}
819	.176	8.78×10^{-3}
	.176	8.78×10^{-3}
827	.285	1.42×10^{-2}
	.285	1.42×10^{-2}
	.314	1.56×10^{-2}
	.267	1.33×10^{-2}
844	.639	3.18×10^{-2}
	.639	3.18×10^{-2}
	.639	3.18×10^{-2}
	.639	3.18×10^{-2}
868	1.74	8.64×10^{-2}
	1.74	8.64×10^{-2}
	1.70	8.47×10^{-2}
	1.70	8.47×10^{-2}

The average of the rate constants at each temperature are tabulated in Table 5.2.

Table 5.2 Data for an Arrhenius Plot for the Thermal
Isomerisation of Cyclopropane

Temperature T/K	$1/T \times 10^3$	Rate Constant k/s^{-1}	$\ln k$
801	1.248	3.58×10^{-3}	-5.632
806	1.241	4.48×10^{-3}	-5.409
819	1.221	8.78×10^{-3}	-4.735
827	1.209	1.43×10^{-3}	-4.247
844	1.185	3.18×10^{-2}	-3.448
868	1.152	8.56×10^{-2}	-2.459

By means of a standard linear regression technique, using least squares 95% confidence limits, these results were found to be given by

$$\log_{10}(k/s^{-1}) = (15.76 \pm 0.36) - (279.2 \pm 5.6) \text{ kJ mol}^{-1}/2.303RT$$

APPENDIX SIX

EXPERIMENTAL RESULTS - TETRAMETHYLSILANE

Appendix 6 Numerical Results For the Thermolysis of
Tetramethylsilane

The results presented below are the data from individual thermolysis experiments. They are presented in three groups; those obtained in the unpacked reaction vessels, those obtained in the packed reaction vessel, and some subsequent experiments using an unpacked reaction vessel to check the reproducibility of earlier results.

The nomenclature is as follows:-

CH_4 = amount of methane formed as measured by G.L.C. and divided by the appropriate molecular weight factor.

3MS = amount of trimethylsilane formed as measured by G.L.C. and divided by the appropriate molecular weight factor.

4MS = amount of tetramethylsilane formed as measured by G.L.C. and divided by the appropriate molecular weight factor.

All the above are corrected to a recorder sensitivity of 2 mV F.S.D.

C = units of the above amounts

PW = grams of paper

NI = number produced by numerical integration procedure

T = reaction temperature

V = volume of reaction vessel

τ = residence time

k = first order rate constant for the formation of methane evaluated from equation (3.14)

The results are presented in chronological order, each horizontal row represents a given experiment. A dash indicates that the compound although formed was not measured. The figures in brackets are powers of ten, i.e. 1.23(-4) is read as 1.23×10^{-4} .

Table 6.1 Data Obtained from Unpacked Reaction Vessels

1. $T = 954\text{K}$ $C = \text{NI}$
 $V = 60.19 \text{ cm}^3$
 $\tau = 66.5 \text{ s}$

CH_4	3MS	4MS
10322	458.5	13898
16108	772.7	19385
5896	186.8	8195
5447	146.4	7177

$$k/\text{s}^{-1} = 1.405(-2)$$

$$\log_{10}(k/\text{s}^{-1}) = -1.852$$

2. $T = 932\text{K}$ $C = \text{NI}$
 $V = 60.19 \text{ cm}^3$
 $\tau = 38.2 \text{ s}$

CH_4	3MS	4MS
5079.4	468.4	26871
3658.6	256.8	16604
3490.4	268.2	18078
2053.9	159.8	12834
2075.1	113.5	10872
1731.6	100.1	9875

$$k/\text{s}^{-1} = 5.747(-4)$$

$$\log_{10}(k/\text{s}^{-1}) = -3.24$$

3. $T = 844\text{K}$

$C = \text{PW}$

$V = 60.19 \text{ cm}^3$

$\tau = 121.3 \text{ s}$

CH_4	3MS	4MS
2.392(-3)	2.171(-4)	9.15 (-2)
4.795(-3)	3.69 (-4)	1.45 (-1)
4.298(-3)	3.69 (-4)	1.289(-1)
1.074(-3)	1.05 (-4)	5.15 (-2)
1.571(-3)	1.303(-4)	7.82 (-2)
6.615(-4)	1.306(-4)	6.24 (-2)
1.984(-3)	1.306(-4)	6.651(-2)
1.653(-3)	7.598(-5)	4.82 (-2)
1.240(-3)	4.34 (-5)	4.07 (-2)
9.922(-4)	6.513(-5)	4.99 (-2)

$k/\text{s}^{-1} = 2.219(-4)$

$\log_{10}(k/\text{s}^{-1}) = -3.65$

4. $T = 1013\text{K}$
 $V = 60.19 \text{ cm}^3$
 $\tau = 121.24 \text{ s}$

$$C = PW$$

CH_4	3MS	4MS
3.514(-1)	1.519(-3)	1.95 (-2)
2.37 (-1)	1.682(-3)	1.41 (-2)
5.125(-1)	2.388(-3)	1.955(-2)
7.193(-1)	3.754(-3)	2.57 (-2)
6.32 (-2)	8.684(-5)	3.744(-3)
1.554(-1)	3.69 (-4)	6.988(-3)
1.781(-1)	4.342(-3)	9.651(-3)
3.307(-2)	6.513(-5)	2.579(-3)

$$k/s^{-1} = 1.646(-1)$$

$$\log_{10}(k/s^{-1}) = -0.783$$

5. $T = 1054\text{K}$
 $V = 60.19$
 $\tau = 92.2\text{s}$

$$C = PW$$

CH_4	3MS	4MS
1.565(-1)	6.513(-5)	1.664(-3)
6.281(-1)	3.265(-4)	5.824(-3)
5.542(-1)	3.039(-4)	6.156(-3)
9.680(-1)	1.107(-3)	1.119(-2)
7.783(-2)	6.513(-5)	9.984(-4)
1.418(-2)	1.231(-4)	1.497(-4)

$$k/s^{-1} = 9.55(-1)$$

$$\log_{10}(k/s^{-1}) = -1.99(-2)$$

6. $T = 898\text{K}$

$C = \text{PW}$

$V = 10.4 \text{ cm}^3$

$\tau = 24.46 \text{ s}$

CH_4	3MS	4MS
2.149(-3)	1.303(-4)	5.36 (-2)
2.232(-3)	1.300(-4)	5.07 (-2)
3.885(-3)	2.171(-4)	7.73 (-2)
4.46 (-3)	3.473(-4)	9.40 (-2)
4.87 (-3)	4.342(-4)	1.098(-1)
6.200(-3)	4.993(-4)	1.397(-1)
7.119(-3)	6.73 (-4)	1.597(-1)

$k/s^{-1} = 1.822(-3)$

$\log_{10}(k/s^{-1}) = -2.74$

7. $T = 983\text{K}$

$C = \text{PW}$

$V = 11.7 \text{ cm}^3$

$\tau = 13.32 \text{ s}$

CH_4	3MS	4MS
2.79(-2)	9.335(-4)	4.36 (-2)
3.72(-2)	1.736(-3)	6.36 (-2)
4.50(-2)	2.442(-3)	8.36 (-2)
5.45(-2)	2.870(-3)	8.77 (-2)
5.70(-2)	3.256(-3)	1.023(-1)
1.81(-2)	6.29 (-4)	2.74 (-2)

$k/s^{-1} = 4.80(-2)$

$\log_{10}(k/s^{-1}) = -1.32$

8. $T = 1003\text{K}$ $C = \text{PW}$
 $V = 11.7 \text{ cm}^3$
 $\tau = 13.32 \text{ s}$

CH_4	3MS	4MS
9.25 (-2)	2.985(-3)	6.115(-2)
1.025(-1)	3.636(-3)	7.155(-2)
1.182(-1)	4.179(-3)	8.57 (-2)
1.467(-1)	5.862(-3)	9.98 (-2)
1.57 (-1)	6.839(-3)	1.056(-1)

$$k/s^{-1} = 1.105(-1)$$

$$\log_{10}(k/s^{-1}) = -9.563(-1)$$

9. $T = 1620\text{K}$ $C = \text{PW}$
 $V = 11.7 \text{ cm}^3$
 $\tau = 13.32 \text{ s}$

CH_4	3MS	4MS
1.198(-1)	2.38 (-3)	3.28(-2)
9.92 (-2)	-	2.24(-2)
1.529(-1)	3.691(-3)	5.28(-2)
1.901(-1)	5.21 (-3)	7.36(-2)
1.984(-1)	5.86 (-3)	7.73(-2)
1.943(-1)	5.427(-3)	6.98(-2)
1.07 (-1)	9.118(-3)	4.12(-2)

$$k/s^{-1} = 2.174(-1)$$

$$\log_{10}(k/s^{-1}) = -6.62(-1)$$

10. $T = 1037\text{K}$

$C = \text{PW}$

$V = 11.7 \text{ cm}^3$

$\tau = 17.3 \text{ s}$

 CH_4

4MS

2.14(-2)

2.62(-3)

5.66(-2)

6.53(-3)

7.11(-2)

4.22(-3)

9.09(-2)

5.26(-3)

1.14(-1)

1.35(-2)

2.14(-1)

2.47(-2)

$k/\text{s}^{-1} = 5.01(-1)$

$\log_{10}(k/\text{s}^{-1}) = -3.03(-1)$

Table 6.2 Data Obtained From Packed Reaction Vessel

$$V = 54.4 \text{ cm}^3 \quad \text{surface/volume} = 12.2 \text{ cm}^{-1} \quad C = \text{PW}$$

T/K	τ/s	CH_4	4MS	k/s^{-1}
934	69.99	1.953(-2)	5.793(-2)	4.817(-3)
933	70.62	3.449(-2)	9.518(-2)	5.118(-3)
927	70.62	1.028(-2)	3.653(-2)	3.981(-3)
898	70.62	1.083(-2)	1.372(-1)	1.117(-3)
868	70.62	2.193(-3)	1.111(-1)	2.780(-4)
972	70.62	1.172(-1)	6.135(-2)	2.71 (-2)
1001	70.62	2.755(-1)	3.581(-2)	1.088(-1)
1022	70.62	9.518(-2)	5.518(-3)	2.442(-1)
981	62.3	7.810(-2)	3.167(-2)	3.96 (-2)

$$T = 933\text{K}$$

$$\tau = 70.62 \text{ s}$$

CH_4	4MS
2.985(-2)	8.413(-2)
3.449(-2)	9.518(-2)
4.570(-2)	1.348(-1)
7.585(-2)	2.065(-2)

$$k/s^{-1} = 5.118(-3)$$

$$T = 1001\text{K}$$

$$\tau = 70.62 \text{ s}$$

CH_4	4MS
2.755(-1)	3.581(-2)
3.090(-1)	4.51 (-2)
3.981(-1)	5.888(-2)
5.188(-1)	7.585(-2)
5.623(-3)	9.443(-2)

$$k/\text{s}^{-1} = 1.088(-1)$$

Table 6.3 Data Obtained from Unpacked Reaction Vessel to
Check Reproducibility

T/K	τ/s	CH_4	4MS	k/s^{-1}
1013	14.7	4.523(-3)	1.627(-3)	1.89(-1)
984	15.1	1.370(-2)	1.791(-2)	5.07(-2)
960	15.5	6.167(-3)	2.022(-2)	1.97(-2)
1043	28.5	3.415(-2)	2.206(-3)	5.39(-1)

APPENDIX SEVEN

DETAILS OF COMPOUNDS USED

Appendix 7 Details of Compounds Used

Tetramethylsilane: This was special spectrometric grade obtained from B.D.H. Ltd. It contained no impurities detectable by G.L.C. or mass spectrometry. Some samples were purified by preparative gas chromatography (Aerogram A700 Autoprep), the middle 50% of the 4MS peak being collected. These samples gave identical results to those that had not been so purified.

Methane, ethane, propane and n-butane were obtained from Cambrian Chemicals Ltd.

Trimethylsilane was obtained from the Pierce Chemical Co. Ltd., Rockford, Illinois.

Hexamethyldisilane was prepared by the method of Wilson and Smith and purified by preparative gas chromatography.

TMDS was donated by I.C.I. Nobel Division.

REFERENCES

REFERENCES

- (1) I.M.T. Davidson, and I.L. Stephenson, *J. Chem. Soc.(A)*, 1968, 282.
- (2) J.A. Connor, G. Finney, G.J. Leigh, R.N. Haszeldine, P.J. Robinson, R.D. Sedgwick, and R.F. Simmons, *J.C.S. Chem.Comm.*, 1966, 178.
- (3) J.A. Connor, R.N. Haszeldine, G.J. Leigh, and R.D. Sedgwick, *J.Chem.Soc.(A)*, 1967, 768.
- (4) C. Eaborn and J.M. Simmie, *J.C.S. Chem.Comm.*, 1968, 1426.
- (5) I.M.T. Davidson, C. Eaborn, and J.M. Simmie, *J.C.S. Faraday I*, 1974, 70, 249.
- (6) S.J. Band, I.M.T. Davidson, and C.A. Lambert, *J.Chem.Soc. (A)*, 1968, 2068.
- (7) I.M.T. Davidson, *Quart. Rev.*, 1971, 25, 111.
- (8) I.M.T. Davidson and C.A. Lambert, *J. Chem.Soc.(A)*, 1971, 882.
- (9) M.C. Flowers and L.E. Gusel'nikov, *J.Chem.Soc.(B)*, 1968, 419.
- (10) S.W. Benson, "Thermochemical Kinetics", Wiley, New York, 1968.
- (11) G.B. Watts and K.U. Ingold, *J.Amer.Chem.Soc.*, 1972, 94, 491.
- (12) P. Cadman, G.M. Tilsley, and A.F. Trotman-Dickenson, *J.C.S. Faraday I*, 1972, 68, 1849.
- (13) R.P. Clifford, B.G. Gowenlock, C.A.F. Johnson, and J Stevenson, *J. Organometallic Chem.*, 1972, 34, 53.
- (14) I.M.T. Davidson and A.V. Howard, *J.C.S. Chem.Comm.*, 1973, 323.

- (15) I.M.T. Davidson and A.V. Howard, J.C.S. Faraday I, 1975, 71, 69.
- (16) W.C. Steele and F.G.A. Stone, J.Amer.Chem.Soc., 1962, 84, 3599; F.E. Saalfeld and H.J. Svec, J.Phys.Chem., 1966, 70, 1753.
- (17) I.M.T. Davidson, M. Jones, and H.F. Tibbals, unpublished work.
- (18) R. Walsh and J.M. Wells, J.C.S. Chem.Comm., 1973, 513.
- (19) R. Walsh and J.M. Wells, J.C.S. Faraday I, 1976, 72, 100.
- (20) P. Potzinger, A. Ritter, and J. Krause, Z. Naturforsch, 1975, 30a, 347.
- (21) G.W. Gear, "Information Processing 68", Ed. Morrell, North Holland, Amsterdam Vol. I, p.187.
- (22) A.C. Baldwin, I.M.T. Davidson, and A.V. Howard, J.C.S. Faraday I, 1975, 71, 972.
- (23) D.R. Mason and E.L. Piret, Ind.Eng.Chem., 1950, 42, 817.
- (24) K. Denbigh, "Chemical Reactor Theory", Cambridge, 1965.
- (25) H.M. Frey and R. Walsh, Chem.Rev., 1969, 69, 103.
- (26) M.F.R. Mulcahy and D.J. Williams, Australian J.Chem., 1961, 14, 535.
- (27) J.P. Langwell and M.A. Weiss, Ind.Eng.Chem., 1955, 47, 1634.
- (28) J.L. Stephensen. Ph.D. Thesis, University of Leicester, 1967.
- (29) C.A. Lambert. Ph.D. Thesis, University of Leicester, 1969.
- (30) M. Jones. Ph.D. Thesis, University of Leicester, 1971.
- (31) G.L. Pratt and J.H. Purnell, Anal.Chem., 1960, 32, 1213.
- (32) G.H. Gady and D.P. Seigwarth, Anal.Chem., 1959, 31, 618.

- (33) Gow-Mac Instrument Co.
(a) "Instructions for use Gow-Mac gas density detectors"
(b) Bulletin S.B. GADE 1065.
- (34) C.L. Giullmain and F. Auricourt, J.Gas Chrom., 1964, 20, 156.
- (35) C.L. Giullmain, F. Auricourt, and P. Blaise, J.Gas Chrom., 1966, 4, 338.
- (36) J.L. Wittink, G.A. Junk, G.V. Calder, J.S. Fritz, and H.J. Svec, J.Org.Chem., 1973, 38(17), 3066.
- (37) M.F.R. Mulcahy and D.J. Williams, Australian J.Chem., 1961, 14, 535.
- (38) J.M. Sullivan and T.J. Hauser, Chem.Ind., 1965, 1057.
- (39) Ref. 29,
- (40) Ref. 24, p72.
- (41) Cooper and Jeffreys, "Chemical Kinetics and Reactor Design" Oliver and Boyd, 1971.
- (42) M.F.R. Mulcahy and M.R. Pethard, Australian J.Chem., 1963, 16, 527.
- (43) J.T. Batten, Australian J.Appl.Sci., 1961, 12, 11.
- (44) M.F.R. Mulcahy, "Gas Kinetics", Nelson, 1973.
- (45) W.C. Herndon, M.R. Henly, J.M. Sullivan, J.Phys.Chem., 1963, 67, 2842.
- (46) W.C. Herndon, and L.L. Lowry, J.Amer.Chem.Soc., 1964, 86, 1922.
- (47) W.C. Herndon, J.Chem.Educ., 1964, 41, 425.
- (48) Ref. 24, p86.
- (49) Ref. 44, p62.
- (50) A.C. Baldwin, I.M.T. Davidson, and A.V. Howard, J.C.S. Faraday I, 1975, 71, 972.

- (51) D.R. Mason and E.L. Piret, *Ind.Eng.Chem.*, 1950, 42, 817.
- (52) Ref. 44, p51.
- (53) S.W. Benson, "The Foundations of Chemical Kinetics", McGraw-Hill, 1960, Chapter IV.
- (54) Ref. 53, Chapter II.
- (55) D.L. Allara, D. Edelson, and K.C. Irwin, *Int.J.Chem.Kinet.*, 1972, IV, 345.
- (56) R.J. Gelinias, *J.Comp.Phys.*, 1972, 9, 222.
- (57) L.A. Farrow and D. Edelson, *Int.J.Chem.Kinet.*, 1974, VI, 787.
- (58) A. Jones. "Chemical Society Specialist Periodical Reports". Reaction Kinetics, Vol.I., 1975.
- (59) C.F. Curtis and J.O. Hirschfelder, *Proc.Nat.Acad.Sci.U.S.A.*, 1952, 33, 235.
- (60) Ed. D.F. De Tar, "Computer Programs for Chemistry", Benjamin, Vol.I, 1968; Vol.II, 1969.
- (61) C.W. Gear, "Numerical Initial Value Problems in Ordinary Differential Equations", Prentice-Hall, 1971.
- (62) A. Nordsieck, *Math.Comp.*, 1962, 16, 22.
- (63) A.C. Hindmarsh, "Linear Multistep Methods for Ordinary Differential Equations" UCRL-51186 Lawrence Livermore Laboratory, 1972.
- (64) G. Pratt and D. Rogers, *J.C.S. Faraday I*, 1976, 72, 1589.
- (65) J.N. Bradley and K.O. West, *J.C.S. Faraday I*, 1976, 72, 8.
- (66) J.N. Bradley and K.O. West, *J.C.S. Faraday I*, 1976, 72, 558.
- (67) C.W. Gear, *I.F.I.P., Proc.A*, 1968, 81.
- (68) C.W. Gear, "Information Processing 68", Ed. Morrell, North Holland, Amsterdam, Vol.1, p187.
- (69) A.C. Hindmarsh, "Ordinary Differential Equation System Solver" UCID-30001 Lawrence Livermore Laboratory, 1972.

- (70) I.M.T. Davidson, "Reaction Kinetics", Chem. Soc. Spec. Periodical Rep., London 1975, Vol.1, p212.
- (71) P. Robinson and K. Holbrook, "Unimolecular Reactions", Wiles-Interscience, London 1972.
- (72) P. Robinson, "Reaction Kinetics", Chem. Soc. Spec. Periodical Rep., London 1975, Vol.1, p135.
- (73) W.E. Falconer, T.F. Hunter and A.F. Trotman-Dickenson, J.Chem.Soc., 1961, 609.
- (74) D.P. Paquin, R.J. O'Conner and M.A. Ring, J. Organometallic Chem., 1974, 80, 341.
- (75) R.E. Berkley, I. Safarik, H.E. Gunning and O.P. Strausz, J.Phys.Chem., 1973, 77, 1734.
- (76) A. Shepp, J.Chem.Phys., 1956, 24, 939.
- (77) N.A. Continearm, D. Ninelcic, R.H. Schinder and P. Potzinger, Ber. Bunsengesellschaft Phys. Chem., 1971, 75, 426.
- (78) J.B. Pedley and B.S. Iseard, "Catch" tables for silicon compounds, University of Sussex, 1972.
- (79) W.A. Chupka, J.Chem.Phys., 1968, 48, 2337.
- (80) I.M.T. Davidson and J.I. Matthews, J.C.S.Faraday I, 1976, 72, 1403.
- (81) P. John and J.H. Purnell, J.C.S.Faraday I, 1973, 69, 1455.
- (82) R. Walsh, J.Organometallic Chem., 1972, 38, 245.

SUMMARY

The thermolysis of tetramethylsilane was investigated over a wide temperature range, 840K to 1055K, to elucidate the mechanism of the reaction and determine the silicon-methyl bond dissociation energy. At low temperatures, below 955K, the thermolysis was found to proceed by a chain mechanism, however as the temperature was increased the chain length became shorter, until at 955K the reaction became non-chain. The production of methane was then rate determined by reaction (1), and the activation energy could be identified with $D(\text{Me}_3\text{Si-Me})$



$$\log_{10}(k/s^{-1}) = 17.6 + 0.3 - (355.3 + 6) \text{ kJ mol}^{-1}/2.303RT$$

A mechanism was advanced to explain the low temperature chain reaction. Due to its complexity and to the occurrence of several termination reactions of similar rate this mechanism could not be treated by conventional steady state methods. To overcome this problem a computer program using a multi-step, implicit, predictor-corrector formula was used to numerically integrate the differential equations corresponding to the mechanism. Using this method a satisfactory mechanism was arrived at which accounted for all the experimental results.

This in turn enabled a mechanism to be proposed for the thermolysis of a similar compound, trimethylsilane. Although more complicated, due to the presence of two types of hydrogen atom in the molecule, this mechanism satisfactorily rationalised a previous study of this thermolysis.